

**SANDSTONE ACIDIZING USING IN-SITU GENERATED
HYDROFLUORIC ACID**

BY

Ibrahim Hassan Gomaa

A Thesis Presented to the
DEANSHIP OF GRADUATE STUDIES

KING FAHD UNIVERSITY OF PETROLEUM & MINERALS

DHAHRAN, SAUDI ARABIA

In Partial Fulfillment of the
Requirements for the Degree of

MASTER OF SCIENCE

In

PETROLEUM ENGINEERING

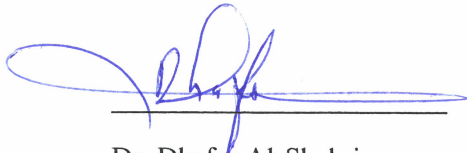
November, 2019

KING FAHD UNIVERSITY OF PETROLEUM & MINERALS

DHAHRAN- 31261, SAUDI ARABIA

DEANSHIP OF GRADUATE STUDIES

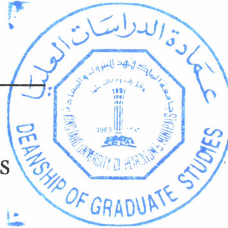
This thesis, written by **Ibrahim Hassan Gomaa** under the direction of his thesis advisor and approved by his thesis committee, has been presented and accepted by the Dean of Graduate Studies, in partial fulfillment of the requirements for the degree of **MASTER OF SCIENCE IN PETROLEUM ENGINEERING**.



Dr. Dhafer Al-Shehri
Department Chairman



Dr. Salam A. Zummo
Dean of Graduate Studies



16/12/19
Date



Dr. Mohamed Mahmoud
(Advisor)



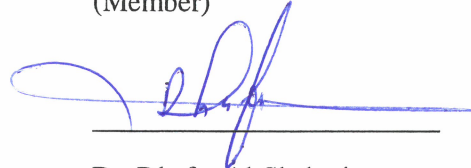
Dr. Mohamed BaTaweel
(Co-Advisor)



Dr. Abdulazeez Abdulraheem
(Member)



Dr. Abdullah Sultan
(Member)



Dr. Dhafer Al-Shehri
(Member)

© Ibrahim Hassan Goma

2019

This work is dedicated to

My Parents and sisters whom prayers always support me in hard times...

My wife and daughter who shared this master's journey with me...

Acknowledgment

All Praise be to **Allah**, Lord of all creation for all the knowledge gained and for all the success achieved throughout this research.

All thanks and gratitude to **King Fahd University of Petroleum and Minerals** for providing me with a scholarship to pursue my master's degree in petroleum engineering.

My sincere gratitude and appreciation go to my advisor, **Dr. Mohamed A. Mahmoud**, who never scrimped his time, efforts or knowledge from me. All thanks to him for his professional guidance and support throughout this research.

My true acknowledgment is extended to my committee members, **Dr. Mohamed BaTaweel, Dr. Abdulazeez Abdulraheem, Dr. Abdullah Sultan and Dr. Dhafer Al-Shehri**, for their valuable contribution, feedback and support.

My deep gratitude for the man who has the greatest favor, after Allah, in joining the College of Petroleum and Geosciences, **Dr. Salaheldin Elkatatny**.

Finally, I would like to express my gratefulness to the whole family of the petroleum engineering department; professors, researchers, students, lab engineers and workers, who helped me throughout this work.

TABLE OF CONTENTS

ACKNOWLEDGMENT	V
TABLE OF CONTENTS	VI
LIST OF TABLES.....	VIII
LIST OF FIGURES.....	IX
LIST OF ABBREVIATIONS	XVI
ABSTRACT	XVII
ملخص الرسالة.....	XIX
CHAPTER 1 INTRODUCTION.....	1
1.1 Sandstone Formation Damage and Treatment.....	1
1.2 Problem Statement.....	7
1.3 Thesis Objectives.....	9
1.4 Thesis Description	11
CHAPTER 2 LITERATURE REVIEW	12
2.1 Mud Acid Treatment	12
2.1.1 Reservoir Problems Associated with Conventional Mud Acid Treatment	14
2.1.2 Conventional Mud Acid Treatment Stages.....	18
2.2 Mud Acid-Sandstone Reaction Stoichiometry	25
2.3 Mud Acid-Sandstone Reaction Kinetics.....	28
2.4 The Problems of Stimulating High Clay Content Sandstone Formations using Mud Acid	30
2.4.1 Problems of Acidizing Illitic Sandstone Reservoirs using Mud Acid	33
2.5 Safety Hazards and Precautions of Dealing with Mud Acid.	34
2.6 Trials of Replacing the Conventional Mud Acid	35
2.6.1 The Use of Organic Acids/HF Mixtures.....	35
2.6.2 Retarded HF Acid Systems.....	37
2.6.3 The Use of Chelating Agents in Sandstone Acidizing.....	41
2.7 Ammonium Fluoride Oxidation.....	44
2.8 Applications of Thermochemicals in Oil Field	46

CHAPTER 3 RESEARCH NOVELTY, METHODOLOGY AND EQUIPMENT	48
3.1 Research Novelty	48
3.2 Methodology and equipment	49
3.2.1 Phase 1- Materials Preparation.....	49
3.2.2 Phase 2 – Proving the Concept (Quartz Solubility Test).....	55
3.2.3 Phase 3 – Clay Solubility Test	59
3.2.4 Phase 4 – Core Flooding	61
3.2.5 Phase 5 – Pore System and Core Integrity Evaluation	72
CHAPTER 4 RESULTS AND DISCUSSION	75
4.1 Results of Testing Different Oxidizers	75
4.2 Different Clay Minerals solubility in the in-situ HF generating fluids	80
4.3 Acidizing Berea and Scioto Cores without using Thermochemicals	85
4.3.1 Gray Berea Sandstone Core	85
4.3.2 Scioto Sandstone Core	93
4.4 Pore System Change Monitoring using NMR Scanning.....	100
4.5 Rock Integrity and Strength Monitoring.....	102
4.6 The effect of the pressure pulse generated from the thermochemicals on the stimulation process.	112
CHAPTER 5 CONCLUSIONS AND RECOMMENDATIONS	122
5.1 Conclusions.....	122
5.2 Recommendations for Future Work	125
REFERENCES	126
VITAE	140

LIST OF TABLES

Table 1.1	Damage risk assessment matrix for wells drilled in sandstone formations.	8
Table 2.1	The solubility of different sandstone mineral constituents in mud acid	13
Table 2.2	The selection criteria of the preflush acid used for mud acid treatment.....	20
Table 2.3	The basic design guidelines for the main flush stage	22
Table 2.4	The modified guidelines for mud acid main flush after.....	23
Table 2.5	The dissolving power of HF acid at different concentrations with both Quartz and Albite	27
Table 2.6	The different types of clay minerals after	31
Table 3.1	Chemical and physical properties of the used chemical compounds.....	50
Table 3.2	Gray Brea and Scioto cores properties with the saturating fluid properties	65
Table 3.3	The permeability measurement stage and the preflush stage properties for the two core types	67
Table 4.1	The corresponding Si ⁺ ions concentration (ppm) and the quartz samples weight change (mg) with different oxidizer concentrations.....	78

LIST OF FIGURES

Figure 1.1 Formation damage classifications.	3
Figure 1.2 The acid streamlines while passing through the pore spaces during the acidizing process.	4
Figure 1.3 A graphical illustration of the different oil well stimulation techniques.....	6
Figure 2.1 The pore structure and mineral constituents of typical sandstone rock.....	13
Figure 2.2 The three stages of the reaction of mud acid with sandstone matrix.....	15
Figure 2.3 A comparison between the results of stimulating a Nigerian oil well using conventional mud acid first and then using fluoboric acid as reported by	40
Figure 2.4 The amount of HF acid produced under different concentration ratios of both ammonium flouride and sodium bromates	45
Figure 3.1 Sodium bromate solubility in water as a function of temperature.....	51
Figure 3.2 Ammonium persulfate solubility in water as a function of temperature	51
Figure 3.3 Potassium permanganate solubility in water as a function of temperature	52
Figure 3.4 Ammonium fluoride solubility in water as a function of temperature	52
Figure 3.5 Ammonium chloride solubility in water as a function of temperature.....	53
Figure 3.6 Sodium nitrite solubility in water as a function of temperature	53
Figure 3.7 A triple-hot plate with magnetic stirrer solubility set-up	54
Figure 3.8 Highly pure quartz samples	56
Figure 3.9 High accurate digital balance up to 0.1 mg	56
Figure 3.10 A steel aging cell with a Teflon liner of a maximum capacity of 100 ml	57
Figure 3.11 A digital oven with a maximum temperature of 300 °C	57

Figure 3.12 ICP-OES system used for all the elemental analysis carried out within this study.....	59
Figure 3.13 (a) chlorite clay mineral with its dark color, (b) illite clay mineral with its dark brownish color and (c) kaolinite clay mineral with its light brownish color.	60
Figure 3.14 The core cutting desk.....	61
Figure 3.15 The core face grinding machine	62
Figure 3.16 The mineralogy analysis of both Gray Berea and Scioto cores using XRD	63
Figure 3.17 The core saturating set-up	64
Figure 3.18 Gray Berea SS and Scioto SS cores that will be used for this study	66
Figure 3.19 The general sequence of the core flooding test.	68
Figure 3.20 Core flooding set-up.....	69
Figure 3.21 The injection sequence of the acid generating fluids along with the thermochemicals inside Scioto core.....	71
Figure 3.22 An overview of the scratch test machine used in this study.....	73
Figure 3.23 Oxford Geospec NMR rock core analyzer	74
Figure 4.1 (a) shows the quartz sample before going under the chemical reactions, (b) the quartz sample after going under the chemical reactions	76
Figure 4.2 The effluent from the oxidation of ammonium fluoride with sodium bromates in the presence of thermochemicals	77
Figure 4.3 The Si ⁺ ions concentration resulted from the effluent of mixing different concentrations of ammonium persulfate oxidizer with 1 M ammonium fluoride and the thermochemicals	79

Figure 4.4	The effluent of 0.1, 0.5 and 1 M concentration of ammonium persulfate added to 2 M of ammonium fluoride and mixed with the thermochemicals. .	79
Figure 4.5	The XRF results for the chlorite clay showing the different elements in this clay type.....	81
Figure 4.6	The XRF results for the illite clay showing the different elements in this clay type.....	81
Figure 4.7	The XRF results for the Kaolinite clay showing the different elements in this clay type.	82
Figure 4.8	The concentration of the major elements dissolved from illite, chlorite and kaolinite clays by the action of the novel chemical mixture measured by ICP-OES.....	84
Figure 4.9	The dissolved fraction from the three clay groups (illite, chlorite and kaolinite) by the action of the acid generated from the novel chemical mixture...	84
Figure 4.10	The inlet pressure profile (psi) during the different core flooding stage measured versus the cumulative time (min).	87
Figure 4.11	The inlet-outlet pressure profile (psi) measured during the different core flooding stages measured versus the cumulative time (min).....	88
Figure 4.12	The pressure difference profile (psi) measured during the different core flooding stages measured versus the cumulative pore volume injected	89
Figure 4.13	The Gray Berea core permeability values measured in mD as calculated after each treatment cycle using 3 wt.% KCl solution.....	90
Figure 4.14	The chelated Si ion concentration in each flushing cycle as measured from the core flooding effluent that was analyzed using ICP-OES.....	92

Figure 4.15	The cumulative amount of Si chelated calculated in (mg) from the Gray Berea core after each treatment cycle	92
Figure 4.16	The inlet pressure profile (psi) during the different core flooding stages measured versus the cumulative time (min)	94
Figure 4.17	The inlet-outlet pressure profile (psi) measured during the different core flooding stage measured versus the cumulative time (min).....	95
Figure 4.18	The pressure difference profile (psi) measured during the different core flooding stage measured versus the cumulative time (min).....	96
Figure 4.19	The Scioto core permeability values measured in mD as calculated after each treatment cycle.....	97
Figure 4.20	The chelated Si ion concentration in each flushing cycle as measured from the core flooding effluent that was analyzed using ICP-OES.....	99
Figure 4.21	The cumulative amount of Si chelated calculated in (mg) from the Scioto SS core after each treatment cycle	100
Figure 4.22	The relaxation time T2 measured by the NMR technique for both fresh and acidized Gray Berea core	101
Figure 4.23	The relaxation time T2 measured by the NMR technique for both fresh and acidized Gray Berea core	101
Figure 4.24	The groove created along the whole length of the fresh Gary Berea core with the recorded rock strength in MPa.....	104
Figure 4.25	The groove created along the whole length of the fresh Gary Berea core with the recorded rock strength in MPa.....	104

Figure 4.26	The UCS values of the Gray Berea SS core measured in psi before and after the acid treatment measured by the scratch test.	105
Figure 4.27	The compression and shear waves' velocity of the Gray Berea SS core measured in m/s before and after the acid treatment	105
Figure 4.28	The dynamic Young's Modulus of the Gray Berea SS core measured in ksi before and after the acid treatment.....	106
Figure 4.29	The dynamic Poisson's ratio of the Gray Berea SS core measured before and after the acid treatment.....	106
Figure 4.30	The groove created along the whole length of the fresh Scioto core with the recorded rock strength in MPa.....	108
Figure 4.31	The groove created along the whole length of the acidized Scioto core with the recorded rock strength in MPa.....	108
Figure 4.32	The UCS values of the Scioto core measured in psi before and after the acid treatment measured by the scratch test.....	109
Figure 4.33	The compression and shear waves' velocity of the Scioto core measured in m/s before and after the acid treatment.....	110
Figure 4.34	The dynamic Young's Modulus of the Scioto core measured in ksi before and after the acid treatment.....	110
Figure 4.35	The dynamic Poisson's ratio of the Gray Berea SS core measured before and after the acid treatment.....	111
Figure 4.36	The inlet-outlet pressures measured in psi during the 5 successive cycles of stimulating Scioto core using the in-situ HF generating fluids and the thermochemicals.	113

Figure 4.37	The behavior of the inlet-outlet pressures across the stimulated core while flowing the brine solution with different injection rates.....	114
Figure 4.38	A comparison between the core initial permeability and the permeability after acidizing using the in-situ HF generated with the thermochemicals.	115
Figure 4.39	The ICP analysis for the elements in the effluent produced after the treatment of the Scioto core with the in-situ generating HF fluids and the thermochemicals.	116
Figure 4.40	The NMR scan for the Scioto core before and after the stimulation process	117
Figure 4.41	The groove created along the whole length of the fresh Scioto core with the recorded rock strength in MPa before being acidized with the in-situ HF generating fluids and the thermochemicals,	119
Figure 4.42	The groove created along the whole length of the fresh Scioto core with the recorded rock strength in MPa after being acidized with the in-situ HF generating fluids and the thermochemicals,	119
Figure 4.43	The UCS values of the Scioto core measured in psi before and after being stimulated using the acid generating fluids along with the thermochemicals measured by the scratch test.....	120
Figure 4.44	The compression and shear waves' velocity of the Scioto core measured in m/s before and after being acidized with the in-situ HF generating fluids and the thermochemicals,.....	120

Figure 4.45 The dynamic Young's modulus of the Scioto core measured in ksi
before and after being acidized with the in-situ HF generating fluids
and the thermochemicals..... 121

Figure 4.46 The dynamic Poisson's ratio of the Scioto core before and after being
acidized with the in-situ HF generating fluids and the thermochemicals.. 121

LIST OF ABBREVIATIONS

β	The gravimetric dissolving power
χ	The volumetric dissolving power
r_A	The surface area-specific reaction rate of species A
R_A	The appearance rate of species A in (mole/sec)
S_B	The surface area of mineral B
E_f	The reaction rate constant
C_A	The concentration of reactant A in contact with the surface area
α	The order of the reaction
HPHT	High pressure high temperature
RHF	Retarded HF acids
PRHF	Phosphonic acid based retarded HF system
ALRHF	Aluminum chloride based retarded HF system
BRHF	Fluoboric acid based retarded HF system
BLPD	Barrels liquid per day
HACA	Hydroxethylaminocarboxylic
HEDTA	Hydroxyethylethylenediaminetriacetic acid
GLDA	Glutamic acid-N, N-diacetic acid

ABSTRACT

Full Name : Ibrahim Hassan Ali Gomaa
Thesis Title : Sandstone Acidizing Using In-Situ Generated Hydrofluoric Acid
Major Field : Petroleum Engineering
Date of Degree : December, 2019

In this research, a novel approach for generating in-situ hydrofluoric acid (HF) by oxidizing the ammonium fluoride (NH_4F) salt in the presence of exothermic reaction has been developed and used for sandstone acidizing. A sensitivity analysis of different oxidizers was carried out in order to choose the most suitable, compatible and safe one. Both sodium bromates (NaBrO_3) and ammonium persulfate ($(\text{NH}_4)_2\text{S}_2\text{O}_8$) showed promising results unlike potassium permanganates (KMnO_4) that showed compatibility issues with the other chemicals. The acid generating reaction is catalyzed by another exothermic reaction between the ammonium chloride (NH_4Cl) and sodium nitrite (NaNO_2). The mixture between the acid generating fluids and the thermochemicals could efficiently dissolve both silica and clay minerals which are the main constituents of sandstone formations.

Core flooding tests showed the high capability of the in-situ generating HF fluids to stimulate both Gray Berea and Scioto sandstone cores. After the injection of three successive cycles of the novel fluid mixture, the permeability of Gray Berea and Scioto cores were enhanced by about 40% and 37.5 % respectively. This was accompanied by the dissolution of various amounts of silica mineral from each core reached up to 49 mg in case of the 6-inch Scioto core. Moreover, the NMR scanning for both cores showed a

porosity enhancement after the acid treatment without affecting the original pore system connectivity. Scratch tests were carried out for the tested cores before and after the treatment in order to assess the effect of the treating fluid on the rocks' integrity and mechanical properties. The results of the scratch test showed that the mechanical response of the tested cores to the treating fluid is highly affected by the original composition of the cores.

Experiments done to check the effect of the pressure pulse from the used thermochemicals on the stimulation process showed a much higher permeability enhancement in the Scioto core than being treated with the acid generating fluids only. A pressure pulse of more than 2,000 psi was generated inside the core while being flooded for five successive cycles of the acid generating fluids and the thermochemicals simultaneously. This results in the generation of tiny micro fractures inside the core and enhanced its flowing capacity. NMR scanning came to confirm the generating of these micro fractures.

This method overcomes some of the persisting problems with sandstone stimulation. Upon application of this new stimulation technology, the true production potential of sandstone reservoirs can be achieved; corrosivity will be minimized and handling hazardous chemicals (HF) will be avoided. Importantly, controlling the reaction rate can also ensure deep acidizing penetration.

ملخص الرسالة

الاسم الكامل: إبراهيم حسن علي جمعه

عنوان الرسالة: المعالجة الحمضية للحجر الرملي باستخدام حمض الهيدروفلوريك المتولد في الموقع

التخصص: هندسة البترول

تاريخ الدرجة العلمية: نوفمبر 2019

في هذا البحث، لقد تم التوصل لطريقة جديدة لتوليد حمض الهيدروفلوريك عن طريق أكسدة أملاح فلوريد الأمونيوم في وجود تفاعل طارد للحرارة ليتم استخدامه في المعالجة الحمضية للحجر الرملي. وقد أجريت دراسة دقيقة لعوامل الأكسدة المستخدمة من أجل اختيار الأكثر ملائمة و الأكثر من حيث عوامل الأمان منهم. كلا من برومات الصوديوم و فوق كبريتات الأمونيوم قد أظهرتا نتائج واعدة علي عكس بيرمنجنات البوتاسيوم الذي أظهر عدم ملائمة مع المركبات الكيميائية الأخرى المستخدمة في هذه الدراسة. و قد تم تحفيز تفاعل توليد حمض الهيدروفلوريد باستخدام تفاعل طارد للحرارة بين كلوريد الأمونيوم و نيتريت الصوديوم. و لقد أثبت هذا الخليط الكيميائي الجديد قدرته علي إذابة معادن السيليكا و الطمي المختلفة و التي تعد المكون الرئيسي لطبقات الحجر الرملي.

و قد اثبتت تجارب الحقن قدرة حمض الهيدروفلوريد المتولد داخل الصخر علي تحسين نفاذية عينات كل من Scioto و Gray Berea بعد حقن ثلاث دورات متتالية من الخليط الكيميائي بنسبة 40% و 37.5% علي الترتيب. و قد صاحب هذا نوبان كميات مختلفة من السيليكا وصلت إلي 49 مجم في حالة عينة من صخر ال Scioto ذات ال 6 بوصات. علاوة علي ذلك فإن مسح الرنين المغناطيسي النووي NMR للعينات قد أظهر تحسن ملموس في المسامية بدون الإضرار بقنوات الأتصال الأصلية بين المسام. و قد أظهرت اختبارات خدش العينات قبل و بعد المعالجة أن تأثير الخصائص الميكانيكية للعينات تتأثر تأثيراً كبيراً بالتكوين الأساسي لكل عينة.

و قد أظهرت التجارب التي أجريت من أجل اختبار تأثير دفعة الضغط الناتجة من الكيماويات الحرارية تحسنا كبيرا في نفاذية عينات صخر ال Scioto بعد معالجتها بخمس دورات متتالية من الخليط الكيميائي. فقد نتج عن ذلك ضغط كبير وصلت قيمته ل 2000 رطل/بوصة مربعة. الأمر الذي ترتب عليه خلق كسور دقيقة بداخل العينة مما أدى إلي تحسين قدرة التدفق لديها. و قد جاء مسح الرنين المغناطيسي النووي NMR للعينة ليثبت وجود هذه الكسور.

هذا و قد أثبتت هذه الطريقة الجديدة قدرتها علي تخطي المشكلات المتأصلة في مجال تحسن إنتاجية الحجر الرملي. و أنه فور تطبيق هذه الطريقة فسوف يتم استعادة القدرة الإنتاجية لخزانات الحجر الرملي بالإضافة إلي تقليل مشاكل التآكل و التعامل مع المواد الكيماوية الخطرة. و الأكثر أهمية من ذلك هو التحكم الكبير في معدلات التفاعل و إنتاج الحمض مما يحقق العمق المرجو من عملية المعالجة الحمضية.

CHAPTER 1

INTRODUCTION

1.1 Sandstone Formation Damage and Treatment

The term “formation damage” refers to the decrease in the formation permeability by different improper activities. Operationally and economically, formation damage is considered an undesirable problem that is expected to take place at any stage of the reservoir life (Civan, 2005). As expressed by Amaefule et al. (1988), “Formation damage is an expensive headache to the oil and gas industry.” Bennion (1999) described formation damage as, “The impairment of the invisible, by the inevitable and uncontrollable, resulting in an indeterminate reduction of the unquantifiable!”

Sandstone formation damage can occur at various phases of the hydrocarbon recovery from the reservoir. Different processes such as drilling, completion, stimulation and enhanced oil recovery can introduce damage to the proposed formation. Formation damage during drilling activities is attributed mainly to the invasion of drilling fluids to the adjacent reservoir area. This type of damage depends mainly on the drilling mode whether it is underbalanced or overbalanced drilling and the differential pressure applied to the formation. Formation pore size distribution and drilling fluid particles size and distribution play an important role in this process as well (Li et al., 2017). It has been reported that the formation damage due to the invasion of drilling particles is as high as 10% for some laboratory study. This percentage is expected to be higher for the field applications especially for high porous and permeable zones where the depth of particles invasion is high.

Cementing operations can cause formation damage by forming calcium silicate hydrate as a result of reacting the high pH cement slurry with the silica particles in sandstone formation. In addition, the precipitation of the insoluble salts such as calcium carbonate (CaCO_3) and calcium sulfate (CaSO_4) during the cementation stage is considered a main source of damage (Yang and Sharma, 1991).

Plugging the near wellbore area with formation fines, inorganic and organic scales leads to a rapid production decline and severe formation damage. Asphalts and waxes are the major organic deposits that harm formation permeability (Kamal et al. 2019).

The process of enhanced oil recovery using polymer and/or surfactant can harm the reservoir original permeability. This is because of the adsorption and retention of these chemical particles on the rock surface (Yu et al., 2011). The same damage mechanism occurs when using the viscoelastic surfactants and polymers in activities such as drilling and completion. The retention and adsorption of these chemical particles plug in the rock pore throats and decrease its permeability (Audibert et al., 1999).

The minerals present in the sandstone rocks such as sand, clays, oxides, carbonates and zeolite can interact with the injected fluids and form a formation damage problem (Mahmoud et al. 2015). The most critical content of the sandstone rock are the clay minerals that can interact with the injected water or HCl and result in dissolution, precipitation, clay swelling, pore throat plugging and fines migration (Kamal et al., 2019; Al-Yaseri et al., 2015; Clarke, 2014).

All the previously mentioned cases of sandstone formation damage can be summarized in the following schematic, Figure (1.1), after (Radwan et al., 2019). The damage is

classified to mainly natural damage that is caused by the natural production of reservoir fluids and induced damage that is caused by any external operation carried on the well. The main focus of this research will be on those natural damage types related to the presence of clay minerals such as fines migration and clay swelling problems.

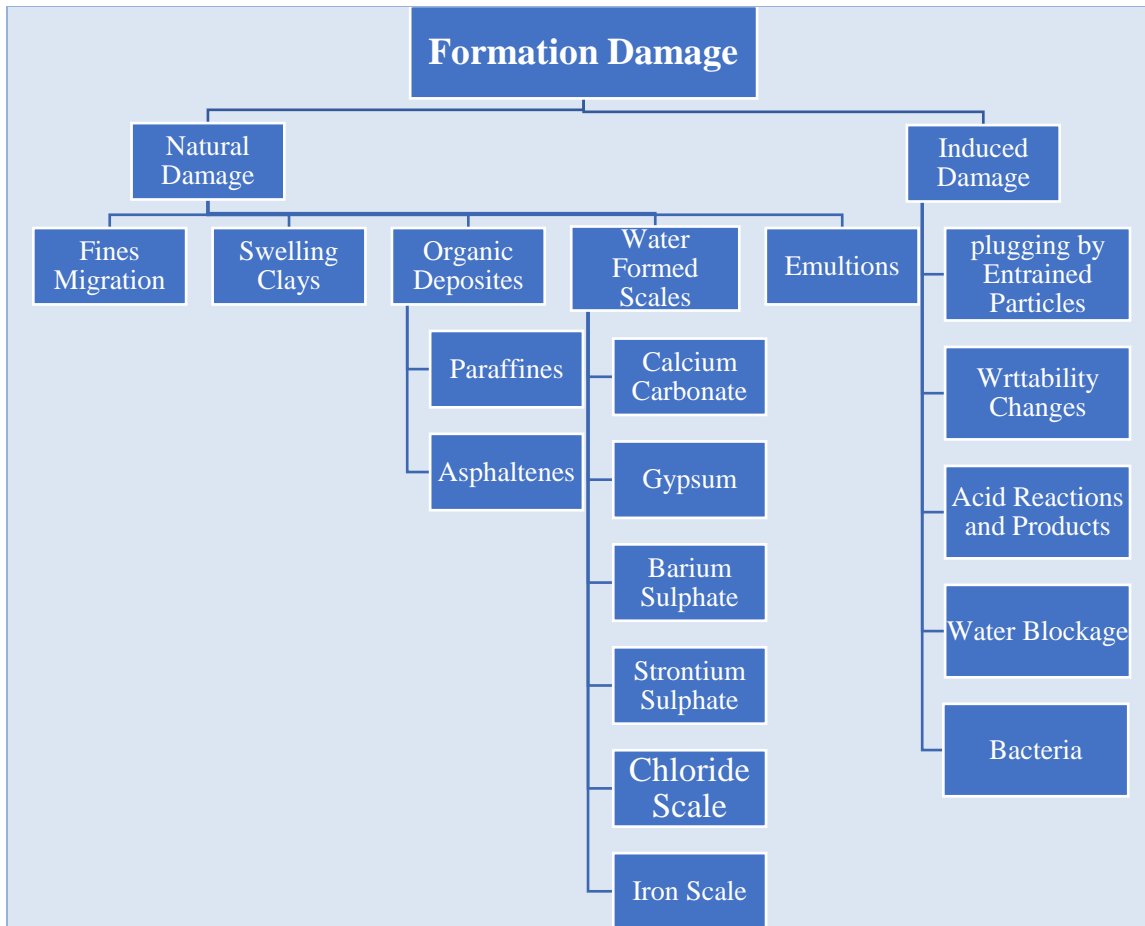


Figure 1.1 Formation damage classifications (Radwan et al., 2019).

Formation acidizing and hydraulic fracturing are both two common solutions to mitigate the formation damage problem. The hydraulic fracturing process aims to bypass the damaged zone around the wellbore by creating a high permeability path within the reservoir that is connected to the well (Economides, 1987). Till now, hydraulic fracture still represents the greater sector of formation stimulation activities.

On the other hand, acidizing treatment aims generally to enhance the well productivity by either dissolving the formation rock itself or removing the well induced damage (Vogt and Anderson, 1974; McLeod, 1984; Hongjie, 1994; Zou et al., 2014; Zakaria et al., 2015). Figure (1.2) illustrates the streamlines of the acid flow through the rock pore spaces. Acid treatment was initially used to stimulate carbonate reservoirs by dissolving the rock matrix. However, with the industry development, special types of acid were evolved to treat sandstone reservoirs from the damage occurs during drilling, completion or even production period (Coulter et al., 1987).

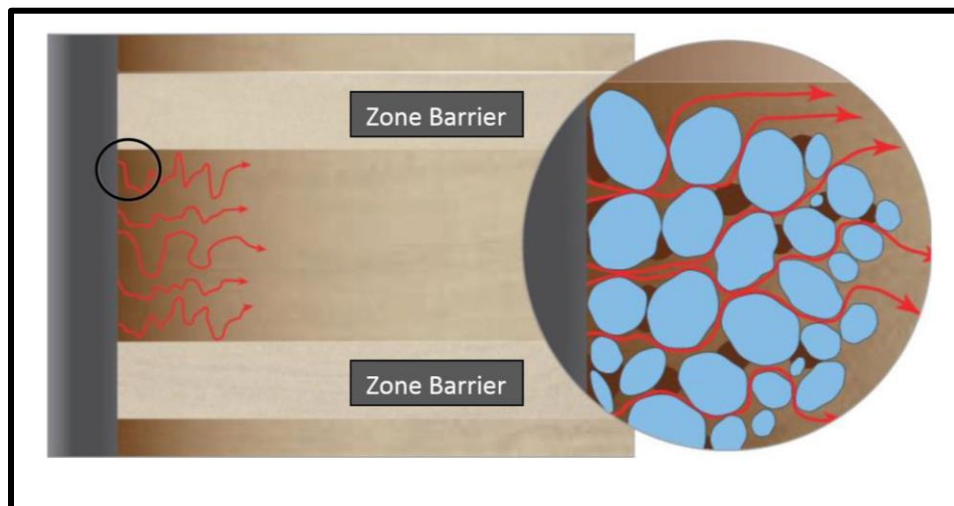


Figure 1.2 The acid streamlines while passing through the pore spaces during the acidizing process (Davies and Kelkar, 2007).

Sandstone matrix acidizing, where the acid is injected at a pressure lower than the formation fracture pressure and reacts near the wellbore area, can reach as deep as only one foot (Leong and Ben Mahmud, 2019). The main goal of sandstone acidizing is not to influence a large deep portion of the reservoir but to highly improve or restore the near wellbore permeability (Kalfayan, 2008 and Economides et al., 2013). Sandstone formations are therefore commonly stimulated using hydrofluoric-acid-based (HF) systems, which may also be blended with strong mineral acids, organic acids, esters and combinations of them (Kume et al., 1999).

The decision of going for formation fracturing or acidizing should be based on technical and economic factors such as the production history, the formation geology and the well-intervention objectives (Al-Harthy et al., 2009). The high-intensive hydraulic fracturing activities are recommended for tight formations with low porosity and permeability. Whereas, a lower-intensive fracturing can be applied to formations with relatively high porosity and permeability. In all cases, formation permeability is considered to be one of the controlling factors that should be carefully considered before performing hydraulic fracturing (Holman, 1982). Loose formations with weak bonds between their grains are not recommended to be hydraulically fractured to avoid formation collapsing. In such cases, going for matrix acidizing is considered to be a better choice. Moreover, the damage results from drilling and production activities is better to be removed by acid treatment rather than going for hydraulic fracturing (Houseworth, 2014). The different well stimulation techniques are shown in Figure (1.3).

Since acid stimulation has a low penetration depth in sandstone formations, it is not recommended to use it with low permeability formations that require deep acid penetration for successful treatment. However, sandstone acidizing is much more suitable for naturally fractured wells that have been damaged by the drilling, completion or production activities. Hence, the function of the stimulation process is to remove the near wellbore damage by dissolving the plugging minerals and retrieve/enhance the well permeability (Economides et al., 2013).

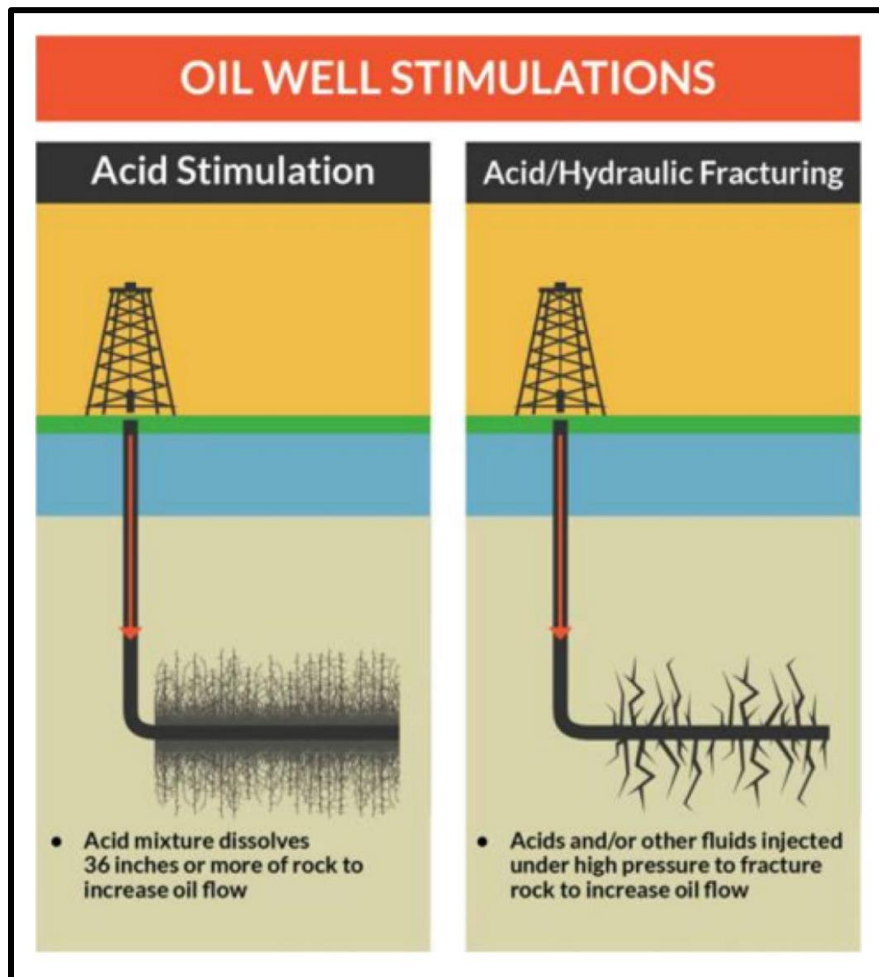


Figure 1.3 A graphical illustration of the different oil well stimulation techniques (Leong and Ben Mahmud, 2019).

1.2 Problem Statement

Sandstone formations are mainly stimulated using hydrofluoric acid-based fluid mixtures. The most common technique is to use a mixture of HF-HCl acids (mud acid) with a specified concentration. However, the reaction of mud acid with sandstone formations is considered to be very fast reaction and the acid is spent quickly before reaching the proper depth. Fines migration would probably occur after mud acid treatment and restore the formation damage. The reaction of HF with silicate minerals exist in sandstone produces fluosilic acid that reacts with the different cations present in the formation and produces precipitates such as CaSiF_6 , Na_2SiF_6 , and K_2SiF_6 .

In addition to the reservoir problems caused by the use of conventional HF acid, surface handling of the stimulating chemicals is very risky to the working crew as well as to the used equipment. Both HF and HCl acids are highly corrosive and require high safety precautions to deal with.

It has been reported that high risk of formation damage is associated with sandstone acidizing and could reach to 80% as shown in Table (1.1) (Byrn, 2009). This percentage is considered so high for a process supposed to remove the damage not to increase it. However, the problem even is more sever when trying to remove this damage resulted from the stimulation treatment as it comes as a late stage in the well life. This gives the damage during this stage the highest importance value of 80 for the risk assessment matrix. Accordingly, one can clearly observe how complicated and sensitive the sandstone stimulation process is.

Although there are so many trials done already to replace and overcome the drawbacks of the conventional mud acid treatment. There is still no method that is completely efficient and risk-free to be used for sandstone acidizing formation. The objective of this research is to achieve this goal throughout designing a novel way for generating in-situ HF acid using environmentally friendly chemicals to overcome the previously stated problems.

Table 1.1 Damage risk assessment matrix for wells drilled in sandstone formations (Byrn, 2009).

Operation	% of total damage	Impact / removable? (1-5)	Importance
Drilling	25	2	50
Completion	25	3	75
Attempted Stimulation	20	4	80
Production	15	3	45
Well Intervention	5	4	40
Injection	10	2	20

1.3 Thesis Objectives

There are so many trials that were carried out to enhance the sandstone formations permeability and remove the different types of damage attached to them as it will be shown in the literature review part. However, all these methods suffer from one or more drawbacks as stated before. The objectives of this work are;

- Generating in-situ hydrofluoric acid (HF) using a combination of thermochemical reaction and an acid precursor (ammonium fluoride NH_4F). The acid precursor will react with a suitable oxidizer in the presence of an exothermic reaction to generate HF in the wellbore.
- Testing different oxidizers such as sodium bromate (NaBrO_3), ammonium persulfate ($\text{NH}_4)_2\text{S}_2\text{O}_8$) and potassium permanganate (KMnO_4) and identifying the best one regarding the reaction kinetics, the amount of HF generated, the byproducts resulted and the economic feasibility.
- Evaluating the effect of pH and temperature on the reactions triggering mechanisms. The two triggering mechanisms will be evaluated in terms of efficiency, generated heat and pressure, the reaction products and the effect of the whole stimulation process.
- Investigating the effect of the pressure pulse generated from the exothermic reaction on the stimulation results.
- Applying the HF generating reaction on pure clay minerals.
- Applying the acid generating reaction by the aid of external temperature sources other than the exothermic reaction.

- Carrying out a sensitivity analysis on different sandstone core types with different clay content, e.g. Berea and Scioto sandstone, using core flooding experiments. The core flooding effluent will be analyzed using inductive coupled plasma - optical emission spectroscopy (ICP-OES) technique.
- Evaluating different soaking times and cycles with core stimulation in order to determine the optimum soaking conditions.
- Checking the effect of the HF- silica tertiary reaction products on the core structure and properties.
- Examining the effect of the new chemical mixture on rock integrity by carrying out a scratch test on the core samples. In addition, the NMR technique will be used to check the effect of the stimulation process on the pore structure.

1.4 Thesis Description

This thesis comes in five main chapters. The description of each chapter is as following;

Chapter 1: represents a brief introduction to the area of this research. It covers the definition and types of formation damage. Then, it spots the light on the problem related to the sandstone stimulation process. Finally, it states the main objectives of this work.

Chapter 2: literature review for sandstone stimulation techniques is discussed in this chapter. So many techniques of sandstone stimulation have been utilized in the petroleum industry. The concept, procedures, advantages and disadvantages of each technique are discussed intensively. Finally, a brief literature review about the ammonium fluoride salt oxidation technique and the application of thermochemicals in the oil industry are discussed at the end of this chapter.

Chapter 3: at the beginning of this chapter, the novelty of this research is discussed. Then, the methodology followed for achieving the research objectives is stated clearly in detail. All the used equipment is shown with a brief description of each one.

Chapter 4: this chapter contains all the results of this work. A detailed discussion with the supporting graphs, charts and Tables are shown in this chapter. The results shown in this chapter are correlated to the thesis objectives and methodology.

Chapter 5: contains the final conclusions of this study and the recommendations that should be kept into consideration while applying the results from this research. Additionally, it contains a future work plan to enhance this research even more.

CHAPTER 2

LITERATURE REVIEW

2.1 Mud Acid Treatment

Hydrofluoric acid (HF) or one of its precursors is being heavily used to stimulate sandstone formations after the discovery of HF in the early 1990s. Hydrofluoric acid reaction with sandstone formation particles is considered to be an exceptional reaction. Unlike hydrochloric, sulfuric and nitric acids, hydrofluoric acid with the fluoride ion (F^-) can effectively react with the silica and clay particles. The reaction of HF with the silicates (quartz) minerals can be described in Eq. 2.1 (Smith and Hendrickson, 1965). Figure (2.1) shows the pore structure of the typical sandstone rocks. Quartz is the most dominant element represented in the rock grains. The pore-filling and pore-lining clays can be found among the quartz grains. Carbonates and feldspars can exist as a cement material or within the rock grains. Table (2.1) shows the different minerals that may present in sandstone formations and the corresponding solubility of each mineral in both HCl and HF. It is clear that almost all the sandstone constituents are soluble in mud acid to different extents.



The first trial of sandstone formation acidizing using a mixture of HCl and HF acids was run by Halliburton in 1933 in Texas. Unexpectedly, the results were disappointing and discouraging. After that, in 1939, a mixture of 12% HCl – 3% HF was introduced under the name of “mud acid” or “regular strength mud acid” and it gave promising results once pumped downhole (Portier et al., 2007).

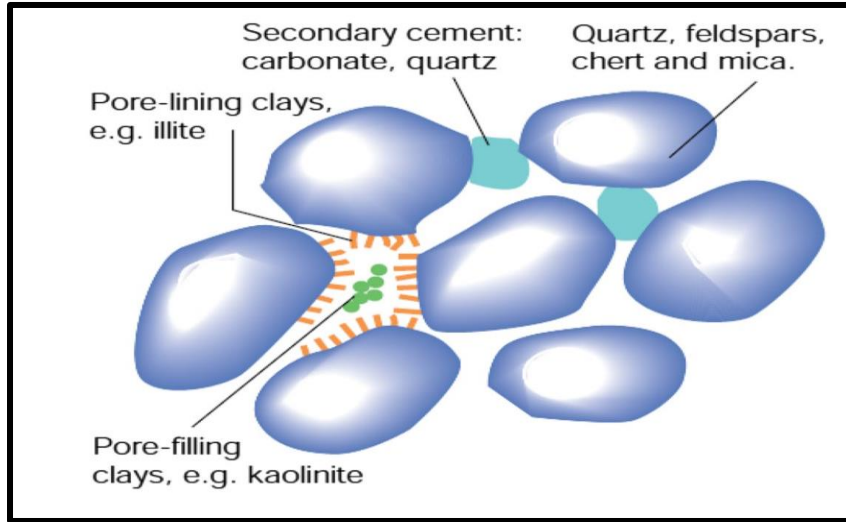


Figure 2.1 The pore structure and mineral constituents of typical sandstone rock (Crowe et al., 1992)

Table 2.1 The solubility of different sandstone mineral constituents in mud acid (Portier et al., 2007)

Minerals	Solubility	
	HCl	HCl-HF
Quartz	Low	Very low
Feldspars	Low	Low to moderate
Mica	Low	Low to moderate
Kaolinite	Low	High
Illite	Low	High
Smectite	Low	High
Chlorite	Low to moderate	High
Calcite	High	High but produces CaF ₂ ppt.
Dolomite	High	High
Ankerite	High	High
Siderite	High	High

2.1.1 Reservoir Problems Associated with Conventional Mud Acid

Treatment

Since silica is the main mineral constituent of sandstone, its reaction with HF at low temperatures occurs at low rate (Al-Dahlan et al. 2001). On the other hand, aluminosilicates such as clays and feldspars react rapidly with mud acid throughout a three-stage reaction to produce some insoluble precipitates. The primary reaction of HF acid with the aluminum silicates is shown in Eq. (2.2) (McCune et al. 1975; Hill et al. 1981; Ying-Hsiao et al. 1998).



Then the produced fluosilic acid reacts with different aluminosilicates such as potassium feldspars throughout a secondary reaction as shown in Eq. (2.3). It was concluded by Bryant (1991) and da Motta et al., (1992) that the reaction rate of fluosilicic acid with clays and feldspars is slow at room temperature. However, it reaches as fast as the rate of the HF acid reaction with these minerals at temperature greater than 50°C.



After that, the ratio of fluorine (F)/aluminum (Al) ions continues to decrease in the aluminum fluoride compounds due to their reaction with aluminosilicates compounds in the presence of HCl. This tertiary reaction chelates the aluminum ions from the aluminosilicates leaving silica gel as a precipitate, Eq. (2.4).

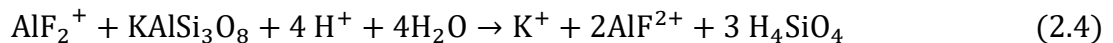


Figure (2.2) represents the occurrence of the previous three stages of the reaction of sandstone rock minerals with conventional mud acid along the offset distance from the well into the reservoir. The primary stage near the wellbore where the aluminum and silica fluorides are produced. The secondary stage where the primary products go under slow reaction to form silica gel which pre precipitates in the reservoir. Further away from the well, a tertiary reaction takes place where more precipitating silica gel is produced, (Al-Harthy et al., 2009). This gives an indication of the failure potential of the sandstone stimulation process with conventional mud acid.

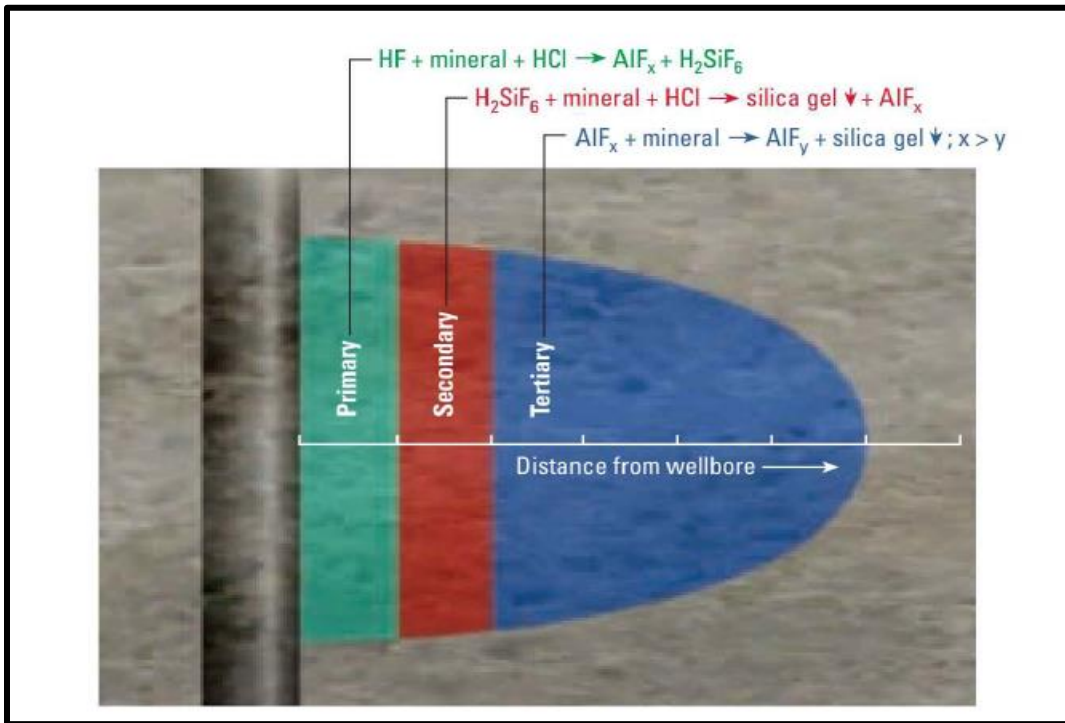


Figure 2.2 The three stages of the reaction of mud acid with sandstone matrix, adopted from Al-Harthy et al., (2009).

Labrid (1975) studied the thermodynamics and kinetics of sandstone acidizing and concluded that colloidal silica (Si(OH)_2) along with fluosilicic acid (H_2SiF_6) are the main products of mineral solubilization by HF. The precipitation of colloidal silica has been proven through several acidizing models and core flooding experiments. The precipitation of silica comes after the reduction of fluorine concentration and the higher ability of the aluminum ions to attract the rest of it leaving the silica to precipitate.

The reaction of mud acid with sandstone formations is considered to be a very fast reaction. Once the acid mixture is injected, it reacts quickly with the near formation area and is spent rapidly. This makes the depth of acid penetration into the formation so small. As a result, fines migrate to the near wellbore area would plug the formation and restore the damage. This makes the production improvements after conventional acid treatment of sandstone formations containing clay minerals to be short-lived (Cheung and Van Arsdale, 1992; Chang et al. 2000).

The reaction of fluosilicic acid (which is the product of HF reaction with silicates) with cations present in the formation brine produces precipitants such as CaSiF_6 , Na_2SiF_6 , and K_2SiF_6 is described by Eqs. (2.5-2.7) (Al-Shaalan and Nasr-El-Din, 2000; Mahmoud et al., 2015).



Gidley (1985) did not recommend the mud acid to be used for stimulating high temperature wells. He stated that the acid efficiency, stability and corrosion rates need to be improved while using mud acid under temperature greater than 200 °F. The problems associated with using mud acid at elevated temperatures are various. The rate of the reaction of mud acid with sandstone minerals at temperature above 200 °F is very fast. This leads the acid to be consumed too early. As a result, the efficiency of the acidizing process drops down and the whole job may fail (Shuchart and Gdanski, 1996; Al-Dahlan et al., 2001; and Al-Harthy et al., 2009).

The acid reaction front is the area where the acid-minerals interactions take place. This area moves radially as long as there is an active acid injected into the formation. As long as the acid proceeds within the area where all the acid soluble minerals have been dissolved, the acid maintains its full strength. The radial extent of the acidized area depends mainly on the formation mineralogy and the reservoir temperature changes. After the acid is totally spent, it transports within the unreacted matrix. The contact between the spent acid and the same matrix is the main reason for the secondary and tertiary reactions that produce different precipitates. This is why it is of high importance to keep the injected acid moving forward to carry out the reaction products far away the critical region around the wellbore (Portier et al., 2007).

2.1.2 Conventional Mud Acid Treatment Stages

The proper design for the sandstone acidizing process can increase the job efficiency and decrease the negative drawbacks associated with such treatment. Hereunder, some stated recommendations that better to be taken as a basis for the design of different sandstone acidizing stages. These guidelines should not be taken as solid rules rather than used as initial design steps. As mentioned by Sutton and Lasater (1972) and Gidley et al. (1996), sandstone acidizing process using mud acid comes in three main phases. The first stage is called a preflush in which the main purpose is to dissolve the formation carbonates and evict the inhabitant salt water using an acid such as HCl. The second stage or the mud acid stage which comprises mainly of HCl and HF acids. The main purpose of this stage is to get rid of all the near wellbore materials that thought to be restricting the production such as clays and feldspars. Finally, the after flush or post flush stage which aims at pushing the mud acid stage further into the reservoir and wash out the byproducts resulted from the previous reactions. The chemicals used in this final stage can vary between hydrochloric acid (HCl), ammonium chloride (NH₄Cl) or even a pure hydrocarbon solvent like diesel oil. Hereunder, a detailed description of each stage of the conventional mud acid stimulation process.

2.1.2.1 The Preflush Stage

Usually, in sandstone stimulation process using mud acid, a preflush fluid is pumped ahead of the main acid flush. This is stage is of great benefit for the main acid treatment. A proper preflush fluid highly affects the success of the acidizing process. As stated by Hill et al., (1981 &1994) and Zeit (2005), the main functions of the preflush stage are to;

- Treat multiple damage mechanisms that may result from the use of mud acid directly with the sandstone formations.
- Condition the rock surface for the main acid treatment.
- Eject the formation water away from the HF acid to avoid the precipitation reaction with the formation brine ions such as K, Na and Ca. This prevents the formation of alkali-fluosilicates such as $CaSiF_6$, Na_2SiF_6 and K_2SiF_6 .
- React with the calcareous materials that exist within the sandstone formation. The dissolution of these materials enhances the rock permeability and leave the quartz surface clear for the HF acid to dissolve. Moreover, this prevents the formation of the calcium fluoride precipitate as a result of the reaction of HF with the calcite mineral.
- Establish good injectivity before the mud acid is pumped.

The most common used preflush fluid for mud acid treatment is HCl acid. Besides all the previously stated objectives of the preflush stage, strong HCl can leach iron, aluminum and magnesium ions from chlorite clays. Chlorite clay is a three-layer clay with high content of iron. In addition, HCl can shrink the hydrated clays present in sandstone formations (McLeod, 1984; Economides and Nolte, 1987).

Ammonium chloride (NH_4Cl) is used as a preflush fluid in some cases. The injected solution of the NH_4Cl can remove the formation brine away from the well vicinity and condition the existing clays. The ammonium ions NH_4^+ have the capability to exchange with and displace the alkali-ions (K, Na and Ca) away from the mud acid. Using

ammonium chloride (NH₄Cl) prior to injecting the main mud acid is an emerging technique and not a part of the conventional treatment process (Portier et al.,2007).

McLeod (1984 &1989) conducted extensive lab experiments and established the main guidelines for the HCl acid concentration used in the preflush stage. These guidelines are then modified by McLeod and Norman (2000) to be the initial step for most of the preflush acid design. These guidelines are mentioned in Table (2.2) where a 10 % cut-off of clay and silt content was taken as main mineralogy threshold. They also categorized the sandstone formations based on three permeability ranges; greater than 100 mD, 20-100 mD and less than 20 mD.

Table 2.2 The selection criteria of the preflush acid used for mud acid treatment after (McLeod and Norman, 2000)

Preflush Fluids			
Mineralogy	Permeability		
	> 100 md	20 -100 md	< 20 md
< 10% silt and <10% clay	15% HCl	10% HCl	7.5 % HCl
> 10% silt and >10% clay	10% HCl	7.5 % HCl	5 % HCl
> 10% silt and < 10% clay	10% HCl	7.5 % HCl	5 % HCl
< 10 silt and >10% clay	10% HCl	7.5 % HCl	5 % HCl

2.1.2.2 The Main Flush Stage

This stage aims at removing the damage and enhance the sandstone formation permeability. The fluid used at this stage is typically a mixture of hydrofluoric (HF) and hydrochloric (HCl) acid. In some cases, organic acids are added to the mud acid mixture. Despite its various hazards, HF is commonly used to treat the sandstone formations. This is because of its high ability to dissolve the siliceous materials present in the sandstone formations. Unlike hydrochloric, sulfuric and nitric acids, hydrofluoric acid with the fluoride ion (F^-) can effectively react with the silica and clay particles. Table (2.1) shows the different minerals that commonly exist in sandstone and the ability of both HF and HCl to dissolve them. It is obvious that HF is capable of dissolving the quartz, feldspars and clay minerals present in sandstone unlike HCl. Moreover, HF is quite abundant and inexpensive.

HCl or organic acid is blended with HF to keep the medium pH low after the HF is spent. This prevents some precipitation reactions. The mixture of HF and HCl is called mud acid because it is initially used to remove the siliceous drilling mud deposited on wellbore walls. McLeod (1984) and Crowe et al., (1992) stated a cut off of 20% of calcite content above which HF is not recommended to treat sandstone formations. The reaction of HF with calcite mineral produces a white precipitate of calcium fluoride. Therefore, it is recommended to use HCl only as the main treating fluid to avoid the undesired precipitates. Table (2.3), after (McLeod, 1984 and Crowe et al., 1992), shows the basic guidelines for the main flush acid mixture based on the formation permeability and the different mineral content.

Table 2.3 The basic design guidelines for the main flush stage after (McLeod, 1984 and Crowe et al., 1992)

Condition	Main Acid	Preflush
HCl solubility (>20%)	Use HCl only	
High permeability (>100 md)		
High quartz (80%), low clay (<5%)	12% HCl, 3% HF	15% HCl
High feldspars (>20%)	13.5% HCl, 1.5 HF	15% HCl
High clay (>10%)	6.5% HCl, 1% HF	Sequestered 5% HCl
High iron chloride clay	3% HCl, 0.5% HF	Sequestered 5% HCl
Low permeability (<10 md)		
Low clay (<5%)	6% HCl, 1.5% HF	7.5 HCl or 10% acetic acid.
High chlorite	3% HCl, 0.5 % HF	5% acetic acid.

The reaction rate of HF acid with the formation clays and feldspars is about 100 to 200 times higher than its reaction rate with silica. This is attributed to the mineral characteristic of quartz that has a more stable structure and comparatively low specific surface area (Leong and Ben Mahmud, 2019). There is a high-risk potential for different precipitation reactions to take place and produce silicon and aluminum insoluble compounds such as SiF_6^{2-} , AlF^{2+} , AlF_2^+ , AlF_3 and AlF_4^- . This may restore the formation damage and plug the stimulated area (Portier et al., 2007).

In a trial to modify the basic design guidelines for the main mud acid flush, Portier et al. (2007) suggested different outlines based on the well conditions as shown in Table (2.4).

Table 2.4 The modified guidelines for mud acid main flush after (Portier et al., 2007)

Well and reservoir conditions	Recommended treatment
Bottomhole treating temperature > 100°C	1.5% HF + 13.5% HCl
Permeability <5 md	1.5% HF + 13.5% HCl
Quartz content:	
• >90%	3% HF + 12% HCl
• 50-90 %	3% HF + 12% HCl or retarded HF
Feldspars, 15- 30%	1.5% HF + 13.5% HCl
Chlorite clay:	
• 1-5 %	3% HF + 10% acetic acid
• >5%	1.5% HF + 10% acetic or formic acid

2.1.2.3 The Post flush Stage

The stage of post flush has a critical role in the success of the whole acid treatment process. The injected post flush fluid must be capable of;

- Pushing the unspent acid deeper into the formation, a minimum distance of 0.9 m, to achieve higher penetration depth.
- Displacing the undesired products of the main flush stage away from the critical area around the wellbore.
- Retrieving the formation original wettability that may change due to the injection of corrosion inhibitors (Nasr-El-Din et al. 2005).

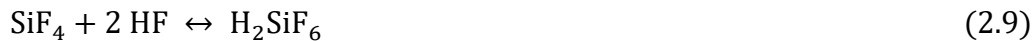
It is recommended to use HCl or acetic acid in the front part of the post flush fluid in order to maintain a low pH into the formation. The volume of the post flush slug should be minimum as twice as the volume of the main acid. This depends on the formation permeability anisotropy that may lead to double or triple this amount of post flush fluids. The produced amorphous silica that results from the reaction of mud acid with sandstone formation can be diluted and transported beyond the critical matrix zone by the post flush fluid. On the other hand, if the volume of the over flush slug is not appropriate, these amorphous silica compound turns to unmovable gel and plug the formation (Portier et al., 2007).

2.2 Mud Acid-Sandstone Reaction Stoichiometry

Reaction stoichiometry helps to determine the amount of acid needed to dissolve a specific amount of mineral based on the balanced chemical reaction between them. In the case of HCl, which is a main constituent of the mud acid, the reaction with the calcite mineral is very simple as described by Eq. (2.8).



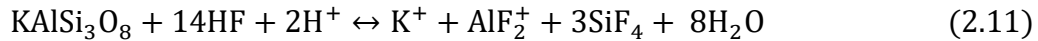
The reaction of hydrochloric acid with calcite is a one-step simple reaction that requires two moles of HCl to dissolve one mole of calcite. On the other hand, the reaction of hydrofluoric acid with silicate minerals is quite complicated. Nevertheless, this situation is much more complicated on the case of HF reactions with different clays and feldspars. Recalling Eq. (2.1) that shows the primary reaction of hydrofluoric acid with silicate, the reaction stoichiometry shows that four moles of HF are required to dissolve only one mole of silicate (SiO_2). However, the produced silicon tetrafluoride (SiF_4) may react with HF in a reversible reaction to produce fluosilicic acid (H_2SiF_6) according to Eq. (2.9).



This reaction shows that six moles not only four of HF are required to dissolve one mole of quartz (Bryant, 1991).

In case of the reaction of HF with feldspars, the number of moles of HF required to dissolve one mole of Albite (sodium feldspars) or Orthoclase (potassium feldspars) can reach as high as 14 moles as shown in Eqs. (2.10 & 2.11), respectively. Moreover,

Schechter (1992) shows that in typical acidizing conditions, about 20 moles of HF are required to dissolve only one mole of feldspars.



The presence of clay minerals in sandstone formations makes it more complicated while calculating the reactions stoichiometry. Each type of clay requires specific number of moles of HF to react with. This number can reach as high as 40 moles as in the case of montmorillonite clay, see Eq. (2.12).



Both the secondary and tertiary reactions of mud acid with the alumino-silicates (mainly clays and feldspars) exist in sandstone formation can severely affect the reaction stoichiometry (Hartman et al., 2006). As illustrated above, the products of these reactions are mainly precipitated amorphous silica.

The gravimetric dissolving power (β) and the volumetric dissolving power (χ) are both two techniques used to express the reaction stoichiometry introduced by (Willimas et al., 1979). Gravimetric dissolving power (β) can be defined as the mass of the mineral that can be dissolved using a specific mass of the acid. It can be calculated by Eq. (2.13). The volumetric dissolving power is defined as the volume of the mineral dissolved by a specific volume of the acid. It is related to the gravimetric dissolving power by the following relation, Eq. (2.14).

$$\beta = \frac{\mathcal{V}_{\text{mineral}} MW_{\text{mineral}}}{\mathcal{V}_{\text{acid}} MW_{\text{acid}}} \quad (2.13)$$

$$\chi = \beta \frac{\rho_{\text{acid solution}}}{\rho_{\text{mineral}}} \quad (2.14)$$

Where $\mathcal{V}_{\text{mineral}}$ and $\mathcal{V}_{\text{acid}}$ are the reaction coefficients of both the mineral and the acid respectively. MW is the molecular weight of the indicated species.

The following Table (2.5) shows both the gravimetric and volumetric dissolving powers of HF acid with both quartz and sodium feldspars (Albite) at different concentrations of the acid, modified after (Economides et al., 2013).

Table 2.5 The dissolving power of HF acid at different concentrations with both Quartz and Albite, (Schechter, 1992)

Acid Concentration (wt%)	Quartz (SiO ₂)		Albite (NaAlSi ₃ O ₈)	
	β	χ	β	χ
2	0.015	0.006	0.019	0.008
3	0.023	0.010	0.028	0.011
4	0.030	0.018	0.037	0.015
6	0.045	0.019	0.056	0.023
8	0.060	0.025	0.075	0.030

2.3 Mud Acid-Sandstone Reaction Kinetics

The term reaction kinetics refers to the rate at which the reaction takes place. The reaction between the acid and the target formations occurs once the acid reaches the mineral surface whether by diffusion or convection. The acid-mineral reactions are termed as “heterogeneous” reactions as they occur between two between aqueous phase (the acid) and solid phase (the rock). The rate of acid-mineral reactions depends mainly on two factors: (1) the rate of acid transportation to the mineral surface by diffusion or convection, and (2) the actual chemical reaction rate on the mineral surface. For HF-sandstone reactions, the surface reaction rates are slower than the rate of acid transport rate. Therefore, the overall HF-Sandstone reactions are controlled by the reaction rate between the acid-mineral surface not the acid transport rate.

Steinfeld et al., (1999) defined the chemical reaction rate as the change in the reactants or the products concentration with time. Another definition of the reaction rate is the ratio of the rate of appearance of a specific species in units of (mole/sec) to the area of the surface exposed to the reaction in units of (m^2) as expressed by Eq. (2.15).

$$r_A = \frac{R_A}{S_B} \rightarrow R_A = r_A S_B \quad (2.15)$$

Where r_A is the surface area-specific reaction rate of species A in (moles/sec- m^2), R_A is the appearance rate of species A in (mole/sec) and S_B is the surface area of mineral B in (m^2).

In case of the fluid-fluid reactions, the reaction rate, r_A , depends on the concentrations of fluid species. However, in the case of the fluid-solid reactions, the solids concentration

is ignored for remaining constant. Involving this concept with the rate expression results the following Eq. (2.16)

$$-R_A = E_f C_A^\alpha S_B \quad (2.16)$$

Where E_f is the reaction rate constant in moles A/ [m² – sec – (moles A/ m³)^α], C_A is the concentration of reactant A in contact with the surface area and α is the order of the reaction.

α is considered an indication about how strongly the reaction depends on the concentration of reactant A. The reaction rate constant, E_f , does not depend only on the concentration of species A, but it also depends on the medium temperature and the concentration of the other chemical species that may be involved into the reaction.

Fogler et al., (1976) and Taylor and Nasr-El-Din (2009) stated two well-known methods used to measure the acid-mineral reaction kinetics. The first one is to use a well-stirred slurry of the specified mineral particles suspended in the acid solution. The other one is to use a rotating-disk apparatus in which a disk of the specified mineral is placed in a large container holding the acid solution. A third indirect method used to measure the acid-mineral reaction kinetics is to match the core flooding results with a model of the whole acidizing process (Economides et al. 2013).

2.4 The Problems of Stimulating High Clay Content Sandstone Formations using Mud Acid

The term “clay” refers to the different types of crystalline minerals formed mainly from hydrous aluminum silicates (El-Aouar, 1962). Guggenheim and Martin (1995) defined ‘clay’ as a naturally existing material formed initially from fine-grained minerals which is generally plastic at specific water contents and will harden once dried or fired. Clays represent a great fraction of sedimentary rocks (Weaver and Pollard, 1973). The existence of clay can be attributed to the drilling, completion or workover fluids that introduce clay minerals into the formation. (Portier et al., 2007). Clays are distinguished for being tiny, layered materials that may exist in the sedimentary rocks as packs of crystals. The clay particles maximum dimension does not exceed 0.005 mm (Weaver,1989).

There are various groups of clays that may exist in sandstone formations such as: (1) Kaolinite group, (2) Montmorillonite or Smectite group and (3) Illite group and (4) chlorite group. However, these groups can coexist together and form a mixed-layer of clay minerals (Grim, 1942; Hughes, 1951). Table (2.6) shows the chemical formula along with the surface area for the typical clays minerals (Welton, 1984; Ezzat, 1990). According to Amaefule et al., (1988), there are two main types of the rock-fluid interactions in sedimentary formations: (1) chemical reactions that take place once the rock minerals become in contact with some incompatible fluids, and (2) physical interactions due to the high flow rates and pressure distribution.

Table 2.6 The different types of clay minerals after (Welton, 1984 and Ezzat, 1990)

Mineral	Chemical elements	Surface area (m ² /gm)
Kaolinite	Al ₄ [Si ₄ O ₄](OH) ₈	20
Smectite	(¹ / ₂ Ca, NA) _{0.7} (Al, Mg, Fe) ₄ [(Si, Al) ₈ O ₂₀] • nH ₂ O	700
Illite	K _{1-1.5} Al ₄ [Si _{7-6.5} Al _{1-1.5} O ₂₀](OH) ₄	100
Chlorite	(Mg, Al, Fe) ₁₂ [(Si, Al) ₈ O ₂₀](OH) ₁₆	100
Mixed Layer	Mix between illite-smectite-chlorite	100-700

The types of formation damage caused by the existence of clay minerals vary according to the nature of the clay mineral itself. For example; Kaolinite clay separates apart, migrates and accumulate at the tiny pore throats resulting in serious plugging and permeability reduction. Smectite clay is very water sensitive. Once Smectite clays get in contact with water, it expands up to 100% causing sever loss in permeability and microporosity. Illite clay can migrate with the other fines causing sever plugging. In addition, once the potassium ions are leached from Illite, it becomes an expandable clay. Chlorite clays are highly sensitive to low pH solutions and oxygenated water. The reaction of chlorite with acids produces (Fe(OH)₃) as a precipitated gel which plugs the pore throats. Finally, the mixed-layer clays can severely reduce the formation permeability when they form a clay-network across the pores (Civan, 2000).

The interactions of aqueous solutions with clay minerals are the main culprit of formation damage in hydrocarbon bearing formations. Mungan (1989) declared the factors that enhance the clay damage as (1) the cation exchange capacity of the clay minerals and (2) the layered framework of the clay minerals. Based on these two factors, the mechanism and severity of the clay damage is determined. The damage process of the three clay groups can be described as following;

- 1- **Kaolinite** has a structure of two main layers and potassium exchange cation with a small base exchange capacity. Kaolinite is a non-swelling clay but it can migrate and disperse easily. Kaolinite is thought to be one of the well-known migratory clays. The damage caused by the migration of kaolinite along with the other fines is localized near the wellbore region within a radius of 3 -55 ft. The damage can even reach the gravel pack. Kaolinite can adsorb some water and held it tightly to the clay surface.
- 2- **Smectite** has a structure of three layers and a large base-exchange capacity up to 90-150 milli-equivalents/100 gm. It can easily adsorb sodium cations causing a high degree of swelling and dispersion. Due to its high ability of swelling, smectite mixtures take water into its structure and expand its volume up to 600% causing severe losses in permeability. The treatment of this clay damage can be accomplished using HF acidizing operation if the depth of penetration is not that deep otherwise hydraulic fracturing will be required to bypass the damage.
- 3- Unlike kaolinites and smectites, **illites** are interlayered. Therefore, illites have the worst characteristics of dispersion and swelling among the other clays. It is very difficult to have stabilized illite clays. Illites suffer from osmotic swelling that takes

place due to the imbalance between the ions concentration at the clay exchange sites and the concentration of the solute content of the contacting fluid (Mungan, 1989 and Mahmoud et al., 2011).

2.4.1 Problems of Acidizing Illitic Sandstone Reservoirs using Mud Acid

Illite is considered one of the pore-lining clays that are attached to the pore walls forming a thin and long clay coating. The permeability of sandstone rocks containing that type of clay minerals is very sensitive to the interactions of clay minerals and the flowing fluids (Kamal et al., 2019). Priisholm et al., (1987) carried out core flooding experiments on sandstone cores containing different types of clays including illite clay. The results of their study show that the permeability and porosity of the formations that contain authigenic kaolinite, chlorite, illite, and mixed layer clays are very sensitive to particle migration and rock/fluid interactions.

Thomas et al., (2001) illustrated that flooding cores contain clays (chlorite and illite) by HCl will damage the cores either by precipitation of reaction byproducts or through fines migration. Moreover, HCl attacks chlorite and illite to produce an amorphous silica residue (Simon and Anderson, 1990; Labrid, 1975). Ali et al., (2002) found out that the clays will be unstable at high temperatures and the reaction will be fast.

Illitic sandstone formations have shown very high sensitivity to HCl-based fluids. The reaction of illitic sandstone with mud acid causes illite to breakdown leading to fines migration and formation damage (Mahmoud e al., 2011). In addition, Velde (1992) and

Gdanski and Shuchart (1998) showed that all the clay minerals are not stable with HCl at elevated temperatures above 300 °F.

Thomas and Crowe (1981) reported significant reduction in the compressive strength of the sandstone formations containing high clay content after mud acid stimulation. This results in formation disintegration and fines migration. Consequently, formation porosity and permeability got reduced.

2.5 Safety Hazards and Precautions of Dealing with Mud Acid.

HCl and HF acids are difficult to handle safely, corrosive to wellbore tubulars and completion equipment, and must be neutralized when returned to the surface. This warrants the need for a delayed acid system where live acid can be controllably released downhole and propagates deeper into the reservoir while treating formation damage (Malate et al. 1998; Leong and Ben Mahmud, 2019).

HF and HCl are very strong acids. Once they become in contact with the skin, they penetrate deeper into the skin layers and mucosa. This leads to harsh ulceration and intensive inflammation (Blodgett et al., 2001). Continuous exposure to HF for several minutes causes corrosion to the skin and the underlying tissues and hurting the blood vessels. The acid may continue and reach the blood. If reached the blood, HF acid may lower the blood pH level. Moreover, it reacts with the calcium and magnesium ions in the blood leading to systematic disorder (Heard and Delgado, 2003; Coffey et al., 2007; Ohtani et al., 2007; Smędra-Kaźmirska et al., 2014).

Intensive caution is highly recommended when dealing with HF acid due to its severe corrosiveness and toxicity. The awareness level of the personnel dealing with mud acid

should be raised to be familiar with all the safety procedures when dealing with the acid. Once the incident of acid contamination occurs, right diagnosis and quick treatment are of very high importance. First of all, the person's regular respiration and pulse should be checked. Immediate decontamination by using antidote is very helpful in stopping the skin adsorption to the HF and minimizing the tissue destruction by the fluoride ions (Burgher et al., 2012). The support from trained medical team is of a great help in such situations. All the persons who are included in the accident site should be transported to the hospital and kept under observation for 24 hrs even if they are not contaminated. During transportation to the medical center, continuous skin and eye irrigation, assistant ventilation and cardiopulmonary resuscitation (CPR) should be provided when needed (Bajraktarova-Valjakova et al., 2018).

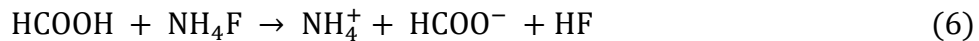
2.6 Trials of Replacing the Conventional Mud Acid

The need for developing new acid mixture that can overcome the drawbacks of the conventional mud acid has recently increased. This comes at the same time of the intensive interest in developing HPHT wells. The alternative acids should have positive impact on both the formation porosity and permeability and achieving positive economic returns as well. There are various types of acids that have been developed to replace the conventional mud acid such as organic acid, chelating agents and retarded acid systems. Following is a summary of the most common acid systems used to replace mud acid in the literature.

2.6.1 The Use of Organic Acids/HF Mixtures

In order to solve the issue of the quickly consumed acid system, Templeton et al. (1975) proposed the approach of self-generating in-situ HF acid. This approach allows the

treatment fluids to be in contact with the formation before generating the HF acid. Templeton et al. used a water-soluble fluoride salt (e.g. ammonium fluoride) along with an organic acid ester (e.g. methyl formate) in order to generate the hydrofluoric acid HF as described by the following reactions.



According to Chang et al., (2000), the aforementioned method suffers from two main issues. First one is the safety objection for using organic esters as they are highly flammable. The second one is the temporary damage caused during the reaction of HF with the formation clays which forms some insoluble products such as ralstonite.

Rogers et al., (1998) proposed the formulation of using 10% Citric acid along with 1.5% HF without any further additives for stimulating sandstone formations containing zeolite mineral. The proposed formulation showed an effective dissolution to the zeolite particles without creating silica gel precipitation. This could prevent the post-damage problem caused by conventional mud acid treatment. After treating five wells with this acid mixture, a production increase from 7400 to 16,000 BOPD was observed. However, the used HF did not penetrate deep into the formation and reacted only with the shallow damage and scale deposits around the wellbore (Chang et al., 2000).

Andotra (2014) could achieve high clay dissolution while causing minimum precipitations by adding 1 wt.% citric acid to 9:1 conventional mud acid. Citric acid reacted as a chelating agent which, in return, enhanced the results of stimulating both Berea and Bandera sandstones. Despite of the technical feasibility of this acid mixture, its economic

feasibility is debatable due to the high cost of citric acid as compared to the conventional mud acid.

Zhou and Nasr-El-Din (2013) carried out a comparative study between formic acid (HCOOH), GLDA and HEDTA. The ability of the three chemicals to remove the carbonate content from Berea sandstone cores (5 wt.% clay content) were tested. All the chemicals could enhance the permeability of tested cores. However, a solution of 9 wt.% formic acid showed the best results among the other chemicals at a temperature of 300 °F.

Shuchart and Gdanski (1996) discovered that there are severe damage caused by the precipitation of aluminum fluoride after using mixtures of HF and some organic acids such as formic and acetic acids. So many factors control the success and failure of the organic acid-HF mixture usage for sandstone acidizing such as; solution pH, the type of the organic acid used, the fluoride ion concentration, the ratio of F/Al ions in the solution and the type of minerals present in the formation (Al-Harbi et al., 2011; Yang et al., 2012).

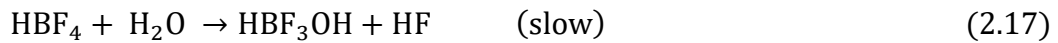
2.6.2 Retarded HF Acid Systems

It is claimed that retarded HF acids (RHF) systems can achieve deeper acid penetration due to their slower reaction rate with the sandstone formation minerals, specially the alumino-silicates (clays and feldspars) (Al-Dahlan et al., 2001). There are three main types of RHF categorized as fluoboric acid (HBF₄) based, aluminum chloride (AlCl₃) based and phosphonic acid based. These acids have shown higher efficiency in stimulating sandstone formations than mud acid. Retarded acids can work as buffer solutions. This enables them to achieve deeper penetration before being fully spent. This positively affects the formation porosity and permeability. In addition, they achieve lower formation strength reduction and

have lower corrosively (Thomas and Crowe 1978; McBride et al. 1979; Kunze and Shaughnessy 1980; Gdanski 1985; Lullo 1996).

Al-Dahlan et al. (2001) evaluated the three aforementioned RHF to find out that phosphonic acid based PRHF has the highest ability to dissolve silicon presented in the sandstone formation followed by aluminum chloride based ALRHF and finally comes the fluoboric acid based BRHF. All the types of RHF precipitate silica gel with increasing the reaction time (after retardation times out) except the PRHF. However, PRHF could not extract the calcium (Ca) and magnesium (Mg) ions from the clay minerals.

One of the retarded methods to generate HF is by hydrolyzing HBF_4 in aqueous solution. This process takes place at a slow rate and has different stages as described by Eqs. (2.17-2.20). The slowness of this process allows the acid to penetrate deeper into the formation. HBF_4 has a positive impact on clay stabilization and the prevention of fines migration (McBride et al. 1979; Thomas and Crowe 1981). As the temperature increases, the hydrolysis of HBF_4 in water is accelerated and hence the rate of generating HF increases. However, the efficiency of using HBF_4 under high temperatures (greater than 150°C) is questionable (Kunze and Shaughnessy, 1983).



Thomas (1979) used fluoboric acid (HBF_4) as an over flush stage after the conventional treatment with mud acid. This could prevent the clay migration problem and hence eliminate the unwanted production decline issue that used to follow the acidizing treatment. However, this approach can be only applicable for formations that do not contain any HCl sensitive minerals such as chlorite and zeolite. Such formations tend to form silica hydrates as precipitates and cause formation plugging (Chang et al., 2000; Portier et al., 2007)

Ayorinde et al., (1992) presented a real field case where a Nigerian oil well experienced various problems due to fines migration issue after the treatment with conventional mud acid. After the mentioned well was treated by conventional mud acid, the daily oil production was about 850 barrels' liquid per day (BLPD). After one year, the well was nearly dead because of the fines migration issues. The well was then treated by HBF_4 which could stop the fines migration problem and increase the production rate up to 2500 BLPD. The efficiency of the fluoboric acid treatment is extended even after one year maintaining a production rate of 2200 BLPD as shown in Figure (2.3).

Adding a retarding agent to the conventional mud acid can solve the problems of the fast acid reaction rate and achieve clay stabilization. Ji et al. (2014) and Ji et al. (2016) formed a new retarded mud acid known as fines control acid by mixing 15% HCl, 1.5% HF with 5% $\text{AlCl}_3 \cdot 6\text{H}_2\text{O}$. The newly designed acid was used to stimulate Berea sandstone cores at two different temperatures of 75 and 200 °F. The test results did not show any aluminum fluoride (AlF_3) precipitation. Moreover, the use of the AlCl_3 retarded acid system could achieve lower acid reaction rate and reach deeper formation penetration (Aneto, 2012).

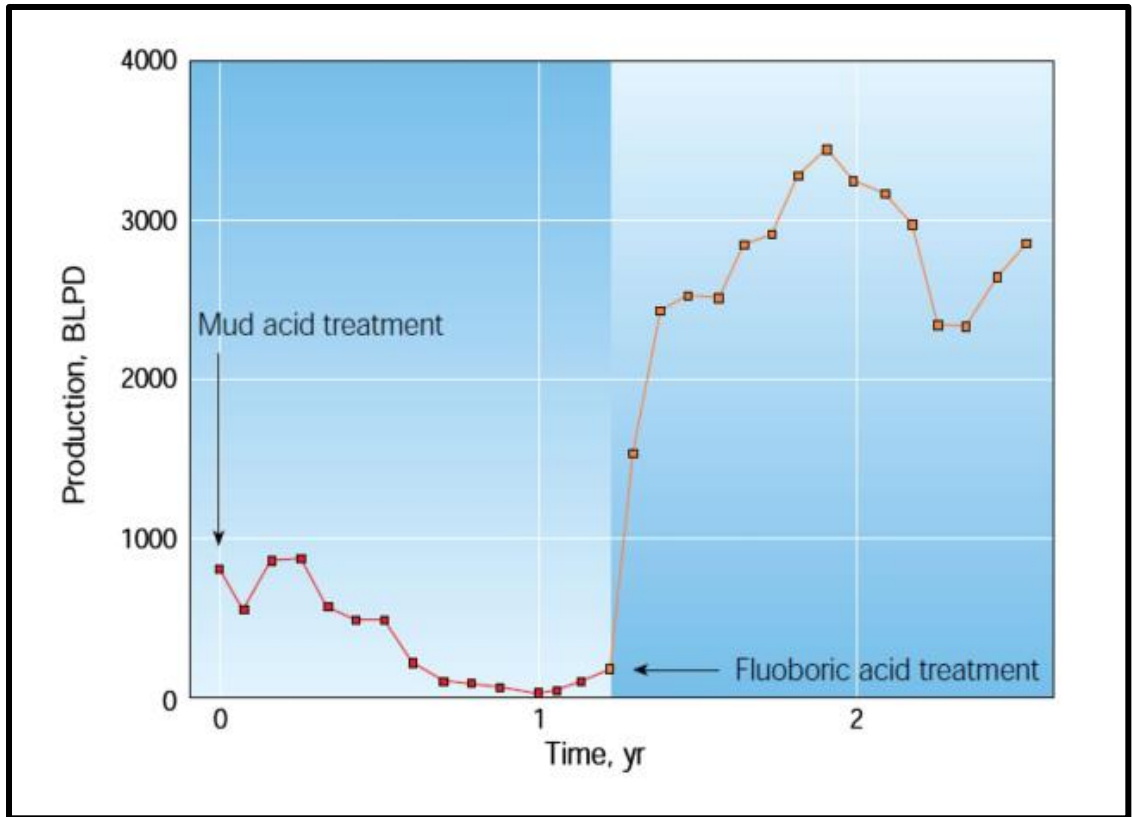


Figure 2.3 A comparison between the results of stimulating a Nigerian oil well using conventional mud acid first and then using fluoboric acid as reported by (Ayorinde et al. 1992).

Shafiq et al., (2014) and Shafiq and Ben Mahmud (2016) tried different acid combinations using different ratios of orthophosphoric (H_3PO_4) acid and HF; fluoroboric (HBF_4) acid and HF; and $HCOOH$ and HF. They investigated the effects of these acids on the porosity, permeability, mineralogy and strength of sandstone cores. The results showed that a combination of 3% HF: 9% H_3PO_4 surpassed the other mixtures and achieved 135.32% permeability enhancement compared to 101.76% for the conventional mud acid.

Zhou and Nasr-El-Din (2016) tested the use of PRHF as an alternative for regular mud acid for sandstone treatment. The acid was tested on both Berea and Bandera sandstone cores with clay content of 5 and 11% respectively. Different parameters were investigated

throughout this study such as the optimum acid concentration, the test temperature and the reaction duration. The study concluded the higher ability of the PRHF to enhance the sandstone permeability up to 177.86% at elevated temperature of 300 °F.

2.6.3 The Use of Chelating Agents in Sandstone Acidizing

Chelating agents were used in oil industry to control the precipitation of ferric and ferrous hydroxide, to remove scale, and as stand-alone stimulation fluids (Frenier et al., 2000; Reyes et al., 2013; Sokhanvarian 2014). Frenier et al., (2004) tried to get rid of the conventional acids used for sandstone stimulation by developing a new chelant from the hydroxethylaminocarboxylic (HACA). They tested the (HACA) on both Berea sandstone and Indiana limestone at high temperatures of 370 and 400 °F. Results showed that HACA could stimulate both sandstone and carbonate reservoirs at elevated temperatures with low reaction rates. Moreover, HACA is distinguished of being used as a corrosion inhibitor. This reduced the corrosion rate accompanied the stimulation process. In addition, HACA has a near neutral pH value which makes its disposal easier.

Tuedor et al., (2006) stimulated Berea sandstone cores (medium to high permeability) with newly developed chelant-based system. The results revealed that the new system is suitable for acidizing sandstone reservoirs with high carbonate content up to 30%. The new acid has a less corrosion effects and safe to handle.

Ali et al., (2008) used sodium hydroxyethylethylenediaminetriacetic acid (Na_3HEDTA) to stimulate sandstone formations of West Africa at high temperature of 149 °C. Although (Na_3HEDTA) has a low pH value, it caused less corrosion to the well

tubulars. Moreover, the solution used in this trials showed high efficiency in increasing the formation permeability.

Mahmoud e al., (2011) stimulated Scioto sandstone cores with high illite content of 18 wt.% using both 15wt% HCl and 0.6M GLDA (glutamic acid-N,N-diacetic acid) under high temperatures up to 300°F. The GLDA dissolved some iron, magnesium, calcium and small amounts of aluminum ions from the sandstone cores. No fines migrations were observed as well as there was no increase in the pressure drop across the core. The core permeability increased up to 84% at 300°F. On the other hand, HCl solution reduced the core permeability by 42% due to the dissolution of the clay minerals leading to fines migration and core plugging.

The mixture of GLDA/HF was proven by Reyes et al. (2015) to be very efficient in stimulating heterogeneous sandstones with high clay content. Their experiments on highly pure Leopard sandstone with more than 95% quartz content showed a reduction in core permeability by about 20%. While the tests on Bandera sandstone with only 65% quartz content showed an enhancement in core permeability by about 30%. The GLDA/HF solution used in this study had a low pH value of 2.5 and the test was carried out at temperature of 360 °F.

Rignol et al., (2015) mixed a low-pH chelating agent with fluoboric acid to stimulate Gulf of Thailand sandstone cores with 9% clay content at high temperatures of 370 °F. The solution did not cause any silica precipitates and increased the core permeability effectively. Moreover, this acid combination showed less corrosivity compared to the conventional mud acid.

Mahmoud et al., (2015) compared the efficiency of HEDTA, and GLDA and 15 wt.% HCl in removing the carbonate content of illitic sandstone cores. The tests were carried out at high temperature of 300 °F. Results showed that HCl had a negative impact on the porosity and permeability of the stimulated cores due to its interactions with the clay minerals. Both GLDA and EDTA showed a positive impact on removing the carbonate content of the stimulated cores without causing damage.

It has been stated that chelating agents are more suitable for carbonate formations or high carbonate content sandstones. In addition, the ability of chelating agents to dissolve quartz ions is very low due to the absence of the fluoride ions. Finally, the cost of chelating agents is considered to be quite high compared to the conventionally used acids (Leong and Ben Mahmud, 2019).

2.7 Ammonium Fluoride Oxidation

Hull et al., (2019) made a comprehensive study about the oxidation of ammonium salts (NH_4X), where X can be Cl, Br, F, ... etc., using a strong oxidizer as sodium bromate (NaBrO_3). Sodium bromate is an inorganic compound based on bromic acid. This reaction requires heating up to 150 °C for 3 hours in order to produce a transparent solution. Bromine gas is expected to be developed in some stage of this reaction. This will be clear from the orange color of the evolved gas. For the oxidation of ammonium fluoride with sodium bromate, Hull et al. found out that the optimum molar concentration ratio of NH_4^+ to BrO_3^- is 2:1 as illustrated in Figure (2.4) at different temperatures of 100 and 150°C. It was also shown that the more soaking time of the reactants under high temperature, the more HF acid generated up to 20 hours of soaking. The reaction of sodium bromate with ammonium fluoride can be represented by Eq. (2.21)



The ammonium fluoride oxidation reaction using sodium bromates is considered to be an autocatalytic reaction. The reaction is defined to be autocatalytic when one of the reaction products acts as catalyst for the main reaction. In this case, the produced HF is the product which works as a catalyst for the oxidation reaction. This is because of the ability of the produced HF to reduce the medium pH. Therefore, if the medium pH is initially low, this reaction will be initiated and completed much faster.

Another oxidizing agents that can be used to oxidize ammonium fluoride and produce hydrofluoric acid (HF) are ammonium persulfate $(\text{NH}_4)_2\text{S}_2\text{O}_8$ and potassium permanganate (KMnO_4) . The solubility of ammonium persulfate is quite high and its reaction with ammonium salts is endothermic reaction as well.

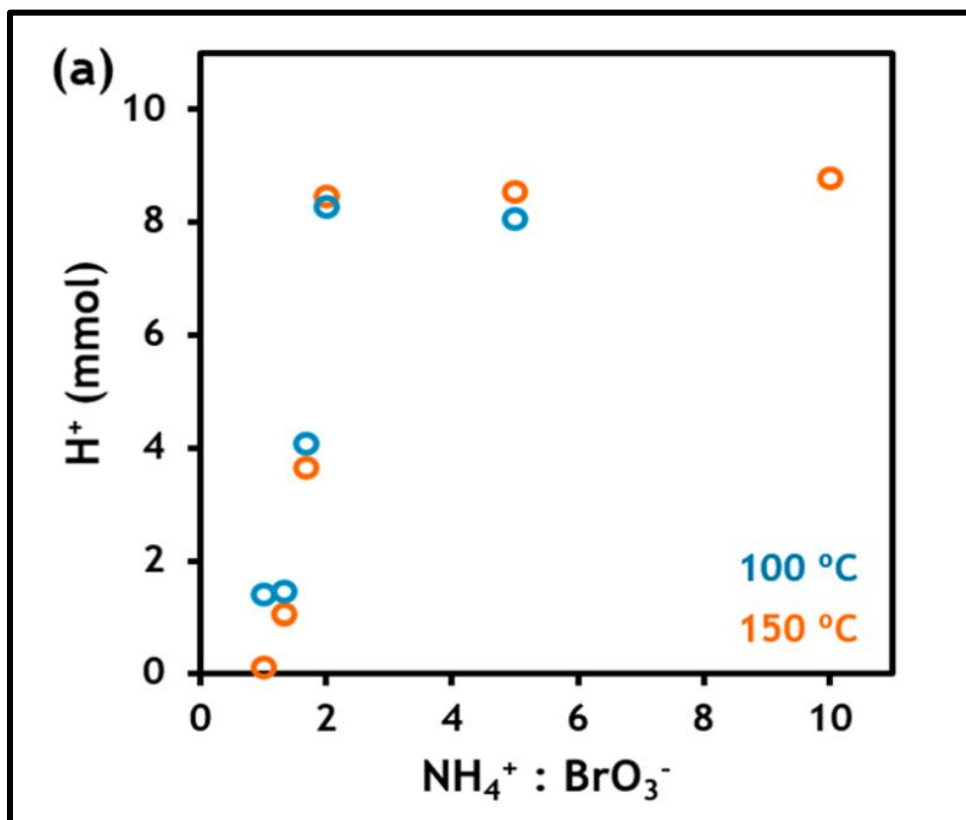
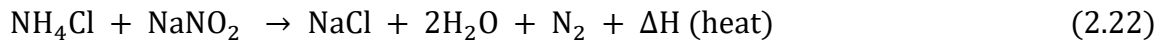


Figure 2.4 The amount of HF acid produced under different concentration ratios of both NH_4F and NaBrO_3 (Hull et al., 2019)

2.8 Applications of Thermochemicals in Oil Field

Karale et al. (2016) patented a novel method for using a pH buffer solution to activate an exothermic reaction downhole. They used sodium nitrite and ammonium chloride as main reactants for their exothermic reactions. One of the reactants can be injected to the formation first or both of them can go together, then a pH buffer solution with pH value ≤ 4 is injected in order to activate the exothermic reaction that is described by Eq. (2.22). The generated heat increases the formation temperature and hence increases the acidizing reaction rate. This method was initially developed for increasing the efficiency of acidizing low temperature dolomite formations.



Nguyen et al., (2003) studies the kinetics of the above reaction and reported that the reaction rate is a strong function in the solution pH. The reaction rate can be increased by a factor of 4000 once the pH drops from 7 to 3. In addition, the reaction is considered a first order reaction regarding the concentration of the ammonium ions where it is considered a second order reaction with respect to the nitrite ions. This kind of exothermic reaction can be used in different applications in the oil industry such as wax, asphaltene and paraffine removal (Singh & Fogler, 1998).

Al-Nakhli et al., (2016) proposed the use of thermochemical reaction as a novel cost-effective way for heavy oil recovery. This new approach is called Exo-Clean technique that provides in-situ steam generation for thermal recovery of deep oil wells. Al-Nakhli et al., reported the increase in system pressure and temperature to be 3470 psi and 600°F respectively after the reaction is completed.

Alade et al., (2019) evaluated the kinetics and energy associated with the thermochemical reaction used for both heavy oil and condensate recovery. They concluded that the system initial temperature highly affects the reaction speed. The reaction time decreased from almost 18 minutes under the ambient temperature of 20 °C to about 6 minutes under 75 °C. Moreover, the change in enthalpy ΔH for this chemical reaction has been shown to be 369 kJ/mol, regardless of the operating temperatures.

Hassan et al., (2019) used the concept of thermochemical treatment for removing water blockage in tight sandstone reservoirs. After treating the tight Scioto sandstone cores with different cycles of the thermochemical mixtures, significant improvement in the core conductivity have been observed. The capillary forces have been reduced by 55% and the productivity index has been increased by 1.79 while the drawdown pressure has been increased by 78%. Moreover, the generated pressure and heat coming from the thermochemical reaction could create micro fractures in the sandstone core sample leading to reduce the capillary forces within the core.

CHAPTER 3

Research Novelty, Methodology and Equipment

3.1 Research Novelty

The idea of this research is to combine what (Hull et al. 2019) and (Karale et al. 2016) did together. In other words, this research aims at combining the application of thermochemical reaction that can generate heat up to 200°F with the application of oxidizing ammonium fluoride salt under high temperature in order to generate in-situ HF acid. Combining the two mentioned concepts together would help in generating the heat required for the endothermic oxidation reaction of ammonium fluoride, producing high pressure pulse that capable of removing any byproduct precipitation. Nitrogen gas is also expected to be produced which would be of a good benefit for diverting the acid solution during the acidizing treatment.

The reaction compounds will be injected separately downhole. This would reduce the corrosion problems generated by pumping conventional acids into the formations. All the chemicals used at the surface are safe to handle in the wellsite. This also eliminates the problem of dealing with hazardous substances on the surface during conventional sandstone acidizing process. Acid generation and reaction rates would be highly controlled throughout controlling the oxidation reaction stoichiometry as well as controlling the exothermic reaction. Moreover, formation true potential could be restored throughout the deeper acid penetration achieved.

3.2 Methodology and equipment

In order to achieve the research objectives, the work flow is carried out along different phases. Phase 1 is to prepare the required chemicals and check their solubility limits and mixing conditions. Phase 2 is to check the validity of the concept of in-situ HF generation by testing the used chemicals against pure quartz samples. Phase 3 is to check the ability of the in-situ generating fluids to dissolve different clay minerals. Phase 4 is to prepare and test different sandstone cores against the new chemical mixture using core flooding set-up. Phase 4 is to determine the optimum number of flooding cycles and the optimum soaking time of each cycle. Phase 5, final phase, is to check the effect of the chemical mixture on the rock mechanical properties and pore system structure. All the phases are discussed in more details below.

3.2.1 Phase 1- Materials Preparation

In this phase we are mainly concerned about the solubility and mixing conditions of the chemicals we will be using. There are three main reactant types that will be initially used for this research. The first type is the oxidizers such as sodium bromates (NaBrO_3), ammonium persulfate ($(\text{NH}_4)_2\text{S}_2\text{O}_8$) and potassium permanganates (KMnO_4). The second type is the acid precursor which is ammonium fluoride (NH_4F). The third type is the thermochemicals which are the sodium nitrite (NaNO_2) and ammonium chloride (NH_4Cl). The chemical and physical properties of these compounds are listed in Table (3.1).

Table 3.1 Chemical and physical properties of the used chemical compounds, after (Haynes, 2010)

Properties	NaBrO ₃	(NH ₄) ₂ S ₂ O ₈	KMnO ₄	NH ₄ F	NaNO ₂	NH ₄ Cl
Molecular weight g/mole	150	228	158	37	69	53
Density g/cc	3.34	1.98	2.7	1.009	2.168	1.519
Appearance	Colorless or white solid	White to yellowish crystals	purplish-bronze-gray	White crystalline solid	White solid	White solid
Melting point °C	381	120	240	100	271	338
Boiling point °C	1390	NA	NA	260	320	520
Standard enthalpy of formation, ΔH KJ/mole	-342.5	- 1411.33	- 813.4	- 466.9	-359	- 314.34
Purity	99%	98%	>99%	95%	97%	99%

Source: PubChem, 2019. URL <https://pubchem.ncbi.nlm.nih.gov/> (accessed 11.14.19).

In order to check the solubility of each compound in water under different temperatures, the solubility curves vs. temperature are constructed as shown in Figs. (3.1-3.6). The solubility limit of each component will determine the maximum concentration that will be used from such chemical in this study.

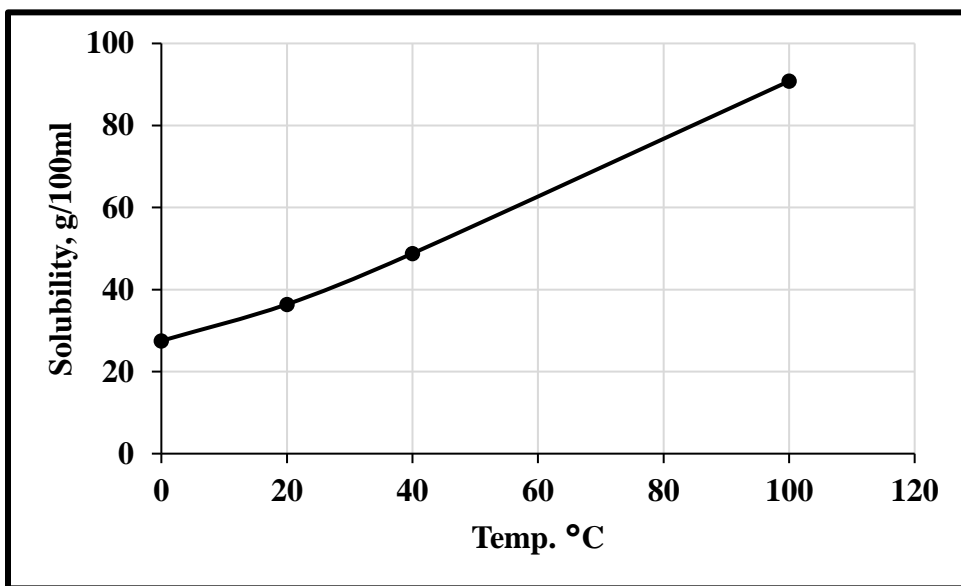


Figure 3.1 Sodium bromate solubility in water as a function of temperature, *PubChem, 2019*.

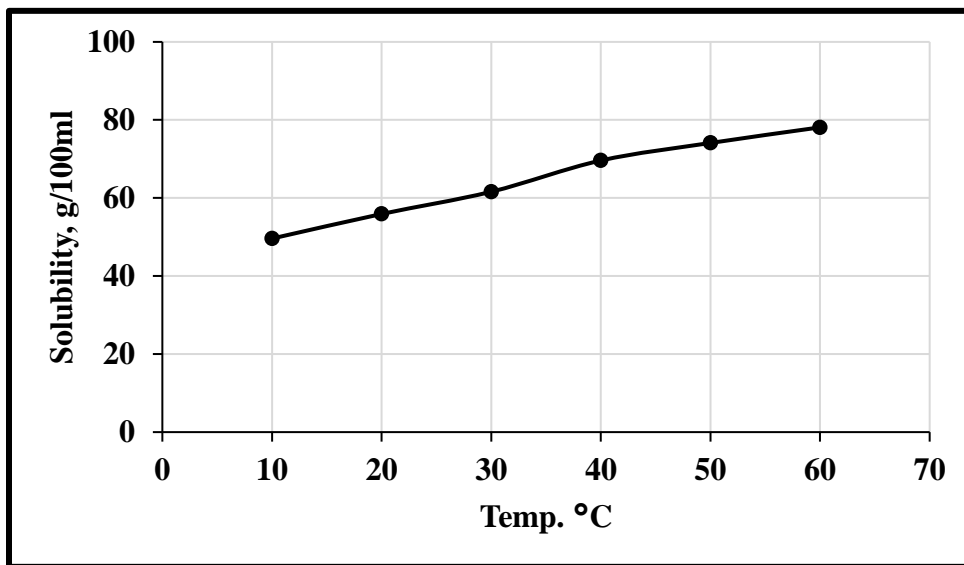


Figure 3.2 Ammonium persulfate solubility in water as a function of temperature, *PubChem, 2019*.

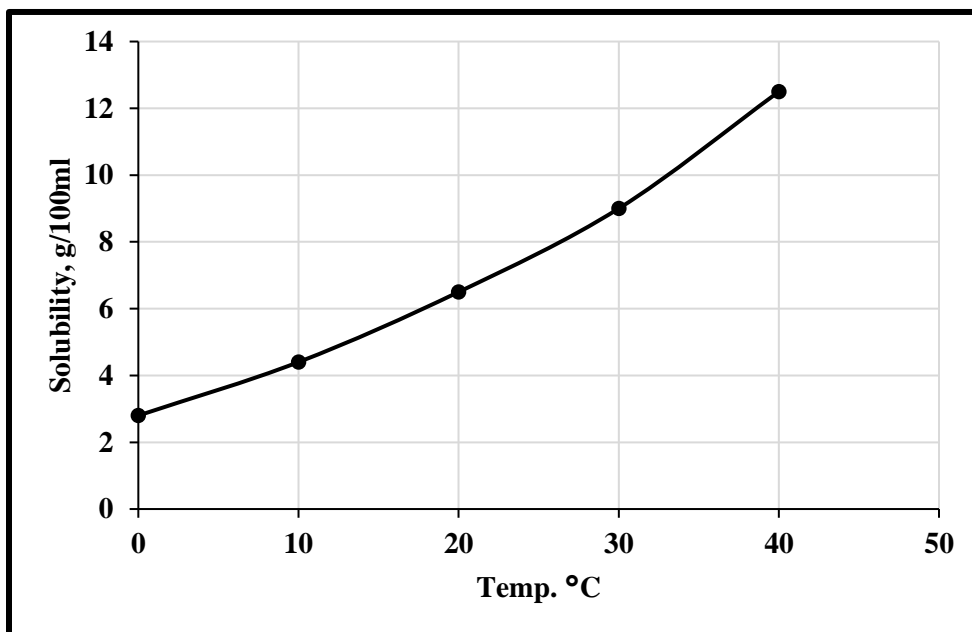


Figure 3.3 Potassium permanganate solubility in water as a function of temperature, *PubChem, 2019*.

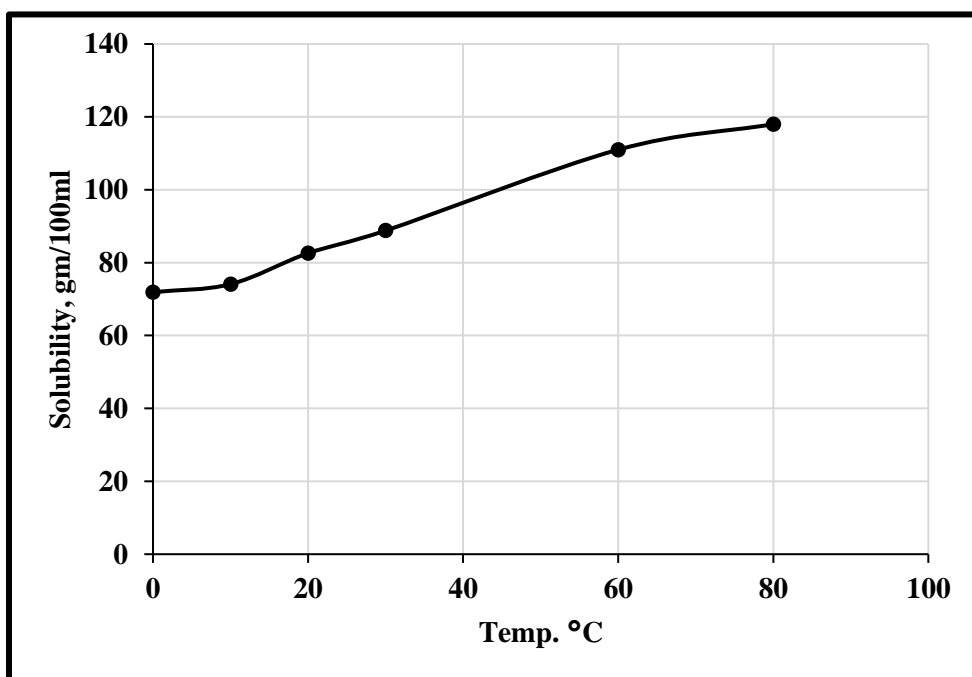


Figure 3.4 Ammonium fluoride solubility in water as a function of temperature, *PubChem, 2019*.

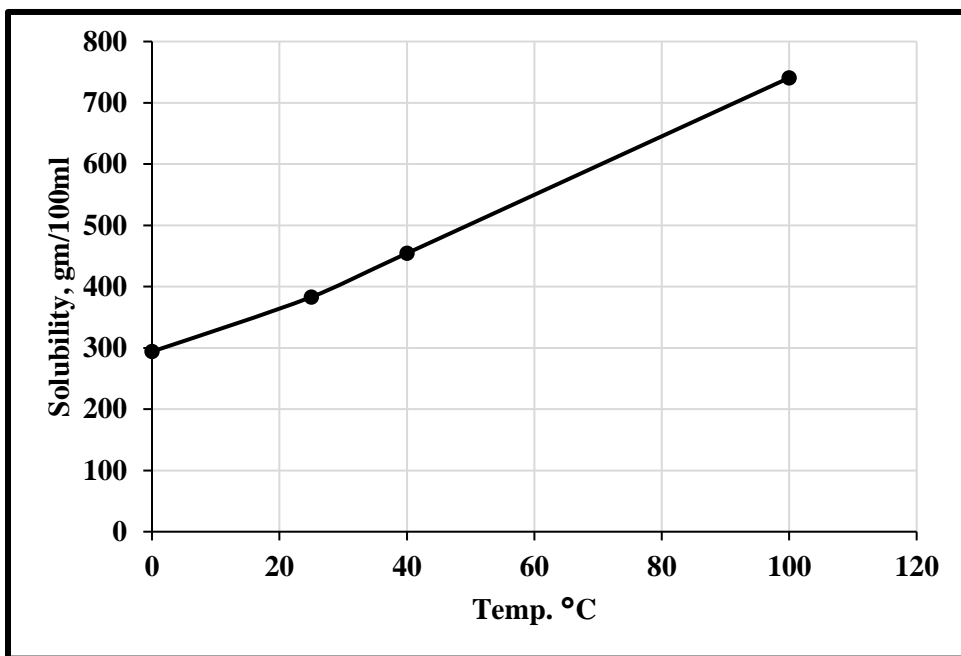


Figure 3.5 Ammonium chloride solubility in water as a function of temperature, *PubChem, 2019*.

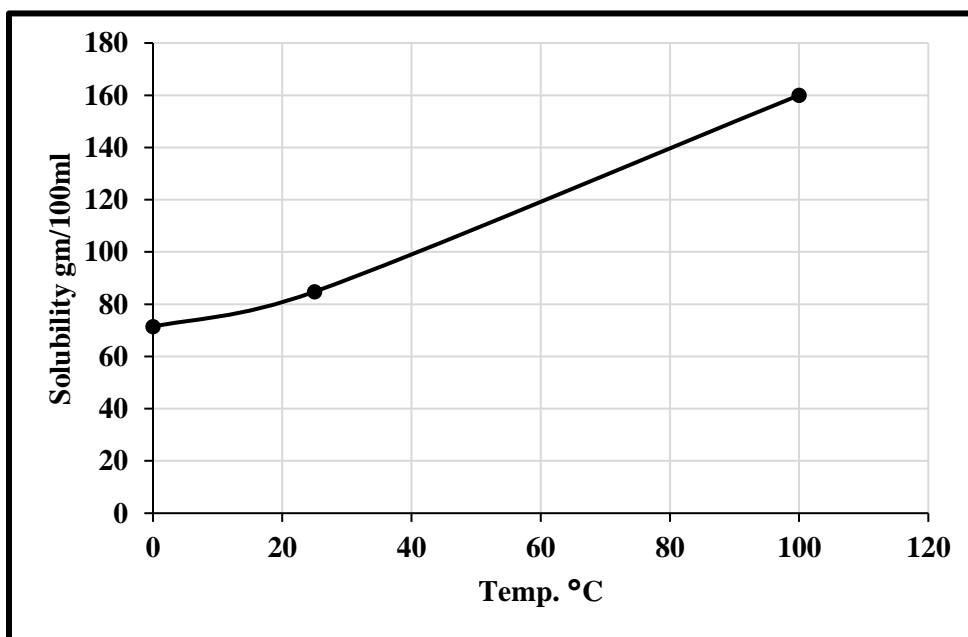


Figure 3.6 Sodium nitrite solubility in water as a function of temperature, *PubChem, 2019*.

As shown in Figure (3.7), the solubility set-up used to prepare and mix the reaction components is a triple-hot plate with magnetic stirrer. The heating range of this apparatus is up to 200 °C while it can go up to 2000 rpm. This allow proper mixing of the chemicals to ensure homogeneous solutions. The solubility set-up is fixed with a ventilation fume hood system to extract any unwanted gases that might evolve. All the chemicals are mixed at a high stirring rate of 1000 rpm.



Figure 3.7 A triple-hot plate with magnetic stirrer solubility set-up

After different mixing trials and based on the data found in the literature, we found out that the optimum ratio of mixing the sodium bromates with the ammonium fluoride is 1:2 as a molar concentration ratio. For both the ammonium persulphate and potassium permanganates, we tried different concentrations of 0.1, 0.5 and 1 molar while keeping the ammonium fluoride concentration constant at 2 molar. Ammonium fluoride mixing can be

done at room temperature unlike the mixing of sodium bromate oxidizer that should be carried out very slowly at temperature of 85°C. The mixing of the other oxidizers can be done at room temperature. Regarding the thermochemical reaction, the ratio of ammonium chloride to sodium nitrite would be 1:1 with a corresponding concentration of 1 molar for both of them. Room temperature is sufficient for the thermochemical mixing.

3.2.2 Phase 2 – Proving the Concept (Quartz Solubility Test)

The work of this phase is done to prove our main concept and the capability of the chemical mixture to generate HF acid as designed. A weighed amount of highly pure quartz, shown in Figure (3.8), is dispersed in the acid-generating medium (contained in a sealed Teflon bottle) and stirred for a given period. The pure quartz is used to avoid any reaction complication due to the impurities, clays and feldspars that may exist in sandstone cores. A highly accurate digital balance is used to measure the weight and weight change of the quartz sample. The used balance, shown in Figure (3.9), can detect up to 0.1 mg. The aging cell is then tightened very well and connected to pressure sensor and temperature thermocouple to monitor both the pressure and temperature inside, Figure (3.10).

The system temperature is then raised to the initiation temperature of the exothermic reaction (90°C) using a digital balance, Figure (3.11). The used digital balance can go as high as 300°C. The system is kept sealed and isolated for 24 hours and then the final weight of the quartz is measured.



Figure 3.8 Highly pure quartz samples



Figure 3.9 High accurate digital balance up to 0.1 mg



Figure 3.10 A steel aging cell with a Teflon liner of a maximum capacity of 100 ml



Figure 3.11 A digital oven with a maximum temperature of 300 °C

The concentration of silicon ions (Si^+) is traced in the solution to quantify the amount of silica dissolved and the corresponding concentration of the generated HF. Inductively Coupled Plasma - Optical Emission Spectrometry (ICP-OES) will be used to analyze the fluid samples for the silicon concentration.

ICP-OES device is used generally to analyze and determine the different ions concentration in the effluent solution at very low levels in terms of parts per billions (ppb). It is based on the concept of analyzing the photons emitted from the excited atoms after losing their energy and return back to the original state. The effluent solution is firstly diluted 100 times and then introduced to the system using a peristaltic pump. The system nebulizer turns the solution into a fine aerosol. A plasma source is then used to excite the different atomic species in the aerosol. The plasma heat current reaches a temperature more than 6000 °K and carried by ionized argon gas. The device main chamber contains prisms and echelle grating used to separate the wavelengths of the different emitted radiations into distinct measurable waves. Based on the element standard emission intensity, the ICP software can detect the types of the elements exist in the sample and report their corresponding concentration. Figure (3.12) shows the complete set-up of the used ICP-OES device.



Figure 3.12 ICP-OES system used for all the elemental analysis carried out within this study

3.2.3 Phase 3 – Clay Solubility Test

In this stage, the solubility of three different clays (chlorite, illite and kaolinite) are tested against a mixture of the in-situ generating HF chemicals and the thermochemicals together. The chemical oxidizer (ammonium persulphate) with a concentration of 1 M is mixed with the HF precursor (ammonium fluoride) solution with a concentration of 2 M concentration in separated vessel. Then, the thermochemicals (ammonium chloride and sodium nitrite) with a concentration of 1 M each are added to the first mixture. The total mixture volume was determined to be 100 ml. The mixture is then contained in a Teflon liner and kept sealed in an aging cell for 3 hrs to make sure the reactions are completed and the acid is generated.

Figure (3.13) shows the three clay groups after being crushed and weighed up to 5 g each. X-ray fluorescence (XRF) analysis is made for the three clays in order to determine their elemental composition. Chlorite clay has a dark-black color due to the abundance of iron oxide in it. Illite clay has a dark brown clay while the kaolinite clay has a light brownish color. The three clays are then added to the whole chemical mixtures while kept stirred under a temperature of 90 °C for 24 hrs. Finally, the solution is filtered and ICP analysis is carried out to determine the amount of each dissolved elements from each clay. The results of this stage shall confirm on the generation of HF acid from the chemicals mixed initially together. Moreover, it tests the ability of the generated acid to dissolve the different clay minerals that commonly exist in sandstone formations.

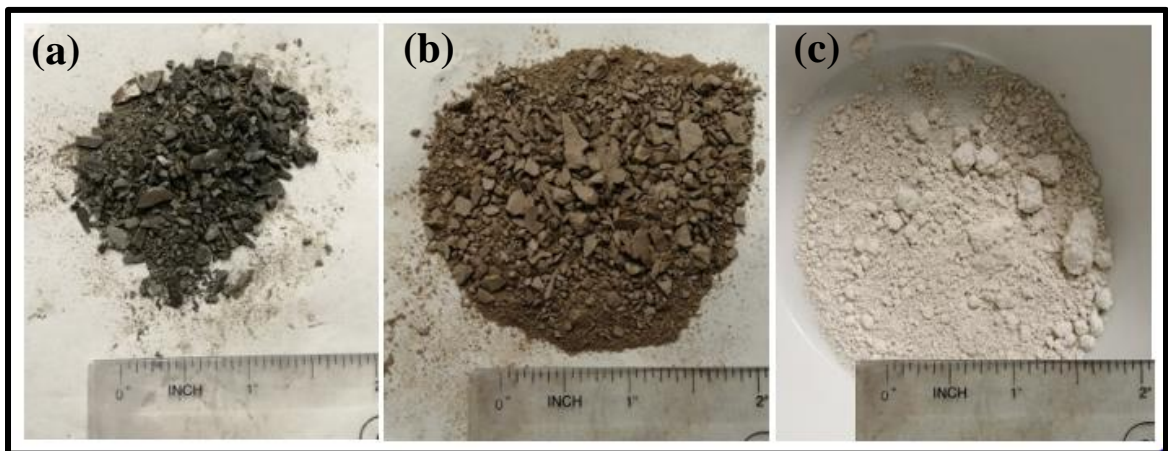


Figure 3.13 (a) chlorite clay mineral with its dark color, (b) illite clay mineral with its dark brownish color and (c) kaolinite clay mineral with its light brownish color.

3.2.4 Phase 4 – Core Flooding

3.2.4.1 Cores preparation

Linear core flooding experiments is designed and carried out to study the ability of the in-situ generated acid to stimulate different sandstone samples at high pressure and temperature conditions. The cores are cut using a sharp core cutting desk, Figure (3.14). After that, core face grinding is done using the face grinding machine, Figure (3.15), in order to assure stable core flooding and avoid any harms for the rubber sleeves used.

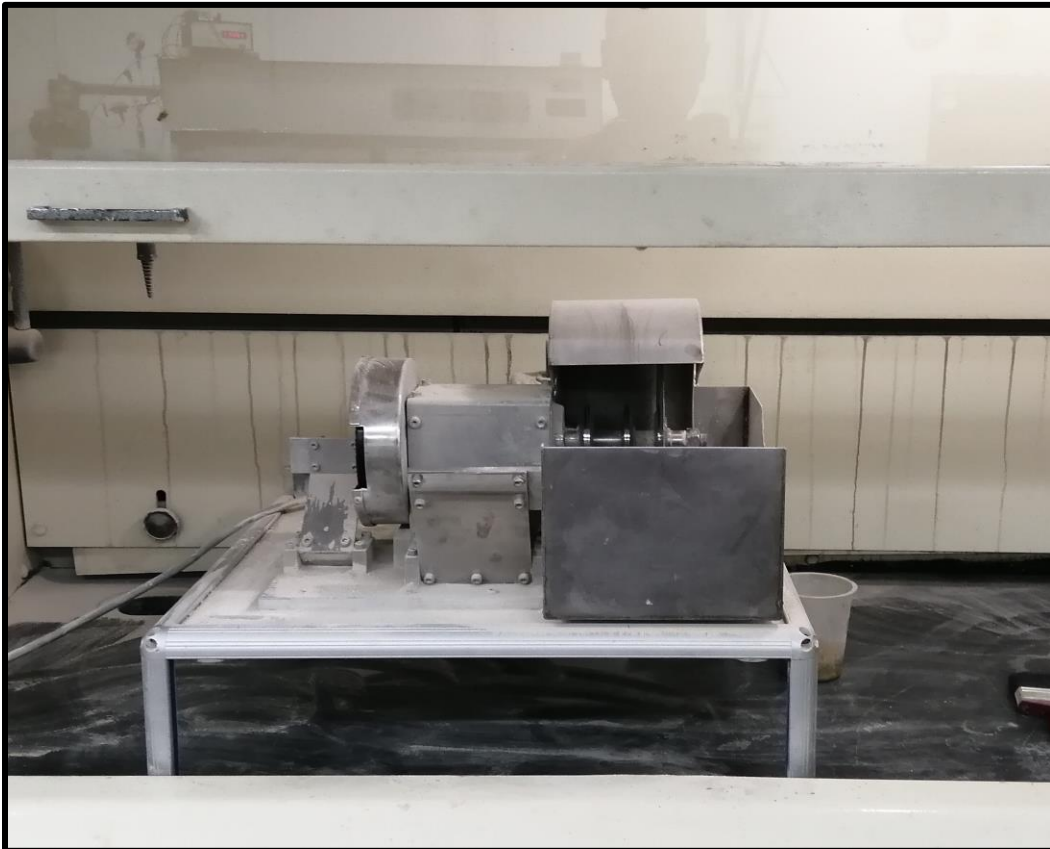


Figure 3.14 The core cutting desk



Figure 3.15 The core face grinding machine

3.2.4.2 X-Ray Diffraction (XRD) Analysis for Gray Berea and Scioto cores

Both Gray Berea and Scioto cores went through X-ray diffraction (XRD) analysis to determine the main minerals present in each core. The results are reported in Figure (3.16). It is clear that both cores have a plenty of quartz content, 87 wt. % and 70 wt. % for Berea and Scioto cores respectively. Both of the cores have almost the same content of potassium feldspars and the different clays except for illite clay and plagioclase feldspars. The high illite clay content of Scioto sandstone core, 18 wt. %, will affect the design of the preflush

stage of the acidizing process. Therefore, only 5 wt.% HCl is used as a preflush for Scioto cores unlike using 7 wt. % of HCl for Gray Berea cores.

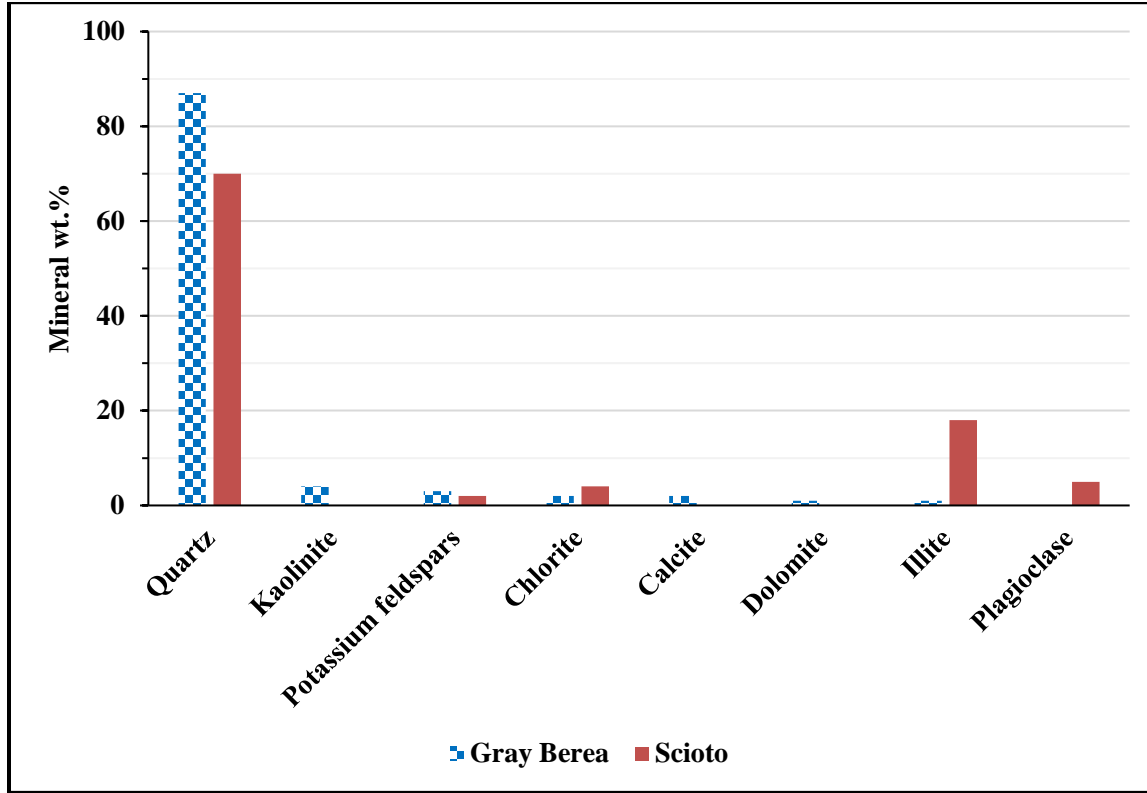


Figure 3.16 The mineralogy analysis of both Gray Berea and Scioto cores using XRD

3.2.4.3 Porosity Measurement for Gray Berea and Scioto cores

Core porosity is measured using the fluid saturation method. The core dry weight is determined and then placed in a transfer cell. A vacuumed pump is used to suck all the air from the core and the cell. Then an injection pump is used to displace the saturating fluid into the cell. In order to make sure that all the rock pores are filled with the saturating fluid, a high pressure of 2,500 psi was applied onto the core for 24 hrs. The following scheme represents the saturation setup, Figure (3.17).

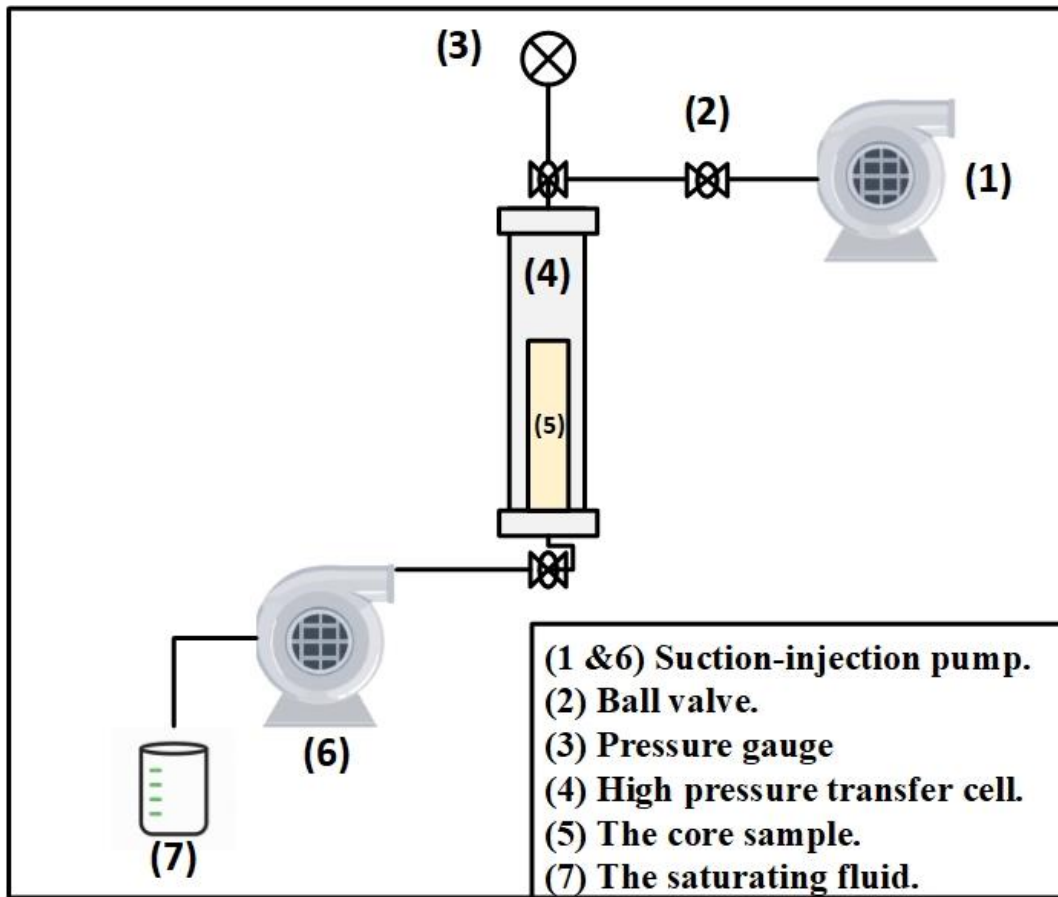


Figure 3.17 The core saturating set-up

The initial porosity of Gray Berea core was about 20 % while it was about 17.5 % for Scioto core. All the parameters used to calculate the cores porosity are mentioned in Table (3.2).

Table 3.2 Gray Brea and Scioto cores properties with the saturating fluid properties

	Gray Berea	Scioto
Dry weight (g)	356.6	375.1
Saturated weight (g)	389.8	405.7
Diameter (in)	1.496	1.494
Core Length (in)	5.856	5.970
Fluid salinity	3 wt.% KCl	3 wt.% KCl
Fluid density (g/cm³)	1.0166	1.0166
Core bulk volume (cm³)	168.68	171.5
Core pore volume (cm³)	33.75	30.1
Porosity	0.2	0.175

Two main types of sandstone cores are tested during this study; Gray Berea and Scioto sandstones, shown in Figure (3.18). The samples initial permeability is measured using 3 wt.% KCl solution with different flow rates suitable for each core. The KCl concentration was chosen based on the recommendations of (Schneider, 1998) to increase the clay stability. A hydrochloric acid (HCl) is then injected through the core to remove any carbonate-based minerals as a preflush stage. Moreover, it helps to condition the rock surface before the acid treatment and eject the previously injected brine solution. This aims to avoid the precipitation reaction between the HF acid and the cations in the brine solution. In addition, the HCl injection should enhance the injectivity for the main flush stage.

The concentration of the preflush acid was determined based on the recommendations of (McLeod and Norman, 2000), see Table (2.2). Then the core permeability is measured for the second time before the main flush stage. All the previous stages are carried out at the ambient conditions. The properties of the permeability measurement stage and the preflush stage for the two core types are mentioned in Table (3.3).



Figure 3.18 Gray Berea SS and Scioto SS cores that will be used for this study

Table 3.3 The permeability measurement stage and the preflush stage properties for the two core types

	Gray Berea	Scioto
Brine salinity	3 wt.% KCl	3 wt.% KCl
Flow rate (cm³/min)	2	0.5
Preflush fluid (HCl concentration)	7 wt. %	5 wt. %
Preflush volume	5 PV	5 PV

3.2.4.4 Core Flooding without Thermochemicals

To examine the effect of the in-situ HF generating fluids only on the core permeability, the HF acid precursor (ammonium fluoride) and the oxidizer (sodium bromates) are weighed based on the 2:1 molar ratio and then mixed together. After the preflush stage of HCl injection finishes, the system temperature is raised to 150 °C. Then, the main fluid mixture is injected with a rate of 2 cm³/min for Gray Berea core and a rate of 0.5 cm³/min for the Scioto core. Once the core is saturated with the full mixture, a 30-minute soaking is allowed for the reactions to take place. The pressure inside the core is monitored during the soaking period by using pressure sensors. After that the core is flushed again by 1 pore volume (PV) of the same mixture and the effluent is collected. Then, the outlet and inlet valves are closed and the sample is exposed to another 30-minute soaking. The same procedures are followed. This is repeated for three successive times and the effluent after each time is collected for ICP analysis.

Finally, the core is flowed back by a solution of 3wt. % KCl to measure its final permeability. The following chart, shown in Figure (3.19), represents the basic sequence of the core flooding operations.

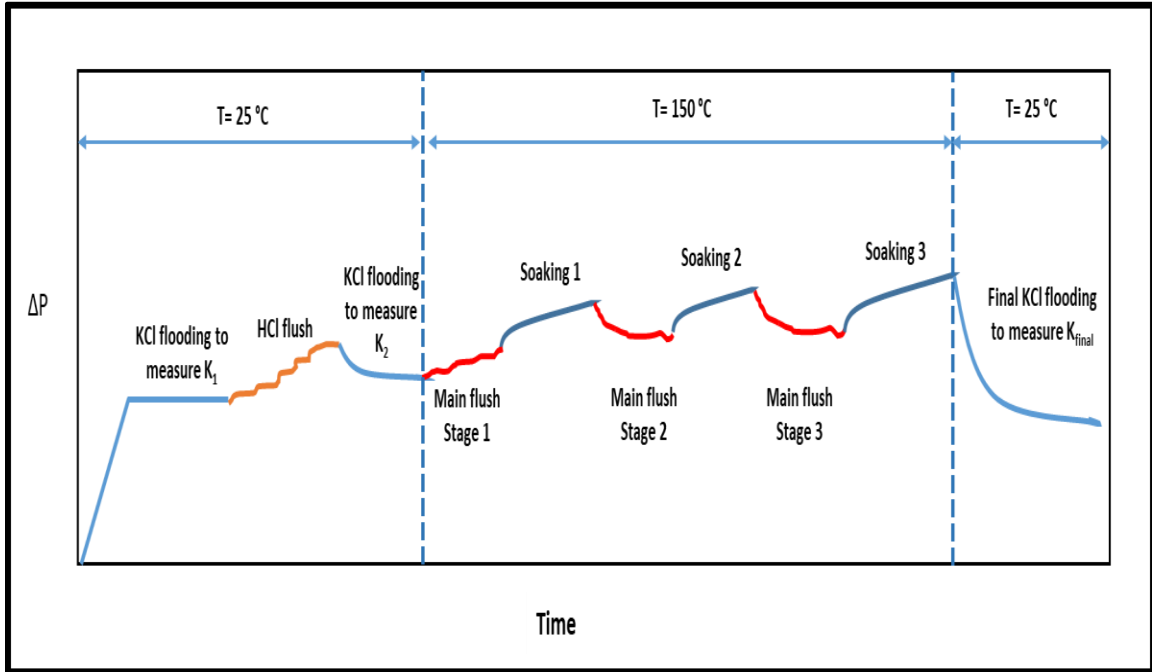


Figure 3.19 The general sequence of the core flooding test. K₁ is the initial core permeability, K₂ is the core permeability after HCl flush and K_{final} is the final core permeability.

Figure (3.20) shows the used linear core flooding system that consists of 6-inch core holder that can withstand high pressure and high temperature conditions. The systems come with three main transfer cells that would contain the different chemicals injected. The cells are connected to a hydraulic pump that capable of injecting the fluids at specified rate with monitoring the total injected volume. A back pressure of 360 psi is kept constant during all the core flooding tests to ensure homogenous stable flow. An overburden pressure of 700 psi is applied around the core to prevent fluid leakage and ensure that all the injected fluids passes through the core. The pressure difference across the core is sensed by differential

pressure transducers which are connected to some lab view software “OMEGA”. The whole system is contained in an oven with temperature sensor to apply the suitable temperature required for the flooding test.

The permeability is measured at the stabilized constant flow rate using Darcy equation (3.1) as following;

$$k = \frac{122.812q\mu L_{core}}{\Delta p d_{core}^2} \quad (3.1)$$

Where K is the core permeability in mD, q is the flow rate in cm^3 /min , μ is the fluid viscosity in cP, L_{core} is the core length in inches, Δp is the pressure drop across the core in psi and d_{core} is the core diameter in inches.

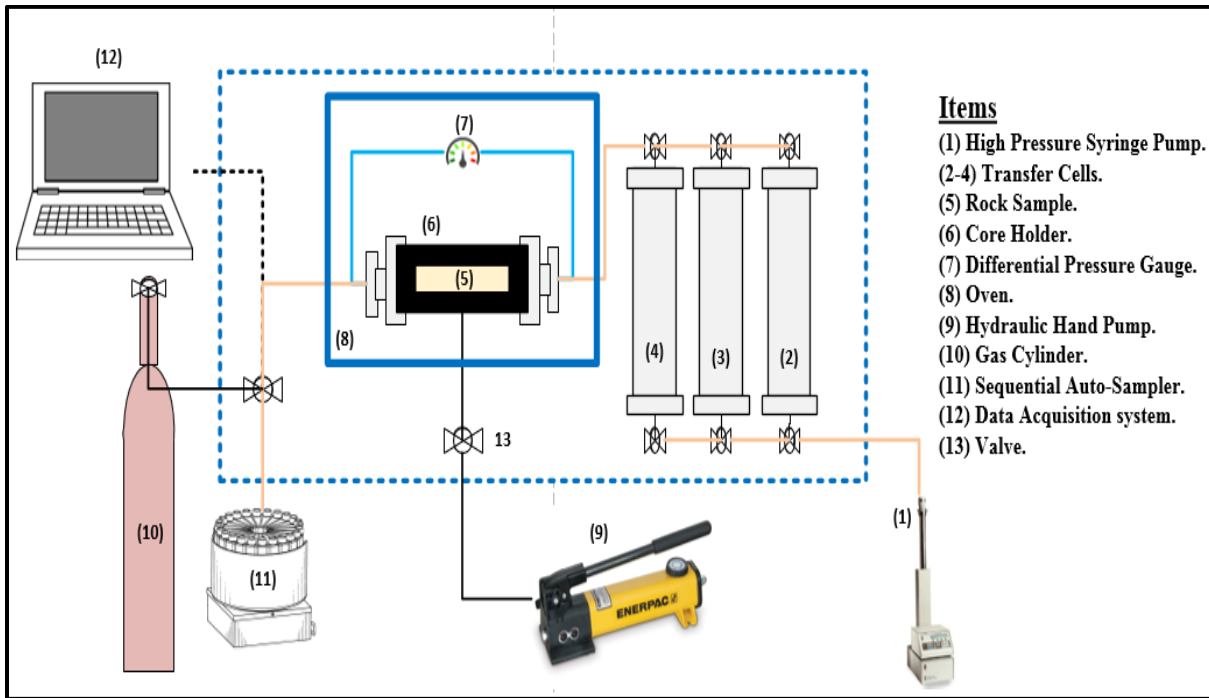


Figure 3.20 Core flooding set-up

3.2.4.5 Core Flooding with Thermochemicals

In order to examine the effect of temperature and pressure generated from the thermochemicals (ammonium chloride and sodium nitrite), a different chemical injection sequence shall be followed regarding the main flush stage. Five successive cycles of injecting the acid generating fluids along with the thermochemical fluids are carried out for Scioto core. The injection sequence of this stage is quite critical. The acid generating chemicals (ammonium fluoride salt and the oxidizer) were weighed, mixed and kept in one injection cell. Each compound of the thermochemicals was kept separated in a transfer cell. Acetic acid was added to one of the thermochemical compounds in order to reduce the medium pH below or equal 4. Firstly, 0.5 PV of the acid generating fluids was injected into the core. Then, 0.25 PV of the thermochemicals first reactant, which the acetic acid was added to it, was injected followed by another 0.25 PV of the other thermochemicals reactant. All the chemicals injection rate was $0.5 \text{ cm}^3/\text{min}$. The following scheme represent the injection sequence of the different chemicals inside the core, Figure (3.21).

This injection sequence has many advantages such as; it helps to achieve deeper acid penetration by pushing the acid generating fluids deep into the formation. The reaction of the in-situ acid generation is an autocatalytic reaction that can be catalyzed by whether increasing the medium temperature up to $150 \text{ }^\circ\text{C}$ or by reducing the medium pH. Therefore, this reaction can be triggered by the acetic acid that is mixed with the first thermochemical compound. This retards the generation of HF from the chemicals at the head of the slug. This, again, helps in achieving deeper acid penetration. In addition, the pressure pulse generated from the thermochemical reaction will push the acid generating fluids much deeper into the formation.

After each injection round, a soaking time of 30 min was allowed for the chemical reactions to take place. This also allowed the pressure to stabilize along the core. The inlet and outlet core pressures were recorded and plotted with time. Effluent was collected for ICP analysis to examine how much elements were chelated from the core during this process.

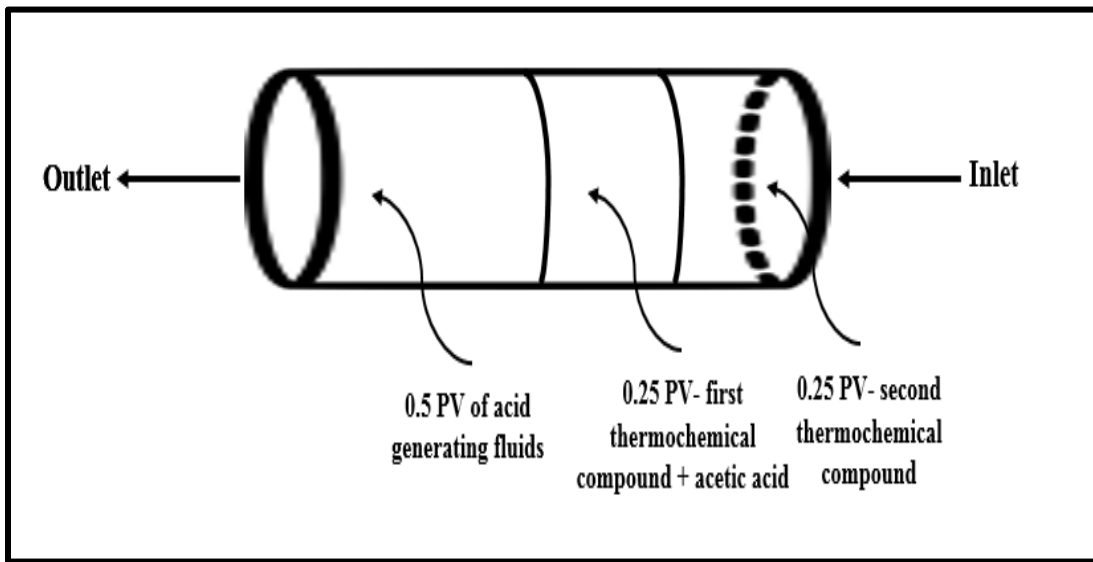


Figure 3.21. The injection sequence of the acid generating fluids along with the thermochemicals inside Scioto core. All the injection rates were constant at $0.5 \text{ cm}^3/\text{min}$.

3.2.5 Phase 5 – Pore System and Core Integrity Evaluation

Core integrity and the change in the core pore system would be evaluated before and after the core flooding stage. This is done by using the scratch test along with the NMR technique. The scratch test is a simple new test that can evaluate the rock mechanical properties. The test provides a continuous measurement for the whole core length. This acquires the test results more measurement resolution than the conventional uniaxial compressive strength (UCS) test. Schei et al. (2000) showed that the accuracy of the scratch test results can be comparable to the UCS test.

Figure (3.22) shows the scratch test machine used for this study. The scratch test involves creating a groove on a surface of a specimen using a cutter. The test is carried out under highly controlled kinematic process as the cutting depth and the cutter speed are highly controlled and kept constant. The groove depth reaches only 1mm or less, depending on the sample strength. The magnitude of the force applied is controlled by different factors such as the rock mechanical properties, the groove geometry and the cutter geometric characteristics. While scratching the sample, the force applied against the cutter is monitored and then interpreted to give an indication of the rock strength, the UCS value (Richard et al. 2012). The test is conducted along the entire specimen length. The cutter in this test has a width of 10 mm with a back rake angle of 15° and velocity of 4 mm/s. The back-rake angle is the angle between the cutter inclination angle with respect to the vertical. By using the sonic mode in the machine, the compressional and shear waves (V_P and V_S) are measured along the sample length. The values of the sonic waves along with the rock density (ρ) can be used to calculate the dynamic elastic properties of the rock sample by using the following two Eqs. (3.2 & 3.3).

$$E_{\text{dyn}} = \rho V_s^2 \left(\frac{3 V_p^2 - 4 V_s^2}{V_p^2 - V_s^2} \right) \quad (3.2)$$

$$v_{\text{dyn}} = \frac{V_p^2 - 2 V_s^2}{2 (V_p^2 - V_s^2)} \quad (3.3)$$

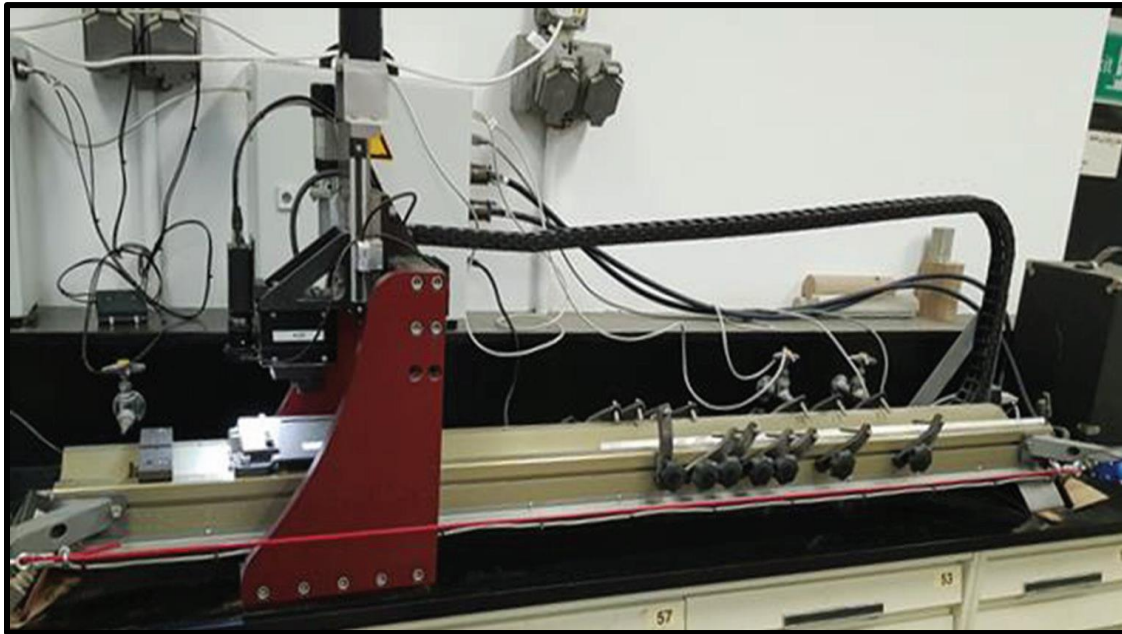


Figure 3.22 An overview of the scratch test machine used in this study

Oxford Geospec NMR rock core analyzer was used for scanning the core with NMR technique before and after the flooding, Figure (3.23). This version comes with an operating frequency of 2 MHz. It has two different cells, the standard one that can withstand samples of 2” diameter and 5” length. The other “P5 Overburden cell” can withstand samples of 1.5” diameter and 2” length. The maximum working pressure and temperature of this device are 5000 psi and 100 °C, respectively.

At the end, a complete screening and parametric design for the optimum stimulation process using this novel approach can be implemented by gathering the results from all the aforementioned steps and phases.



Figure 3.23 Oxford Geospec NMR rock core analyzer

CHAPTER 4

Results and Discussion

4.1 Results of Testing Different Oxidizers

As previously mentioned, this study contains the trials of three different oxidizers which are sodium bromates (NaBrO_3), ammonium persulfate ($(\text{NH}_4)_2\text{S}_2\text{O}_8$) and potassium permanganates (KMnO_4). Sodium bromates was initially examined in the literature and its ability to oxidize ammonium fluoride and generate HF acid was already proven. Moreover, the optimum oxidizer: salt ratio was determined to be 1:2 molar concentration (Hull et al., 2019). The results of adding sodium bromates to ammonium fluoride along with the thermochemical compounds to a pure quartz samples for 24-hours at 90 °C show a change in the quartz sample weight from 3.4040 g to 3.3235 g with some notches on the surface of the quartz sample, see Figures (4.1a and 4.1b). This reduction in weight by 80.50 mg proves the formation of HF acid that could dissolve the silica minerals and reduce the quartz weight.

The ICP results of the aforementioned experiment final solution shows a silicon ion (Si^+) concentration of 91.43 ppm or 0.009143 wt%. The volume of the solution in this experiment was 100 ml. This reflects a mass of dissolved silica of only 19.6 mg. the difference between the mass change of the quartz sample (80.5 mg) and the calculated amount of dissolved silica from ICP analysis (19.6 mg) is attributed to the development of the secondary and tertiary reaction of the dissolved silica with generated HF. These reactions precipitate the Si^+ ions in the solution as previously mentioned. The effluent from this experiment is shown in Figure (4.2). The yellowish-brown color of the effluent

is attributed to the existence of bromide ions. There is some potential of the evolution of bromine gas as a side product of this reaction. Bromine is highly toxic and high safety precautions should be taken while dealing with it. However, in the presence of Ca ions, calcium bromide can be formed and dissolved in the solution.

Heat is not only the desirable product out of the exothermic reaction. Nitrogen gas (N_2) also evolves and increases the system pressure by about 200 psi. These initial observations prove the validity of the concept of the ability to generate HF acid by using ammonium fluoride (NH_4F) as an acid precursor and react it with the strong oxidizer, sodium bromates ($NaBrO_3$), in the presence of the exothermic reaction on the used thermochemicals.



Figure 4.1 (a) shows the quartz sample before going under the chemical reactions with a weight of 3.404 gm with sharp edges and clear surface. (b) the quartz sample after going under the chemical reactions with a weight of 3.3235 gm with notches on the surface due to the effect of HF acid generated.



Figure 4.2 The effluent from the oxidation of ammonium fluoride with sodium bromates in the presence of thermochemicals

The second oxidizer used in this study is ammonium persulfate ($(\text{NH}_4)_2\text{S}_2\text{O}_8$). Concentrations of 0.1, 0.5 and 1 M of the ammonium persulfate were mixed with 2 M of ammonium fluoride salt along with the thermochemicals. All the chemicals are mixed together giving a pure transparent solution then added to highly pure quartz samples. The weight change of the quartz samples after being dispersed for 24-hrs at 90 °C was recorded as well as the concentration of Si^+ ions was monitored using ICP. The initial and final weights of the quartz samples before and after the test are shown in Table (4.1). The ICP results showing the Si^+ ions concentration corresponding to the different oxidizer concentration are shown in Figure (4.3).

From the results of this experiment, we can detect the relationship between the oxidizer concentration and the generated HF that dissolves the silica minerals. Both the weight

change of quartz and the Si⁺ ions concentration show that the more the oxidizer concentration, the more dissolved silica. This essentially means the more the oxidizer concentration, the more the HF generated. This gives us an indication about how to control the amount of HF generated down into the formation. Therefore, the oxidizer concentration will be of critical importance when designing the field acid job.

There is a good compatibility between the ammonium persulfate and the other reactants. This is so clear from the transparency of the effluent samples taken from the previous test with different concentrations of ammonium persulfate, see Figure (4.4). In addition, the Si⁺ ions concentration corresponding to 1 molar of persulfate (329.2 ppm) is much higher than that of using 1 molar sodium bromate (91.43 ppm). These observations give ammonium persulfate a privilege as a more suitable oxidizer than sodium bromates.

Table 4.1 The corresponding Si⁺ ions concentration (ppm) and the quartz samples weight change (mg) with different oxidizer concentrations

Persulfate conc. (M)	Quartz samples initial wt. (g)	Quartz samples final wt. (g)	Quartz samples wt. change (mg)
0.1	2.7699	2.7240	45.9
0.5	2.5100	2.4435	66.5
1	2.6838	2.5969	86.9

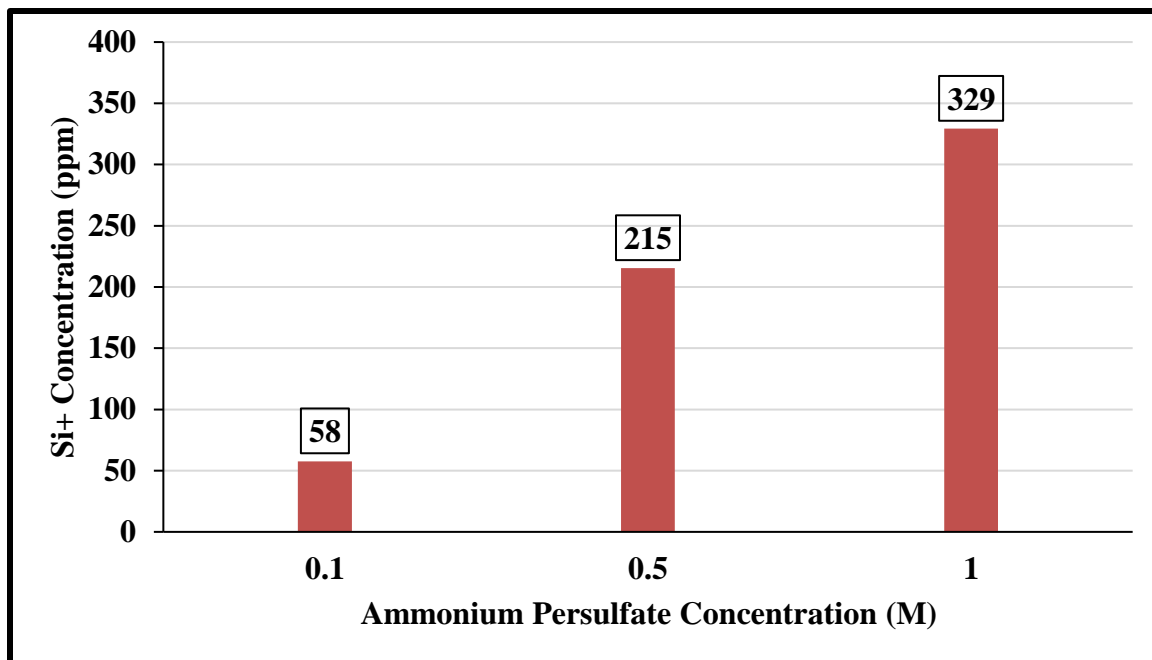


Figure 4.3 The Si⁺ ions concentration resulted from the effluent of mixing different concentrations of ammonium persulfate oxidizer with 1 M ammonium fluoride and the thermochemicals

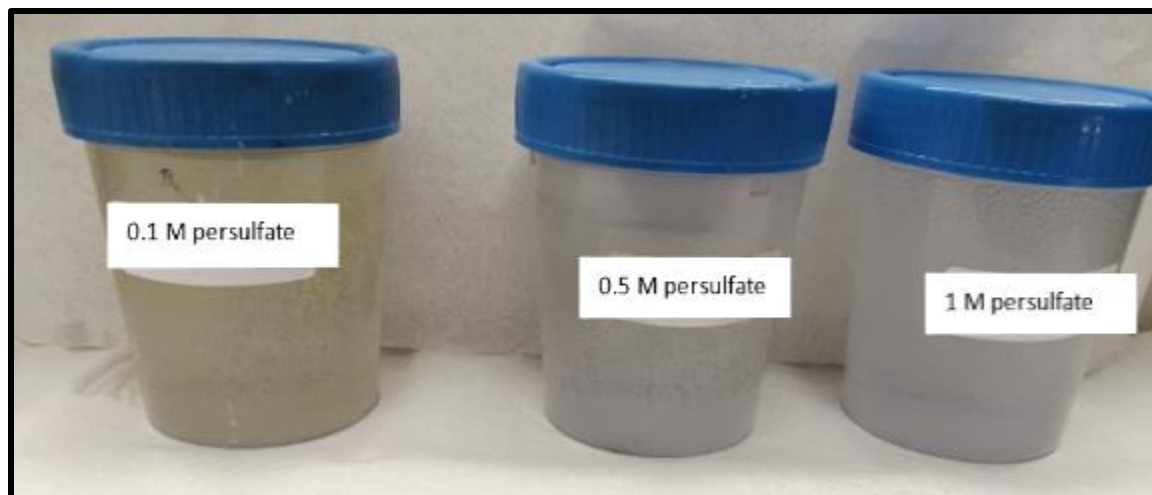


Figure 4.4 The effluent of 0.1, 0.5 and 1 M concentration of ammonium persulfate added to 2 M of ammonium fluoride and mixed with the thermochemicals.

4.2 Different Clay Minerals solubility in the in-situ HF generating fluids

As stated above, one of the main objectives of this research is to check the solubility of three main different clay groups (chlorite, illite and kaolinite) in the new acid generating fluids. Prior to that, XRF analysis is carried out to determine the weight percentage of the different elements exist in each clay group. As shown in Figures (4.5-4.7), all the three clay groups show high silicon (Si) concentration that ranges from 32 % for the kaolinite up to 57% for illite clay. The second most abundant element in the three clays is aluminum (Al). Al represents about 60 wt.% of kaolinite clay where it represents about 21 and 16 wt.% for chlorite and illite clays respectively. Chlorite is distinguished by the high Fe content (23%) compared to the other two clay groups that have much lower Fe content. Additionally, the potassium content of both chlorite and illite is quite close, 10 and 12 wt. % respectively, while kaolinite has almost no potassium ions. This elemental analysis will be of great benefit while analyzing the effluent after the solubility test the acid generating fluids and the thermochemicals.

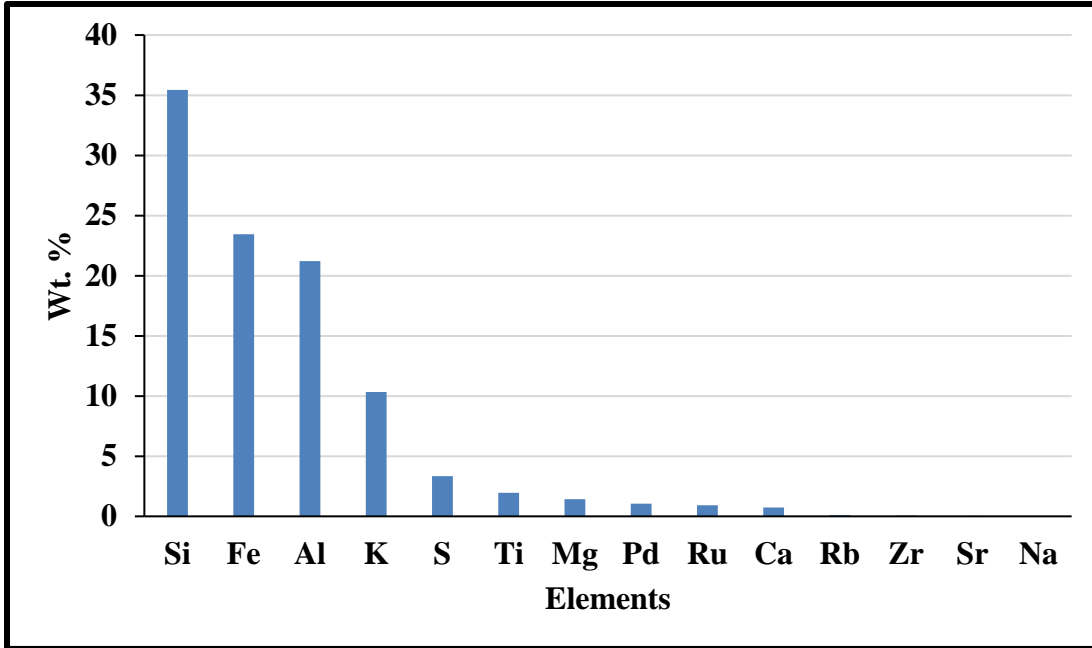


Figure 4.5 The XRF results for the chlorite clay showing the different elements in this clay type.

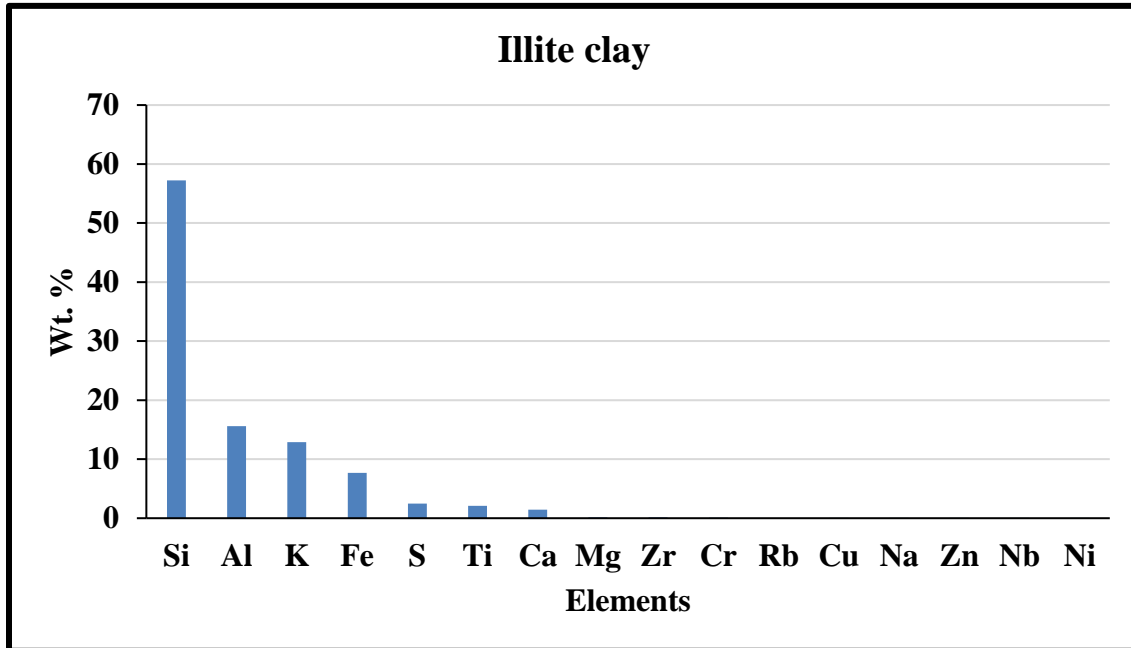


Figure 4.6 The XRF results for the illite clay showing the different elements in this clay type.

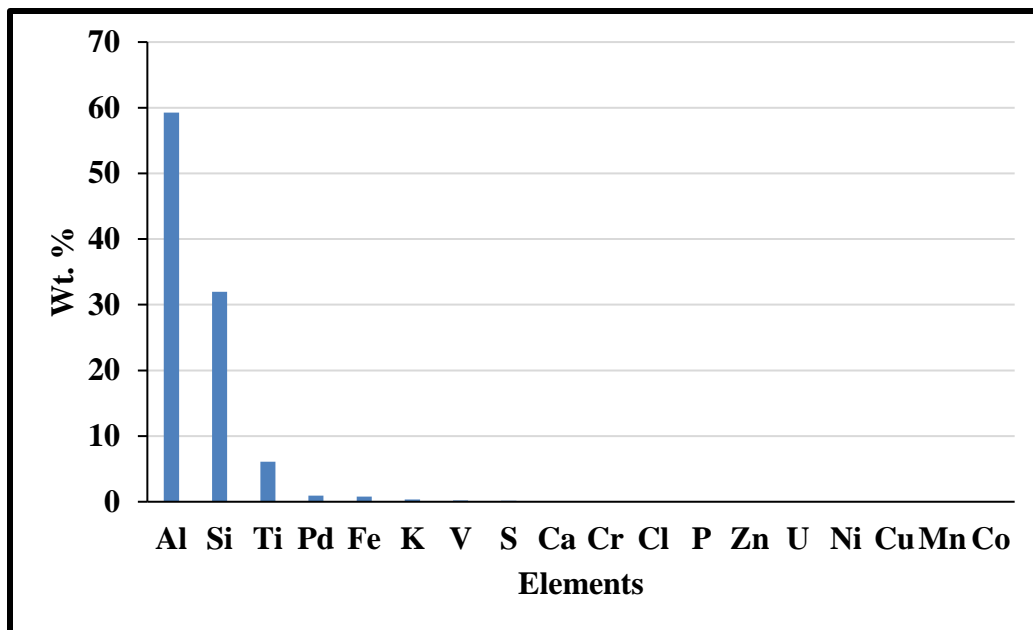


Figure 4.7 The XRF results for the Kaolinite clay showing the different elements in this clay type.

Dispersing 5 g of each clay in 100 ml of the main chemical mixture leads to dissolve the clay mineral to some extent. The ICP analysis for the three effluents measuring the concentration of the major elements in the three clay groups is shown in Figure (4.8). The elements concentration is measured in the unit of mg/l after being diluted up to 100 times. For illite clay, the K ions are of the highest concentration in the dissolution effluent with a concentration of 1534 mg/l. This is followed by the concentrations of Si (830 mg/l), Fe (483.6 mg/l), Al (196.2 mg/l), Mg (53.75 mg/l) and Ca (0.448 mg/l). If we assume these elements to be the only dissolved ones in the solution, this would correlate to 6.2 wt.% of the initial clay dispersed in the solution, Figure (4.9). This means at least 310 mg of the dispersed illite has been dissolved by the action of the generated acid in the presence of the thermochemical reaction. This is -of course- an underestimating assumption since we only measured the concentration of the major elements, not all the elements, in the effluent solution.

For chlorite clay group, K ions are the most abundant ions in the effluent with a concentration of 1063 mg/l. This is followed by the concentrations of Fe (1010 mg/l), Si (733.8 mg/l), Al (266.7 mg/l), Mg (114.4 mg/l) and finally Ca (17.89 mg/l). This would correlate to about 6.4% fraction of the initial clay weight to be dissolved in the acid generating fluid. Since the initial weight of the clay is 5 g, the dissolved clay weight is about 320 mg at least. The same situation is applied for the kaolinite clay where the Si ions represent the most dissolved ions from this clay with a concentration of 1065 mg/l, Figure (4.8). This is followed by the concentrations of Al (767 mg/l), K (60.08 mg/l), Fe (38.44 mg/l) and finally Mg (0.282 mg/l). About 3.9 wt.% (195 mg) of the initial kaolinite weight is dissolved by the action of the acid generating chemicals.

These results confirm on the positive capability of the novel chemical mixture to generate HF acid. The generated acid is capable of dissolving the silica mineral when added to the pure quartz samples. Moreover, it dissolves the different clay minerals such as illite, chlorite and kaolinite. Since silica and clays represent the main constituents of sandstone rocks, the novel chemical mixture that generates in-situ HF acid is highly recommended to stimulate such formations. This recommendation is supported by the coreflooding tests shown in the coming sections.

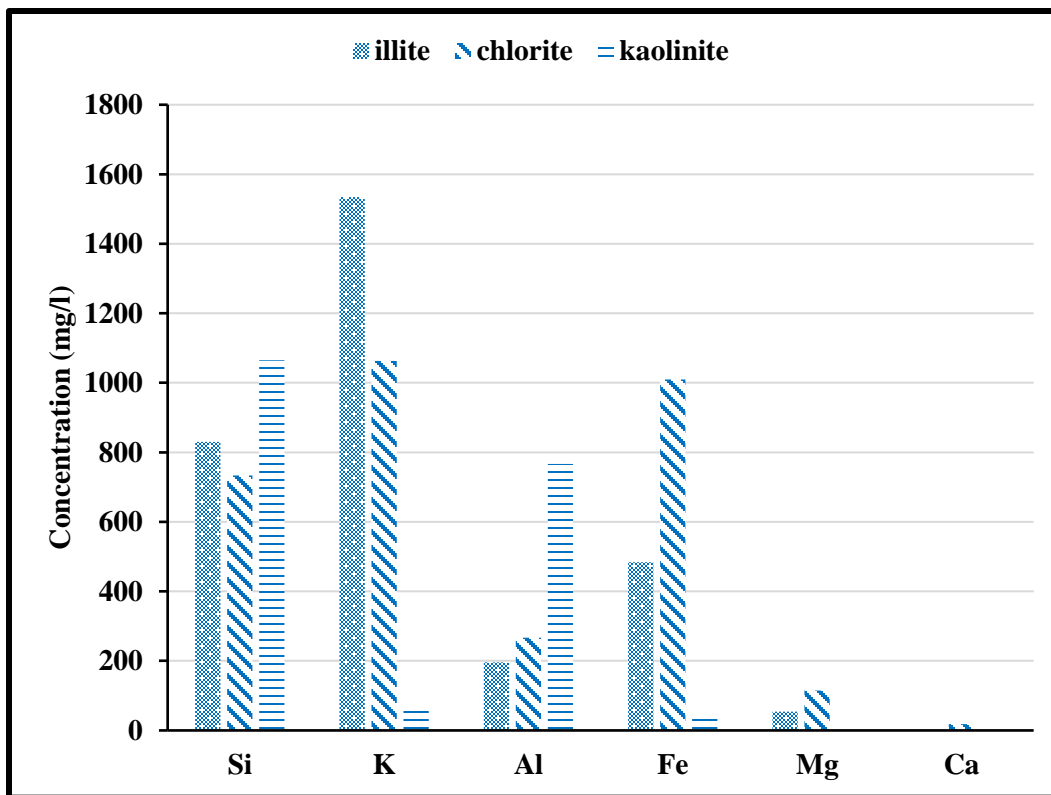


Figure 4.8 The concentration of the major elements dissolved from illite, chlorite and kaolinite clays by the action of the novel chemical mixture measured by ICP-OES

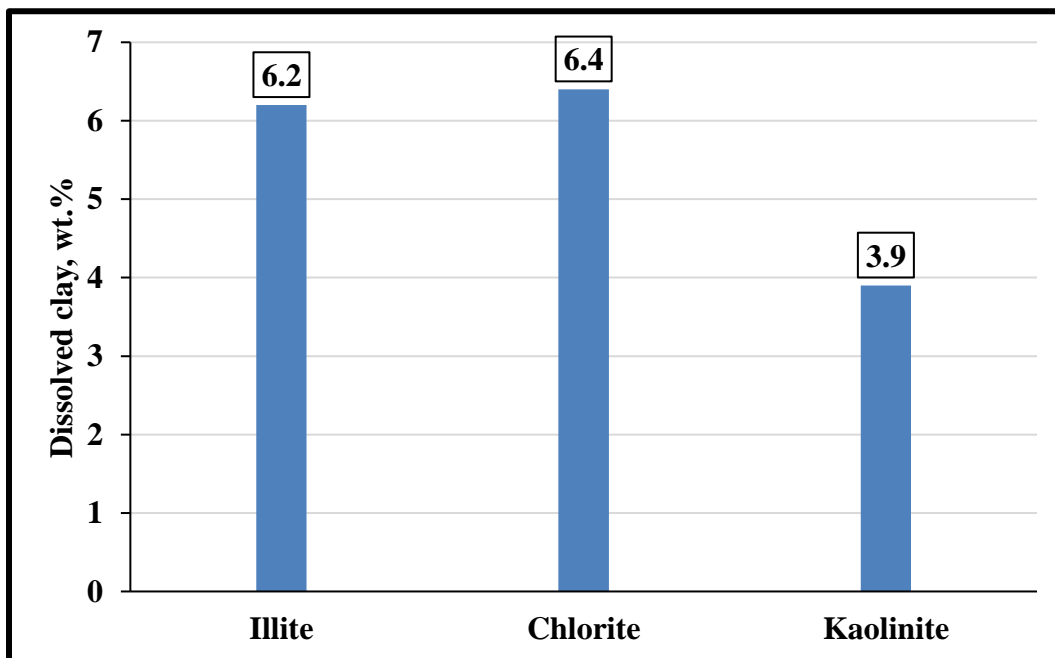


Figure 4.9 The dissolved fraction from the three clay groups (illite, chlorite and kaolinite) by the action of the acid generated from the novel chemical mixture.

4.3 Acidizing Berea and Scioto Cores without using Thermochemicals

The results shown in this part are related to the acidizing process that carried out without using the thermochemical reaction. Instead, an external heating source (an oven) was used to supplement the required heat for the acid generating reaction.

4.3.1 Gray Berea Sandstone Core

The initial core permeability was measured using the 3 wt.% KCl solution. At a stabilized flow rate of 2 cm³/min, the core permeability was calculated to be 33 mD. Flushing the core with 5 PV HCl having a concentration of 7 wt.% led to decrease the core permeability to 31 mD (the core lost about 4.8 % of its original permeability). This can be attributed to the reaction of HCl with the clay minerals (chlorite, illite and kaolinite) existing in the core. This matches with the observations of Thomas et al., (2001) and Kamal et al. (2019) about the effect of HCl acid on the clay containing rocks. HCl reacts with chlorite to produce ferric hydroxide which is a gel material that can plug the pore throats. Also, HCl reacts with both illite and kaolinite and cause fines migration. The main treatment started by injecting 1 PV of the acid generating solutions (ammonium fluoride and sodium bromates). The system temperature is then increased to 150°C to initiate the endothermic reaction of acid generation. The inlet and outlet valves of the core are then closed and the first soaking period of about 30 min was performed. The core inlet pressure started to increase indicating the start of the reaction of HF acid generated with the core minerals. The maximum reached inlet pressure during this stage was about 611 psi. The same flushing and soaking procedures were followed during the second and third cycles. The increase in the inlet pressure during the second and third cycles was 456 and 424

respectively. This is attributed to the inactive acid reaction due to the dissolution of the sandstone minerals from the acid initial path. The inlet pressure profile corresponding to each flooding stage is shown in Figure (4.10) while the profile of the inlet-outlet pressures and the difference between them are shown in Figures (4.11 & 4.12).

Core permeability has increased immediately after the first treatment cycle and reached 41 mD. After the second cycle, the permeability increased more and reached about 44 mD. No noticeable change in the core permeability was found after the third treatment cycle. Finally, the core is flushed by 3wt.% KCl from the reverse direction (back flow) and the final permeability was measured. The final permeability measurement showed an enhancement in the core permeability by about 42 %. All the effluent was collected for ICP-OES analysis to determine the total amount of the dissolved Si^+ ions. The permeability measurement after each flooding stage is shown in Figure (4.13).

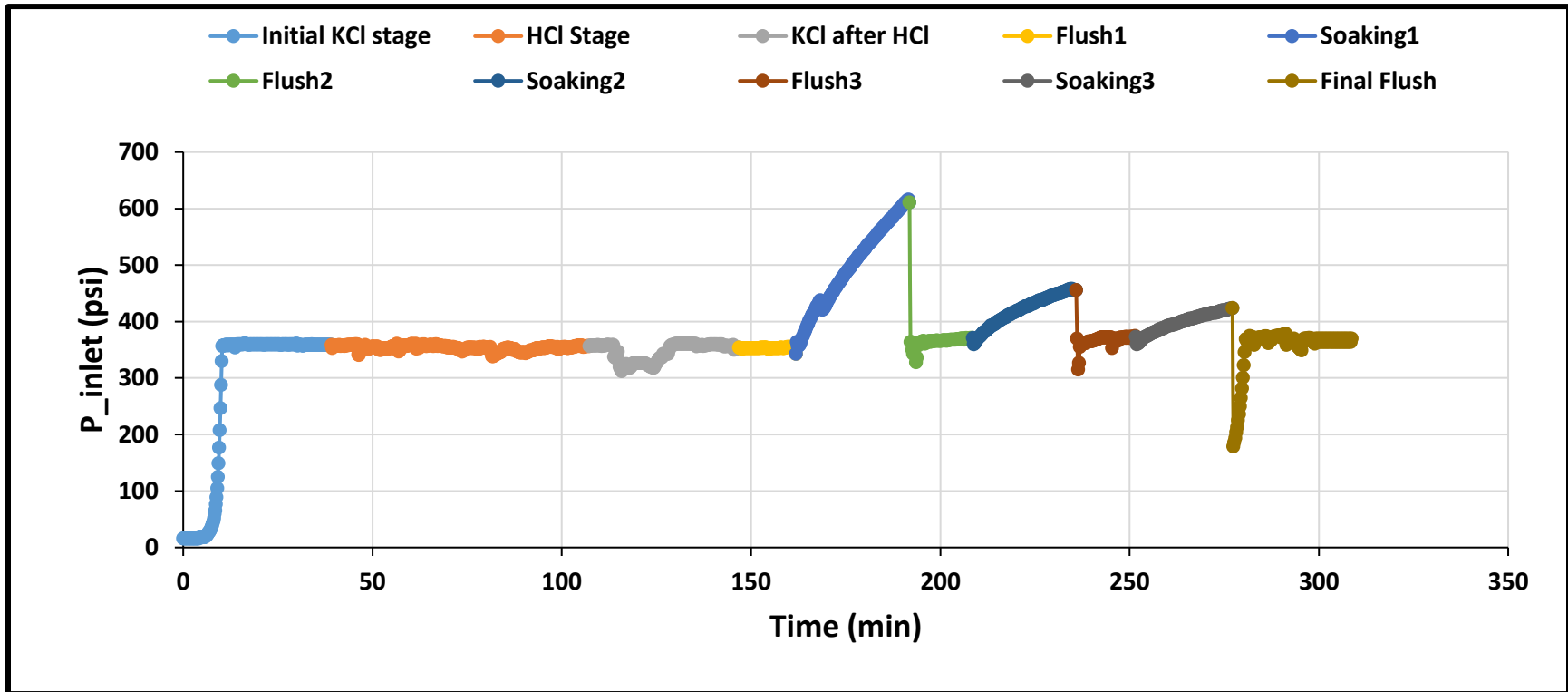


Figure 4.10 The inlet pressure profile (psi) during the different core flooding stage measured versus the cumulative time (min).

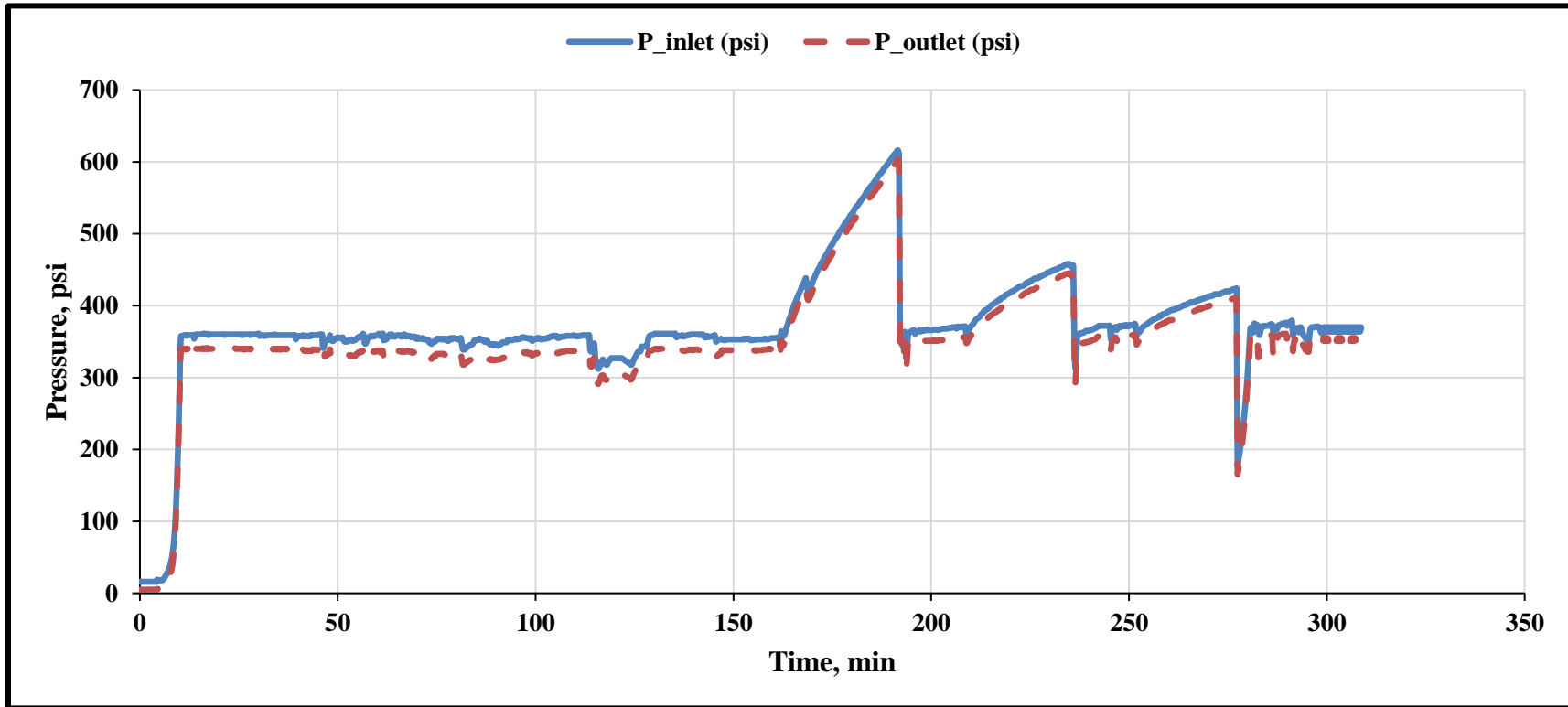


Figure 4.11 The inlet-outlet pressure profile (psi) measured during the different core flooding stages measured versus the cumulative time (min)

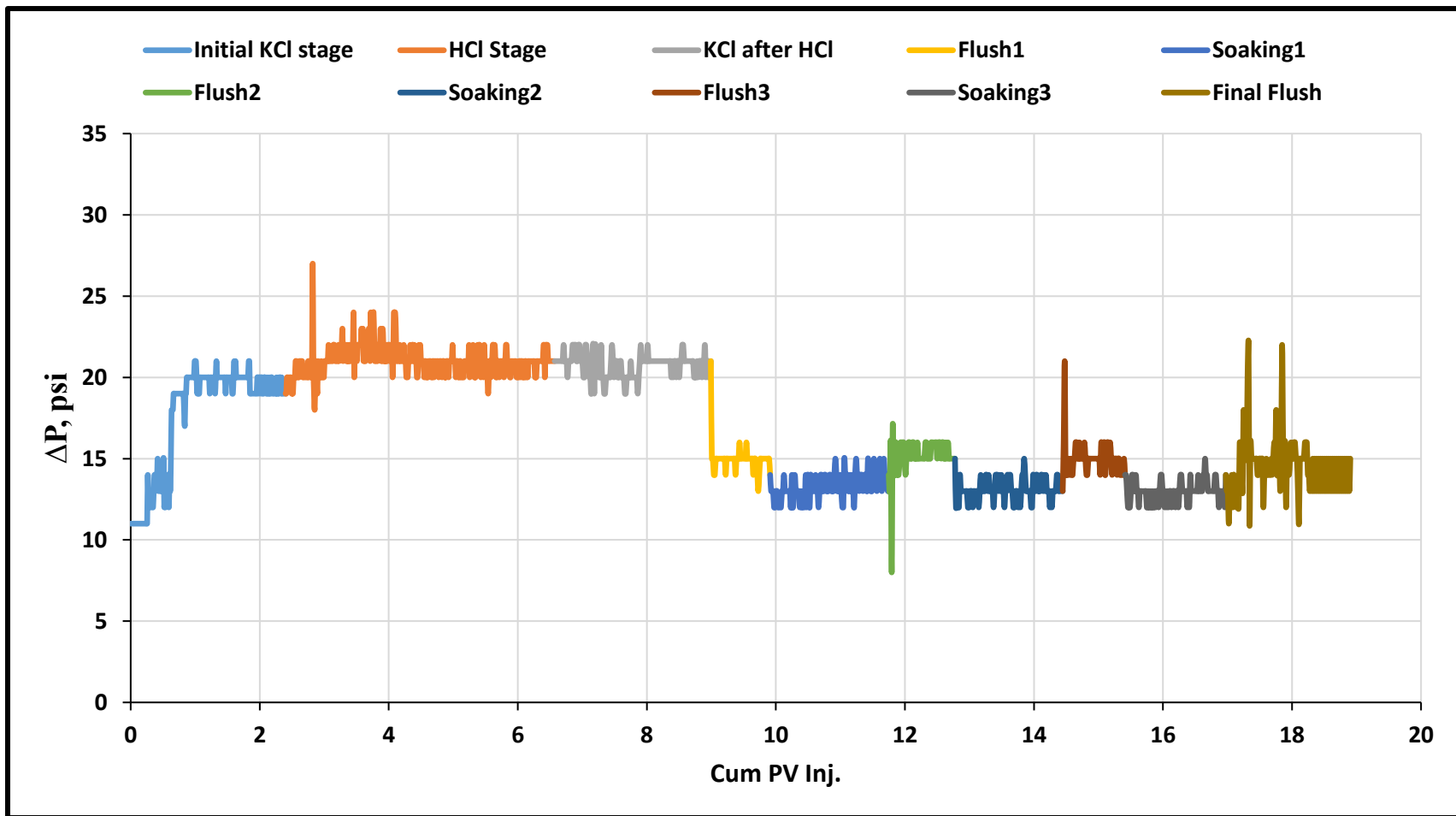


Figure 4.12 The pressure difference profile (psi) measured during the different core flooding stages measured versus the cumulative pore volume injected

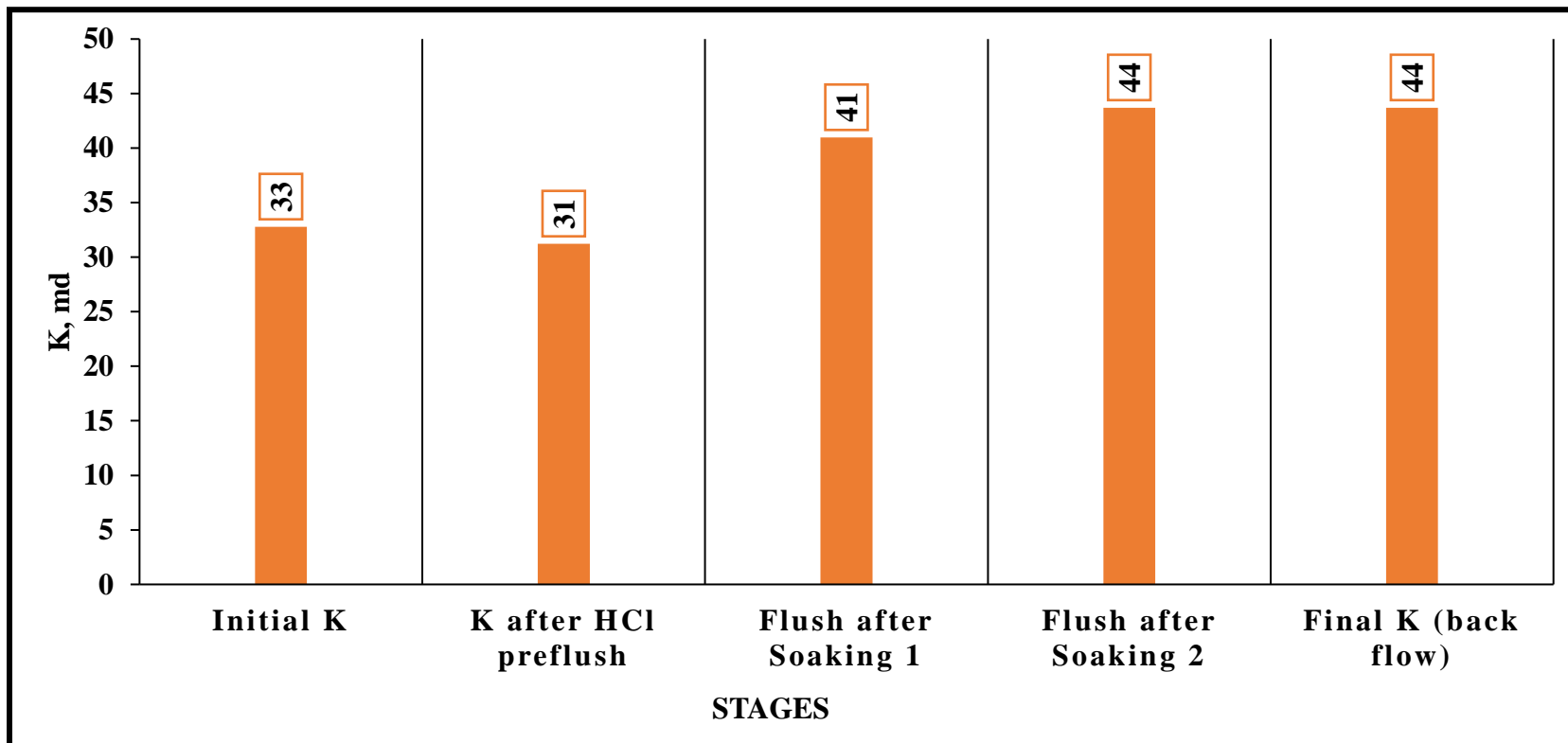


Figure 4.13 The Gray Berea core permeability values measured in mD as calculated after each treatment cycle using 3 wt.% KCl solution

The ICP-OES results showed the presence of Si^+ ions in each effluent after each treatment stage as shown in Figure (4.14). This, again, proves the generation of HF acid inside the Berea sandstone core. Figure (4.15) shows the cumulative amount of the chelated Si^+ ions from the core after each treatment cycle. There is a gradual increase in the cumulative amount of the chelated Si^+ ions after the first two cycles. However, there was a sharp increase in the amount of the Si^+ ions chelated from the core after the third cycle. This is also clear from analyzing the effluent from the after flush stage. The reason behind this is the maturity of the reaction after the first two cycles and the ability of the injected chemical to be exposed to a larger area of the rock. Moreover, back flow of the injected KCl solution during the after flush stage removed all the cations produced from the reaction of the in-situ generated HF and the core minerals. The total chelated amount of Si^+ ions from the core reached 10.5 mg. This is corresponding to a total dissolved amount of 22.5 mg of quartz (silica). This could be the reason behind the permeability enhancement of the Gray Berea sandstone core after this treatment process.

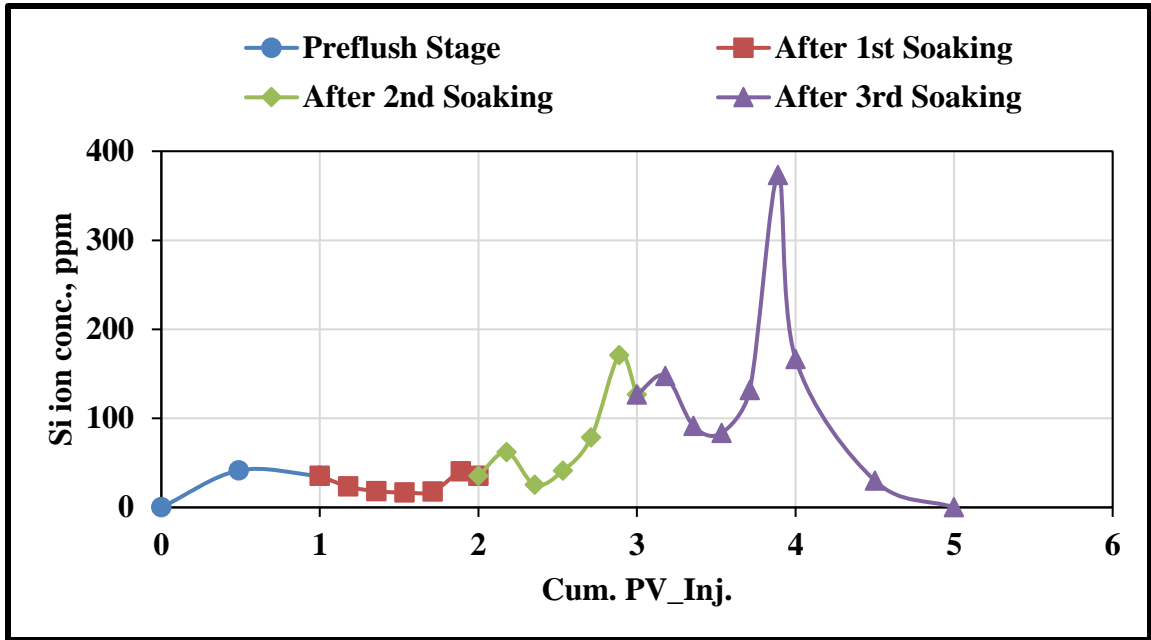


Figure 4.14 The chelated Si ion concentration in each flushing cycle as measured from the core flooding effluent that was analyzed using ICP-OES

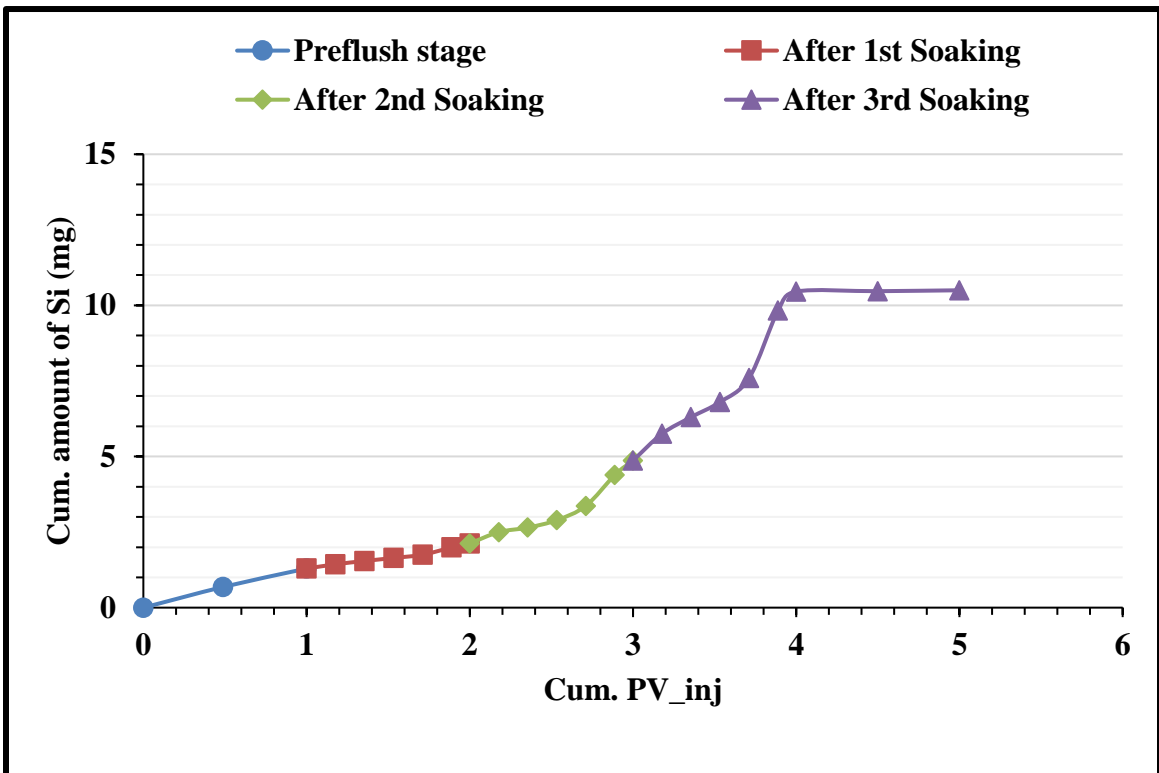


Figure 4.15 The cumulative amount of Si chelated calculated in (mg) from the Gray Berea core after each treatment cycle

4.3.2 Scioto Sandstone Core

The Scioto core sample had an initial permeability of 0.55 mD measured through flooding the core with 3 wt% KCl solution at steady state conditions of flow rate of 0.5 cm³/min. After the core was flooded with HCl, the permeability dropped to 0.48 mD. The reason beyond this is that HCl not only dissolved the calcite content in the core but it also reacted with the clay minerals – mainly illite- inside the core. The reaction of HCl with illite clays broke down the clay particles and led to fines migration and pore plugging. However, permeability got improved after flooding the core with the main flush mixture. The main flush stage consisted of three flushing-soaking cycles of the main chemicals. The inlet pressure profile corresponding to each flooding stage is shown in Figure (4.16) while the profile of the inlet-outlet pressures and the difference between them are shown in Figures (4.17 & 4.18). The in-situ generated HF acid reacted and dissolved the quartz, feldspars and clay particles inside the core. The core permeability was finally increased from 0.48 to 0.66 mD achieving an enhancement of 37.5%. Figure (4.19) shows the Scioto rock sample permeability before and after flooding with the new formulation.

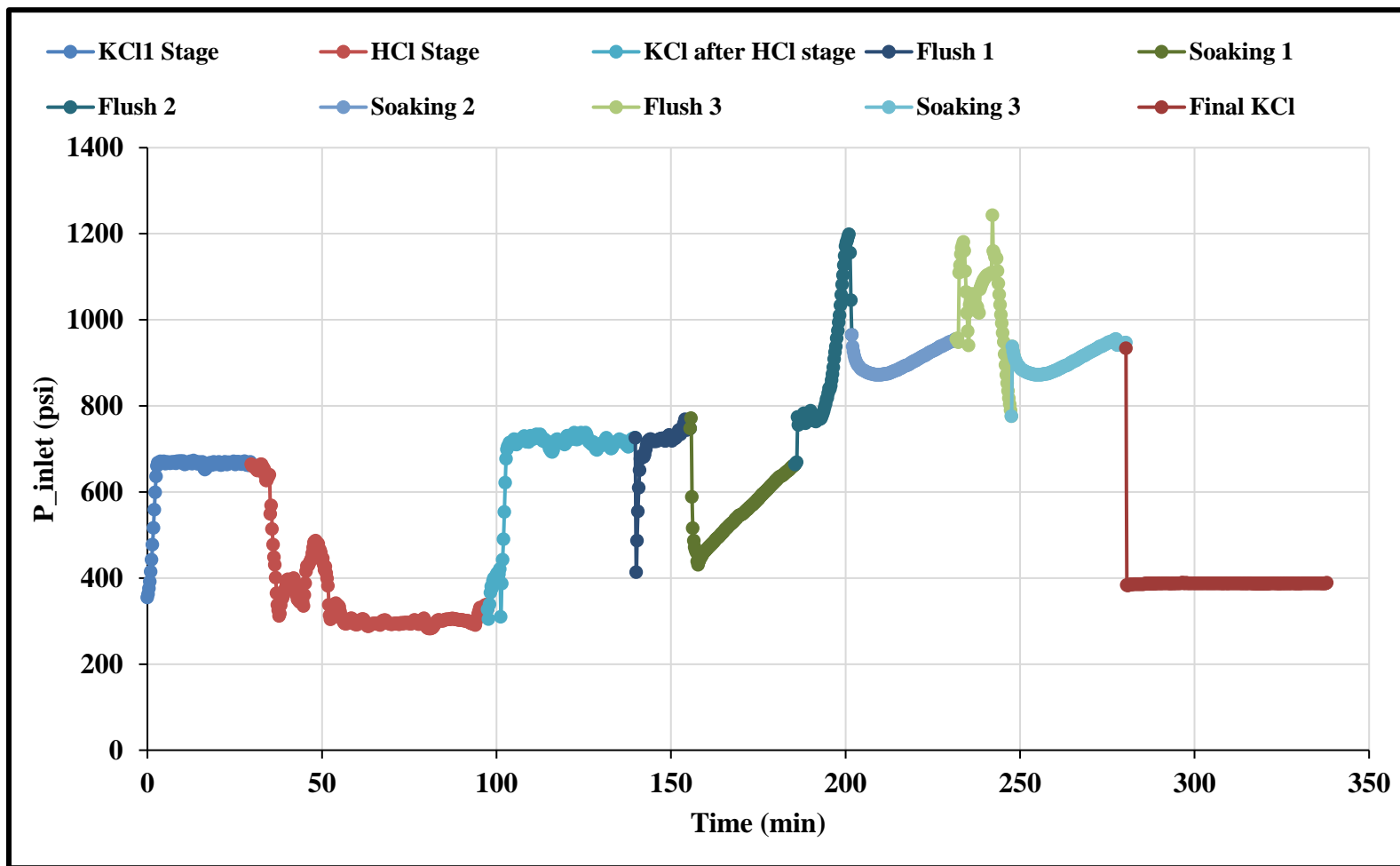


Figure 4.16 The inlet pressure profile (psi) during the different core flooding stages measured versus the cumulative time (min)

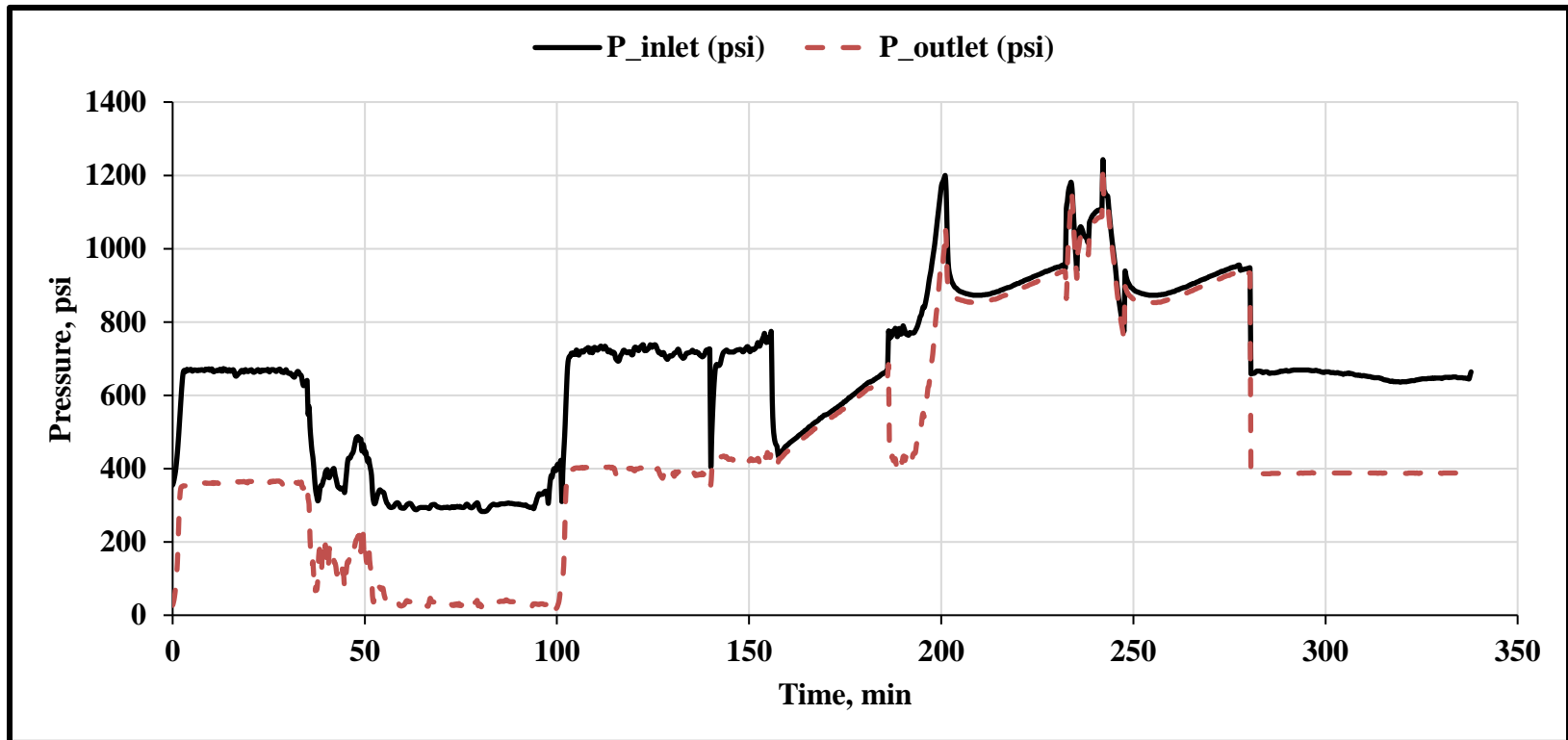


Figure 4.17 The inlet-outlet pressure profile (psi) measured during the different core flooding stage measured versus the cumulative time (min).

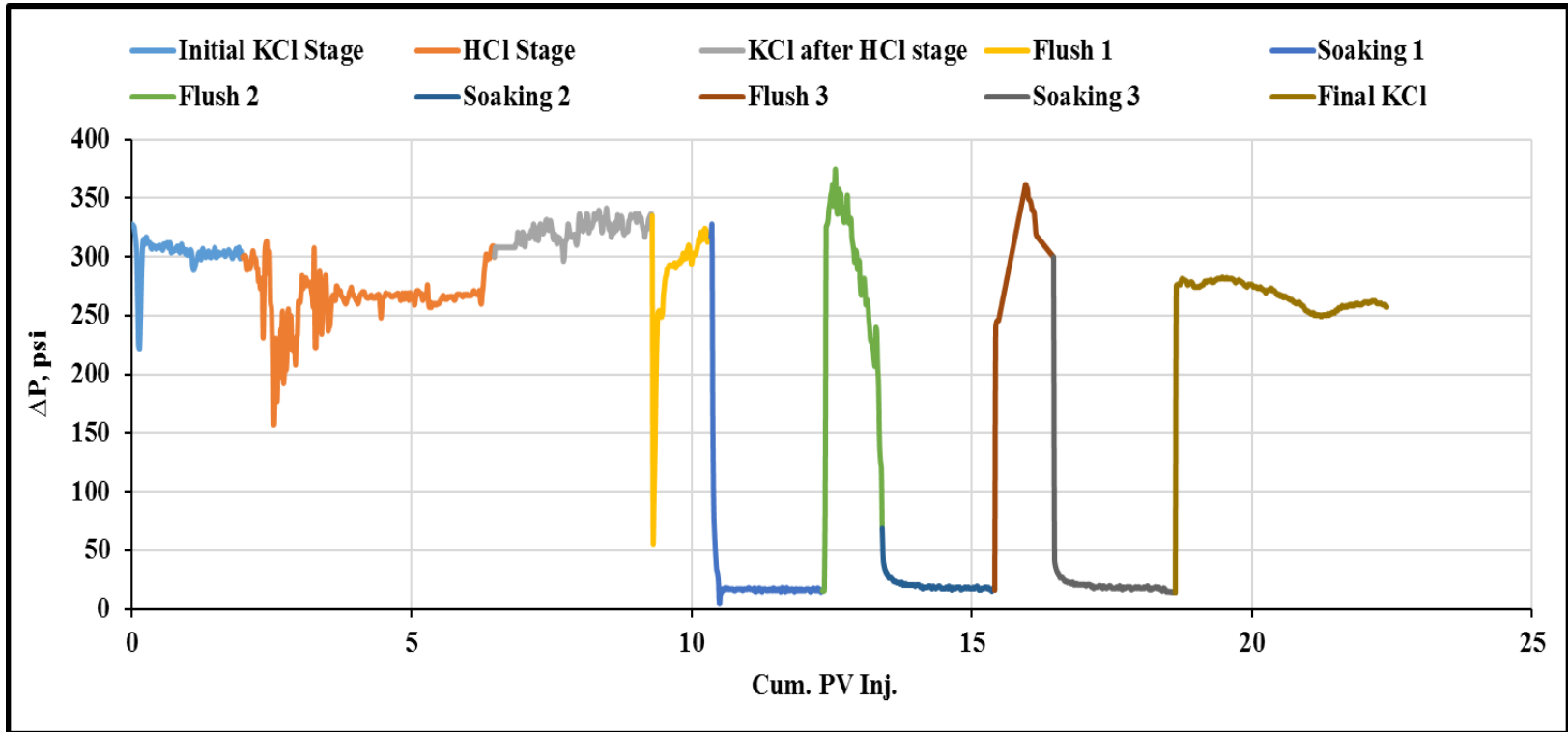


Figure 4.18 The pressure difference profile (psi) measured during the different core flooding stage measured versus the cumulative time (min).

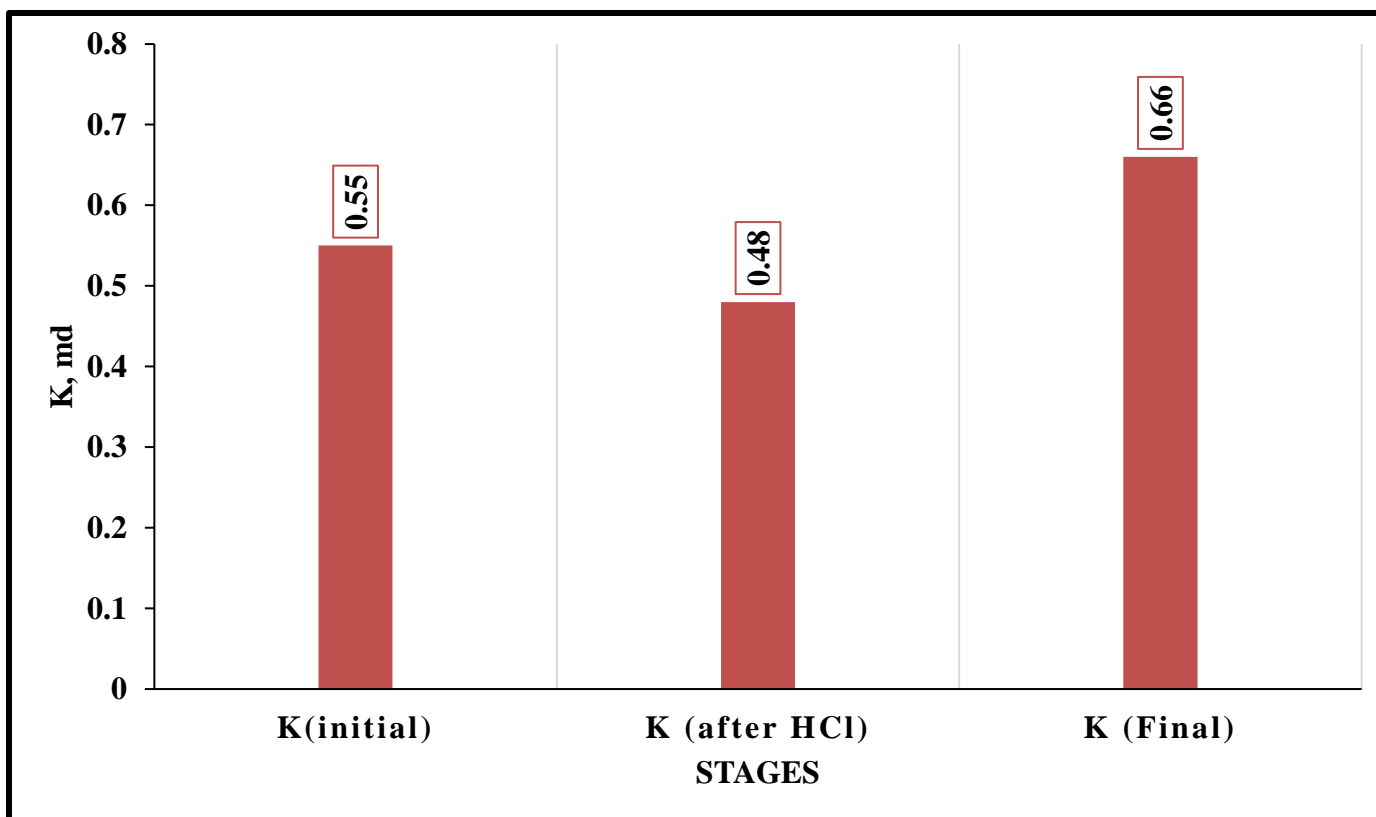


Figure 4.19 The Scioto core permeability values measured in mD as calculated after each treatment cycle using 3 wt.% KCl solution.

To assess the amount of Si^+ ions dissolved from the core, the core flooding effluent after each stage is collected and went through ICP analysis. All the effluent samples show the presence of Si^+ with different concentration, see Figure (4.20). The Si ions concentration in the effluent started to decrease after the third cycle. This indicates the inactive acid reaction with the already flooded parts of the core. This also may give an indication about the development of the silica precipitation reactions. The cumulative amount of Si^+ ions in mg was calculated as shown in Figure (4.21). The total dissolved amount of Si^+ ions from Scioto core reached more than 49 mg. This is corresponding to a total dissolved amount of 104.66 mg of quartz (silica). This dissolved amount of the Si^+ ions enhanced the core permeability and overcame the damage caused by the reaction of HCl with the core clay minerals.

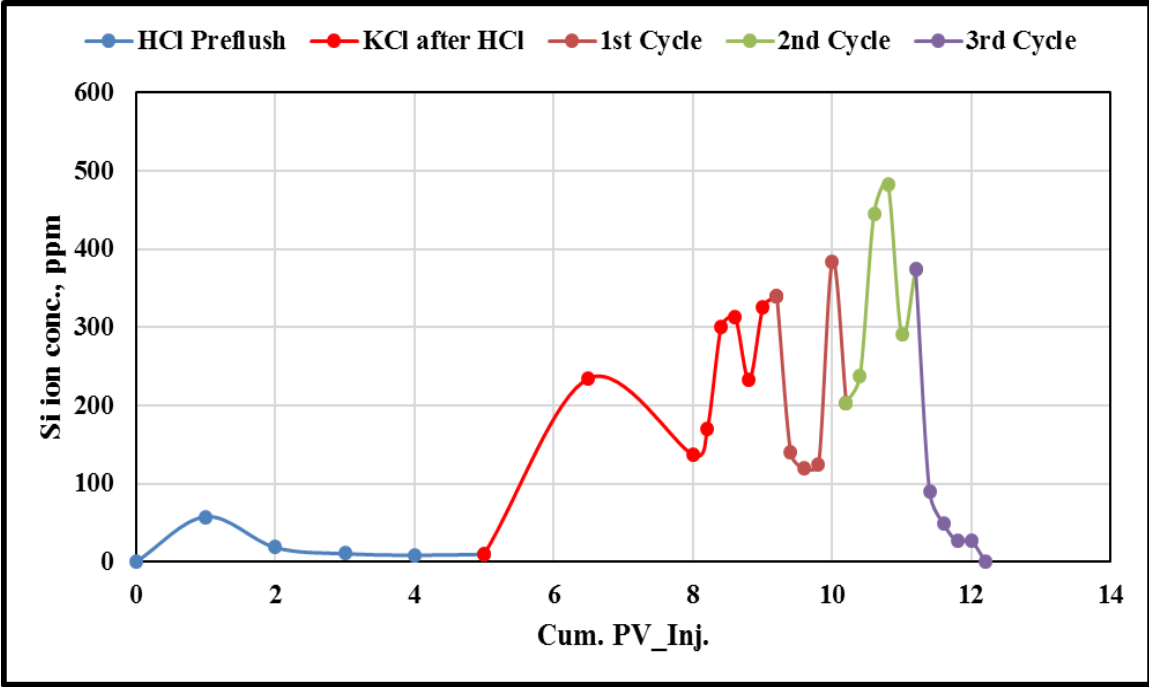


Figure 4.20 The chelated Si ion concentration in each flushing cycle as measured from the core flooding effluent that was analyzed using ICP-OES

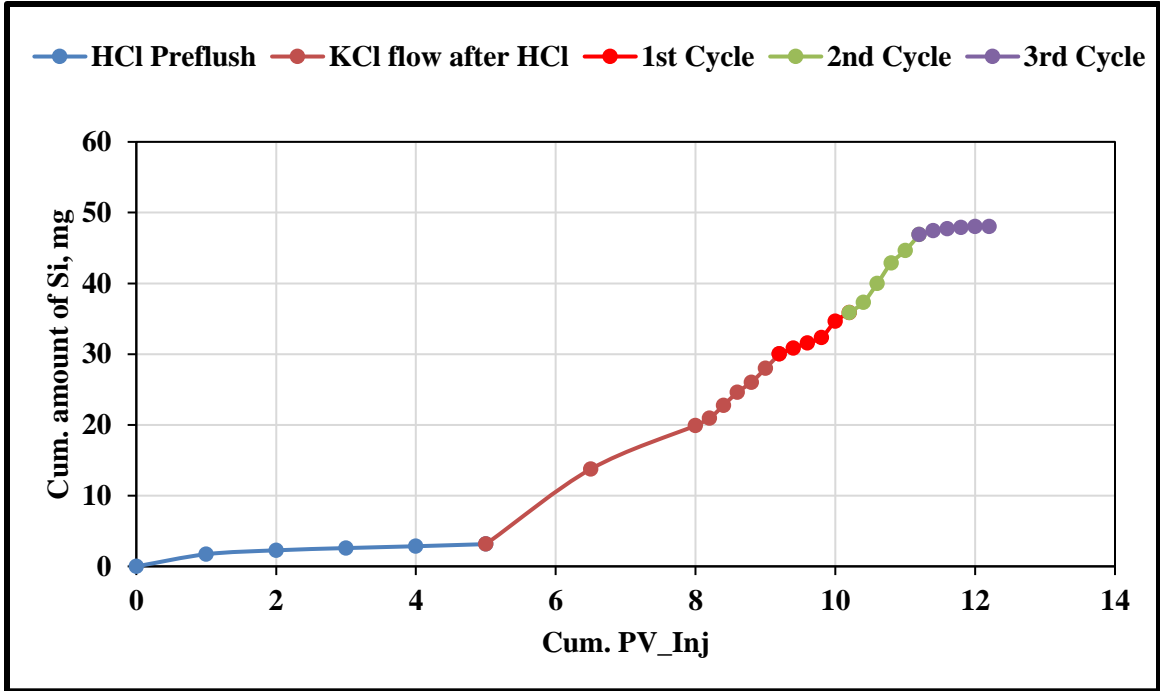


Figure 4.21 The cumulative amount of Si chelated calculated in (mg) from the Scioto SS core after each treatment cycle

4.4 Pore System Change Monitoring using NMR Scanning

NMR measurements for the Gray Berea and Scioto cores before and after the treatment showed an increase in the cores' final porosity. This is attributed to the amount of silica and other minerals that were dissolved from the core by the generated acid. Moreover, the NMR measurement did not exhibit any change in the original pore system which indicates no plugging created. As shown in Figures (4.22 & 4.23), the relaxation time (T_2) curves of the cores before and after the treatment represent only one main peak. This means that the cores preserved only one pore system and no additional pore systems were created, just the existing pores were enlarged. The major T_2 value for the fresh Gray Berea core was about 158 ms while it reached more than 280 ms after acidizing treatment. This indicates the enlargement happened to the core pore system after the in-situ acid treatment. For the Scioto core, the major T_2 measured before and after the treatment was almost the same.

This indicates the generation of new pores with the same size as the old ones. The creation of these new pores is the main reason for the increase in the total core porosity.

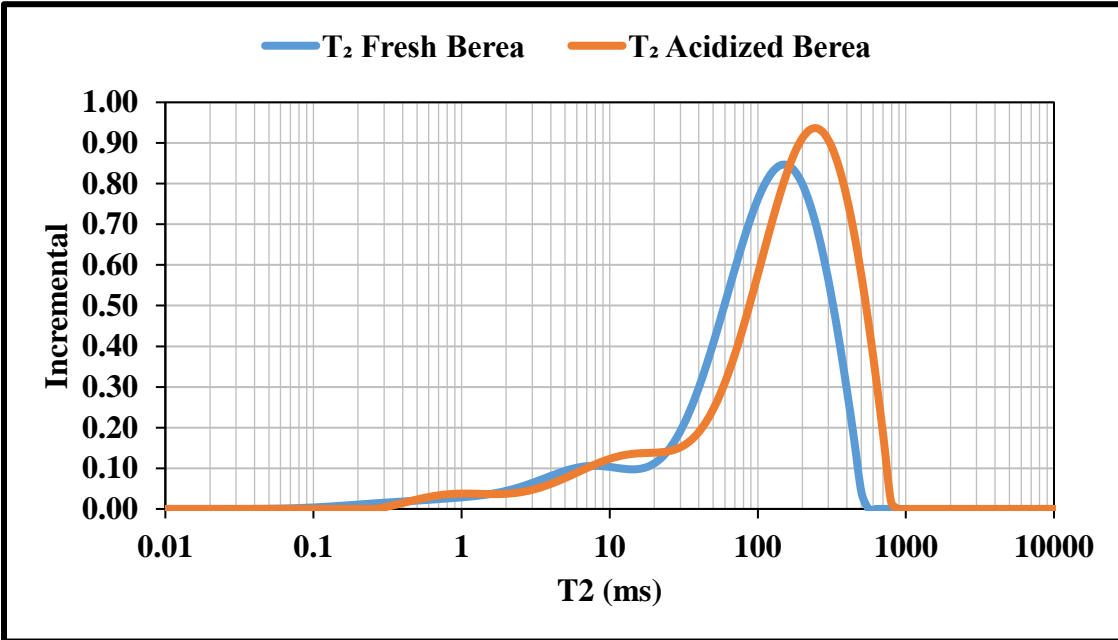


Figure 4.22 The relaxation time T₂ measured by the NMR technique for both fresh and acidized Gray Berea core

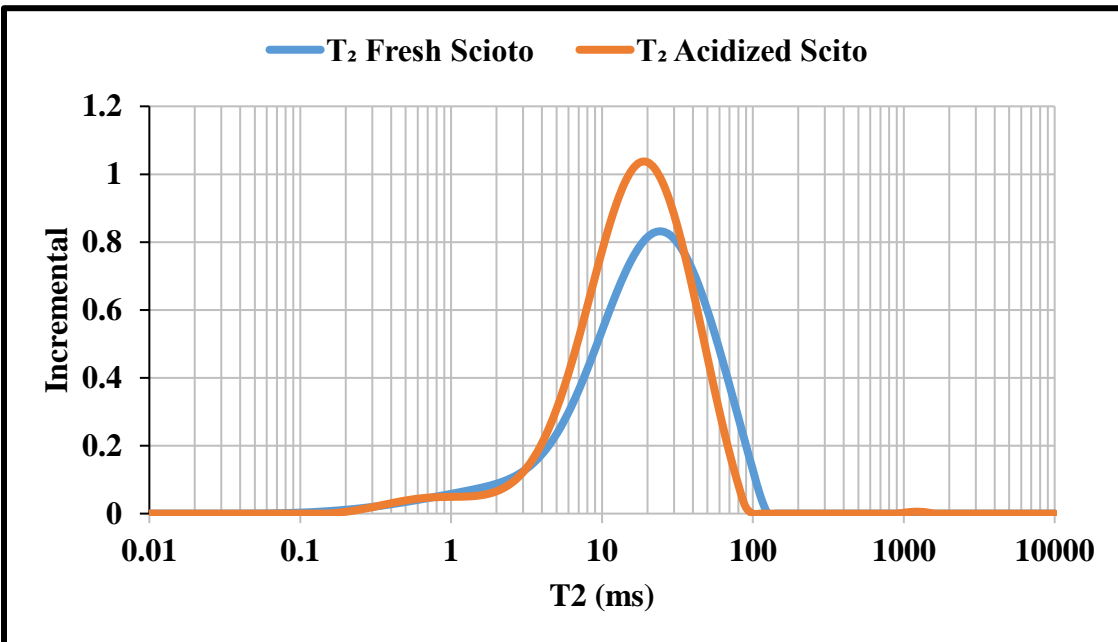


Figure 4.23 The relaxation time T₂ measured by the NMR technique for both fresh and acidized Gray Berea core

4.5 Rock Integrity and Strength Monitoring

The scratch test results can be used to monitor the change in rock integrity and strength before and after the stimulation treatment. **For Gray Berea core**, the results show an enhancement in the rock mechanical parameters such as uniaxial compressive strength (UCS), sonic parameters (compressional and shear waves) and the dynamic elastic parameters (dynamic Young's Modulus and Poisson's ratio). Figures (4.24 & 4.25) show the scratched Gray Berea cores before and after the acid treatment with the groove created along the core whole length. The scratch test machine could also record the core average strength along the whole core length. The UCS value increased by about 1,802 psi after the acid treatment as shown in Figure (4.26). The compressional wave velocity increased from 2471 m/s to about 3227 m/s while the shear wave velocity increased from 1558 m/s to about 1987 m/s, see Figure (4.27). The increase in the sonic waves is reflected by an increase in the dynamic Young's modulus and Poisson's ratio by about 1400 ksi and 0.02 respectively, Figures (4.28 & 4.29).

The increase in the rock mechanical strength can be attributed to the generation of the fluoboric acid from the reaction of the excess amount of HF generated with the bromine source (NaBrO_3) as described by (Pituckchon, 2014), Eq. (4.1). The generated fluoboric acid can react with the potassium source in the Gray Berea core and form a solid precipitate of potassium tetrafluoroborate (KBF_4) under high temperature conditions. This solidification occurred inside the core is the main reason for increasing the core strength. Moreover, the heat generated from the exothermic reaction could increase the strength of sandstone samples due to the solidification of the clays existing inside the core (Szymała et al., 2013).

Moreover, the high temperature applied on the core removed all the moisture and evaporated all the water content inside the core which, in turn, increased the core strength.



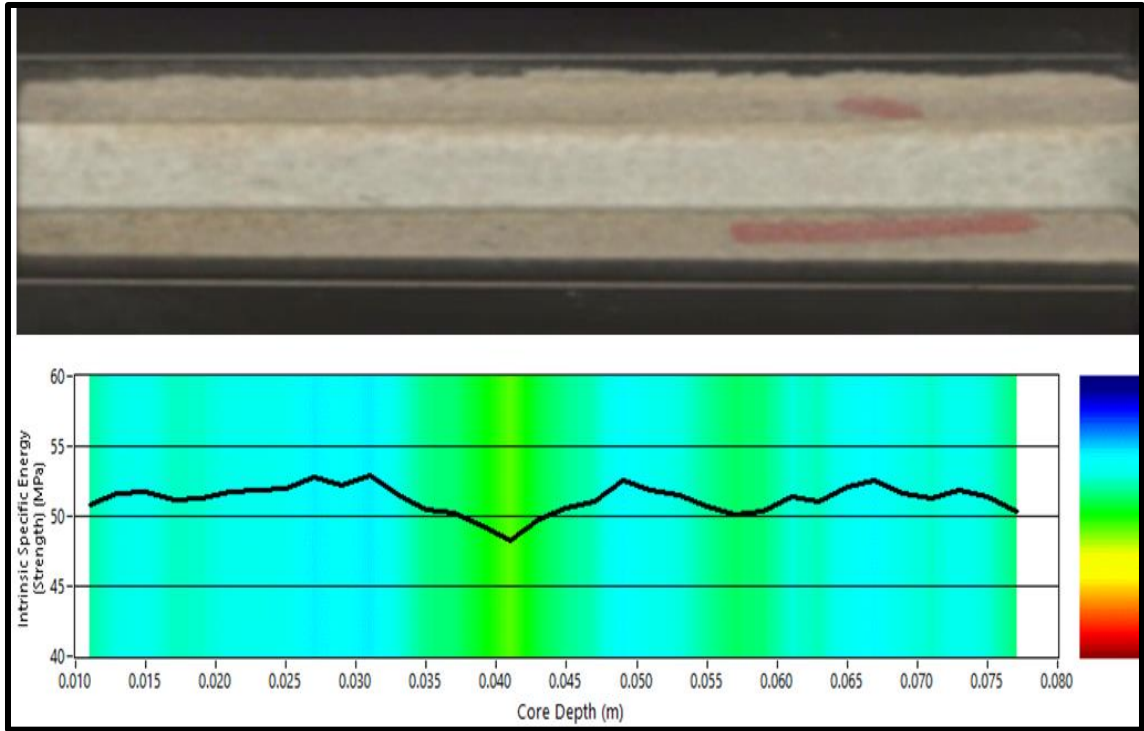


Figure 4.24 The groove created along the whole length of the fresh Gary Berea core with the recorded rock strength in MPa

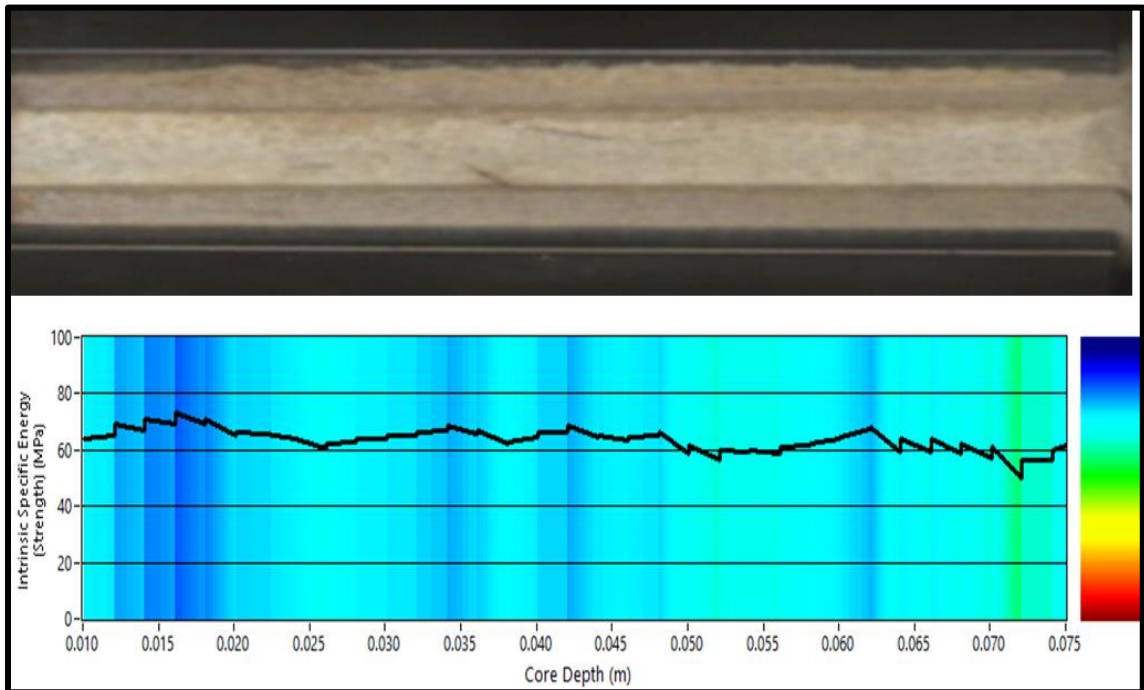


Figure 4.25 The groove created along the whole length of the fresh Gary Berea core with the recorded rock strength in MPa

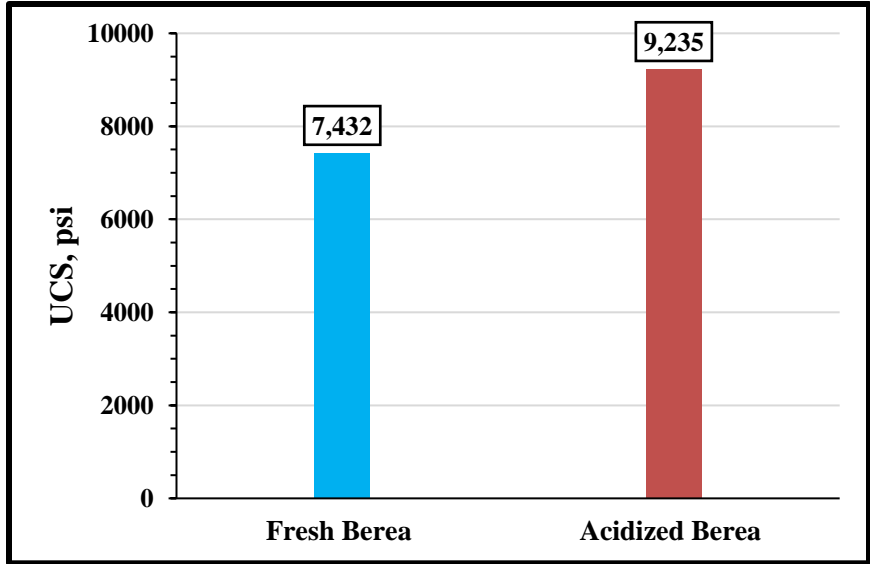


Figure 4.26 The UCS values of the Gray Berea SS core measured in psi before and after the acid treatment measured by the scratch test.

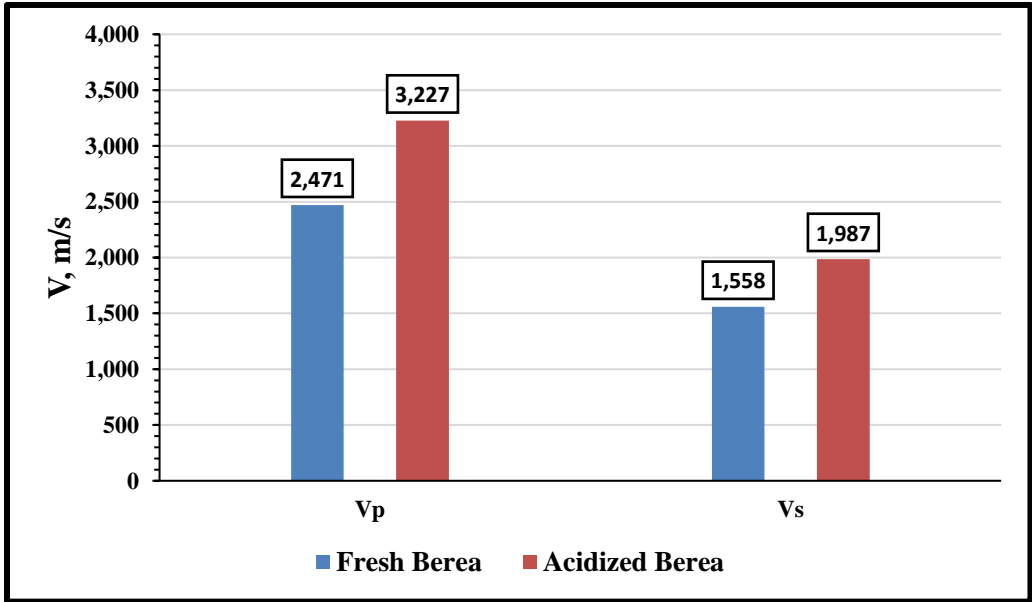


Figure 4.27 The compression and shear waves' velocity of the Gray Berea SS core measured in m/s before and after the acid treatment

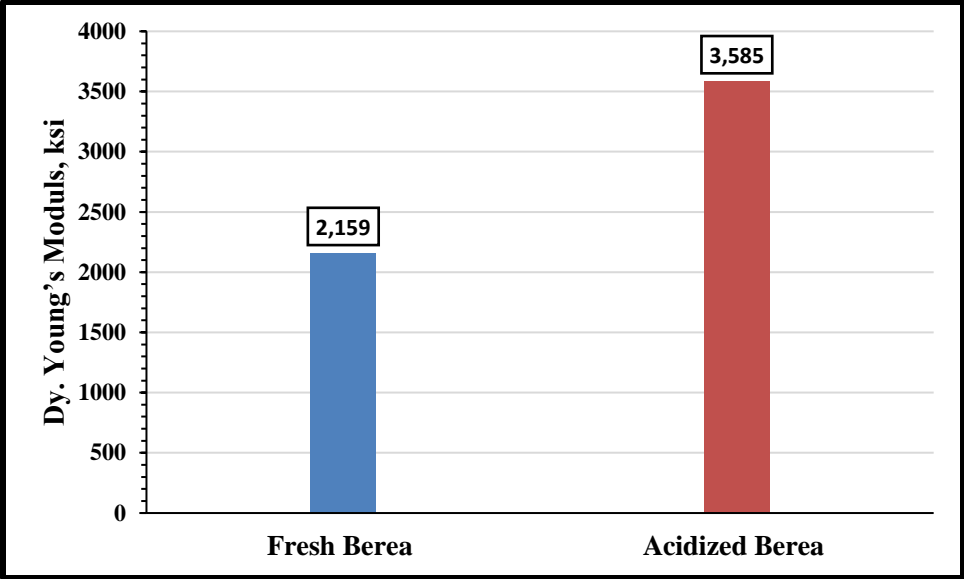


Figure 4.28 The dynamic Young's Modulus of the Gray Berea SS core measured in ksi before and after the acid treatment

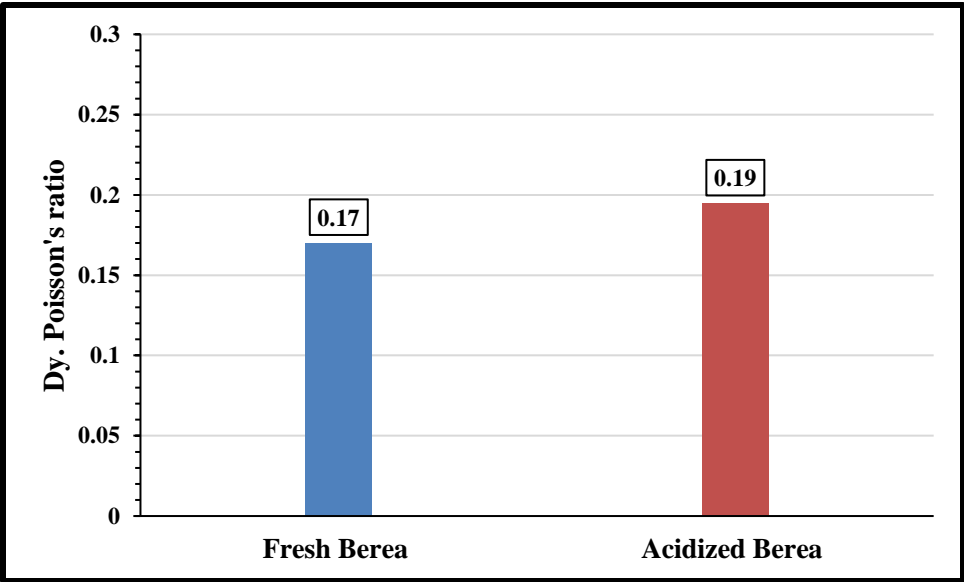


Figure 4.29 The dynamic Poisson's ratio of the Gray Berea SS core measured before and after the acid treatment.

For Scioto sandstone core, the results show that the core had an initial UCS value of 5,781 psi (39.86 MPa). After the stimulation treatment, the core UCS was reduced to 5,011 psi (34.55 MPa) as shown in Figures (4.30 - 4.32). Unlike the Gray Berea core, the stimulation process reduced the core strength by about 770 psi. This can be actually attributed to the tightness of the Scioto core. The small amount of the silica, clays and feldspars that were dissolved from the core represented some of the compacted core grains and the cementing material around them as well. The dissolution of the cementing material, specially, caused the core strength to decrease. It is clear from Figure (4.30) that the core had an almost uniform strength along its whole length. However, after the stimulation treatment, the middle of the core had the lowest UCS value, Figure (4.31). This gives an indication that the main acid reaction with the core minerals took place at the middle of the core.

As mentioned above, Scioto sandstone has a high illite clay content up to 18 wt.% along with some amount of chlorite and potassium feldspars. Another reason beyond the decrease of the core strength is the reaction of its clay and feldspars minerals with the HCl acid during the preflush stage. HCl reacts with chlorite clay to produce iron oxides as precipitates while it reacts with the illite clay causing fines migration.

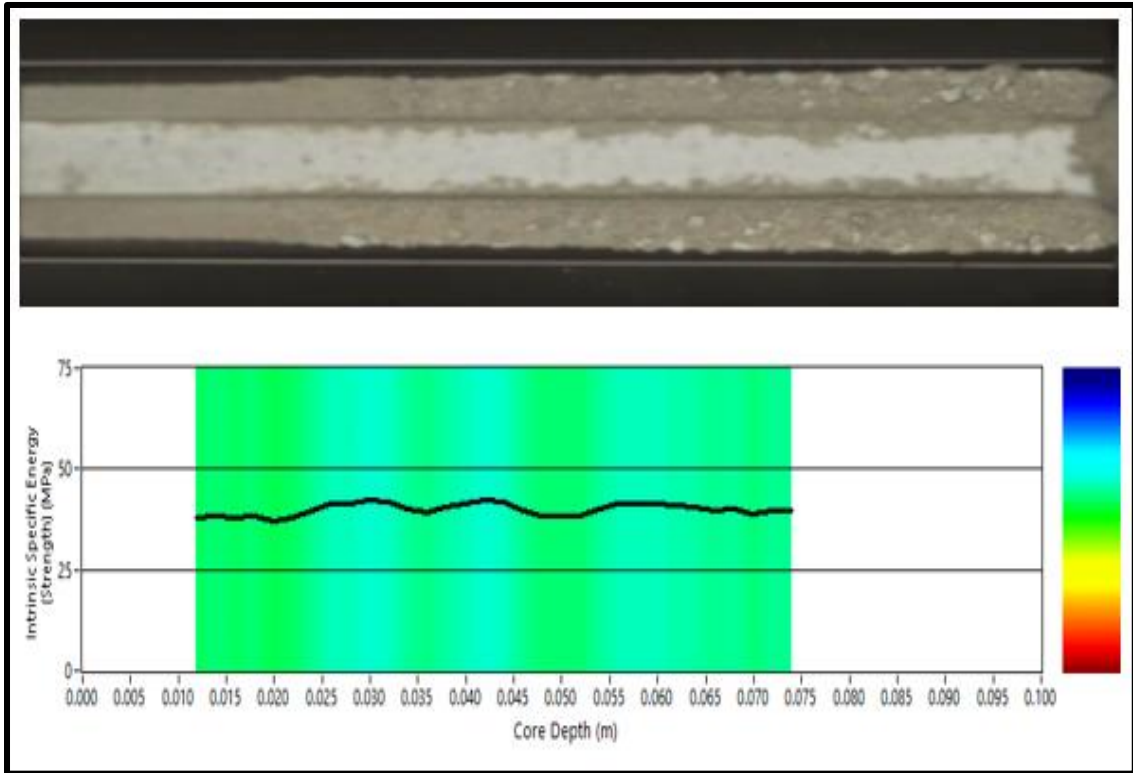


Figure 4.30 The groove created along the whole length of the fresh Scioto core with the recorded rock strength in MPa

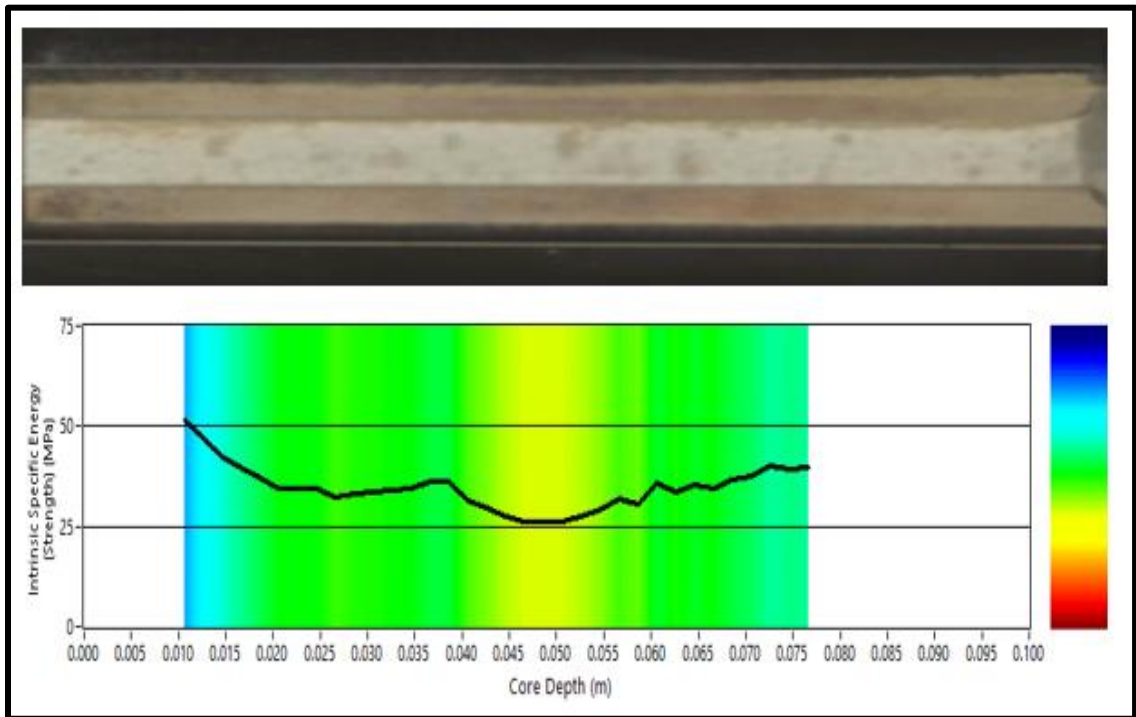


Figure 4.31 The groove created along the whole length of the acidized Scioto core with the recorded rock strength in MPa

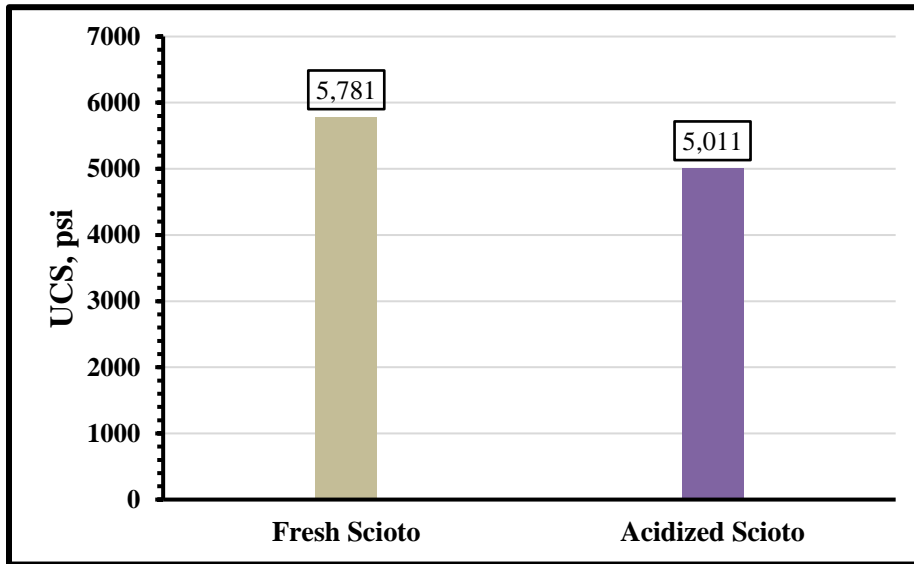


Figure 4.32 The UCS values of the Scioto core measured in psi before and after the acid treatment measured by the scratch test.

In the same way as Gray Berea core, the acoustic data for the Scioto core was measured before and after the acid treatment. The changes in V_p and V_s can be used to calculate the changes in the rock Young's modulus and Poisson's ratio. As shown in Figure (4.33), the compressional wave velocity (V_p) for Scioto core decreased after the stimulation process from 2949 to 2663 m/s. In addition, the shear wave velocity (V_s) decreased as well from 1840 to 1672 m/s.

The decrease in rock strength (UCS) and acoustic waves' velocity (V_p & V_s) was reflected by a decrease in the calculated Young's modulus and Poisson's ratio. As shown in Figures (4.34 & 4.35), the Young's modulus value decreased from 3,074 to 2,524 ksi while the Poisson's ration decreased from 0.18 to 0.17.

These observations confirm the dissolution of some of the rock minerals such as quartz, clays and feldspars. This confirms the generation of HF acid inside the core as a result from the oxidation of ammonium fluoride salt.

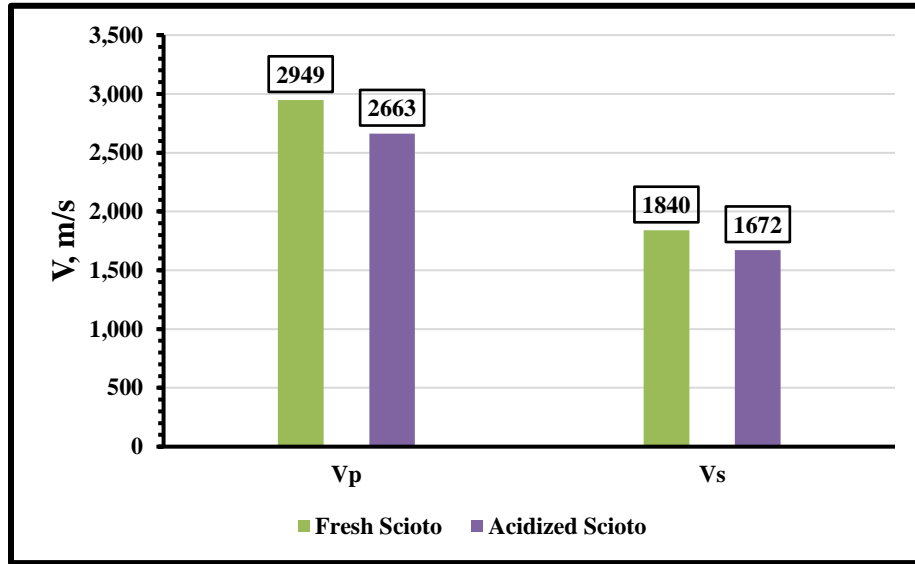


Figure 4.33. The compression and shear waves' velocity of the Scioto core measured in m/s before and after the acid treatment.

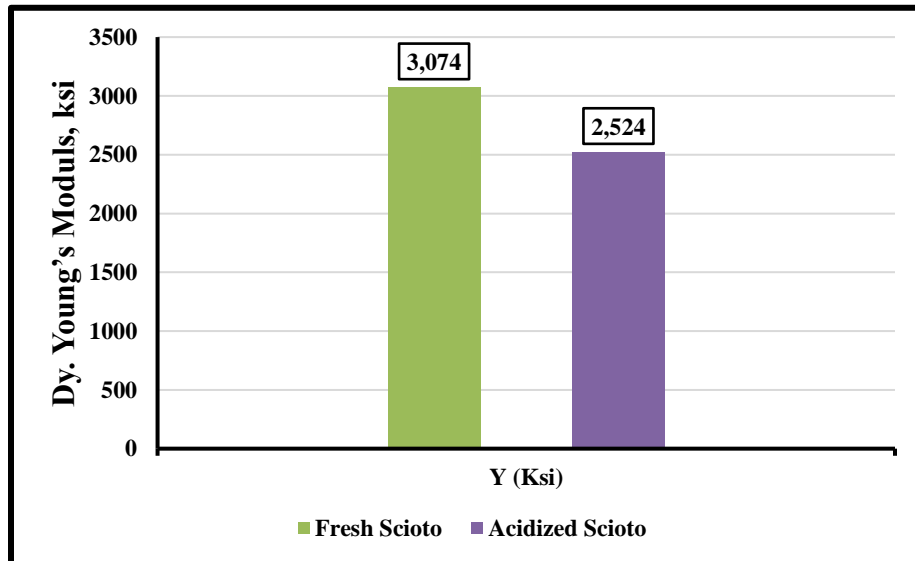


Figure 4.34 The dynamic Young's Modulus of the Scioto core measured in ksi before and after the acid treatment.

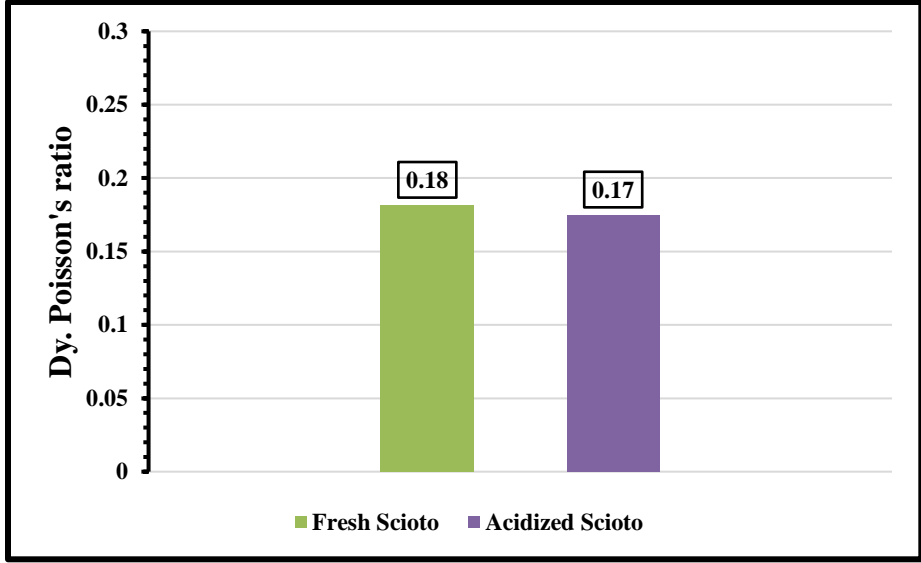


Figure 4.35 The dynamic Poisson's ratio of the Gray Berea SS core measured before and after the acid treatment.

4.6 The effect of the pressure pulse generated from the thermochemicals on the stimulation process.

The generated heat from the exothermic reactions of sodium nitrite with ammonium chloride is not the only product of this reaction. This reaction is capable of generating a pressure pulse that can reach as high as 3,470 psi as illustrated in the literature review part depending on the concentration of the reactants. In this stage, five successive cycles of the in-situ generating HF fluids and the thermochemicals have been injected into Scioto core at a rate of $0.5 \text{ cm}^3/\text{min}$.

The inlet and outlet core pressures were recorded and plotted with time in Figure (4.36). The pressure inside the core kept increasing with increasing the number of injection cycles. This is attributed to the increase in the amount of the thermochemicals inside the core. The maximum pressure reached during this process was 2,075 psi. This pressure is expected to generate tiny micro fractures inside the core and enhance the flow capacity for the stimulated formation. Effluent was collected for ICP analysis to examine how much elements were chelated from the core during this process.

The system was then left to cool down and reach the room temperature in order to measure the core final permeability. The core permeability was measured using a brine solution of 3 wt.% KCl. Different flow rates of 0.25, 0.5 and $1 \text{ cm}^3/\text{min}$ were used to assess the pressure drop along the core. Figure (4.37) represents the core inlet-outlet pressures during the KCl solution injection. The inlet pressure shows a continuous increase at the beginning of the injection while there was no increase in the outlet pressure at the rate of $0.25 \text{ cm}^3/\text{min}$. After the first 1 PV injected of KCl solution, the inlet pressure began

to decrease and stabilize. The injection rate was then increased to $0.5 \text{ cm}^3/\text{min}$ for the next 2 PV injected. It can be noticed that there was almost no difference between the inlet and outlet pressures of the core. After that the injection flow rate was increased to $1 \text{ cm}^3/\text{min}$, however, the pressures trend did not show any change. The pressure transducers showed a pressure drop of only 0.5 psi along the core. This is corresponding to a permeability of 267 mD and produces a $K_{\text{final}}/K_{\text{initial}}$ ratio of 485 for a value of initial permeability of 0.55 mD. A comparison of the core initial and final permeability is represented in Figure (4.38).

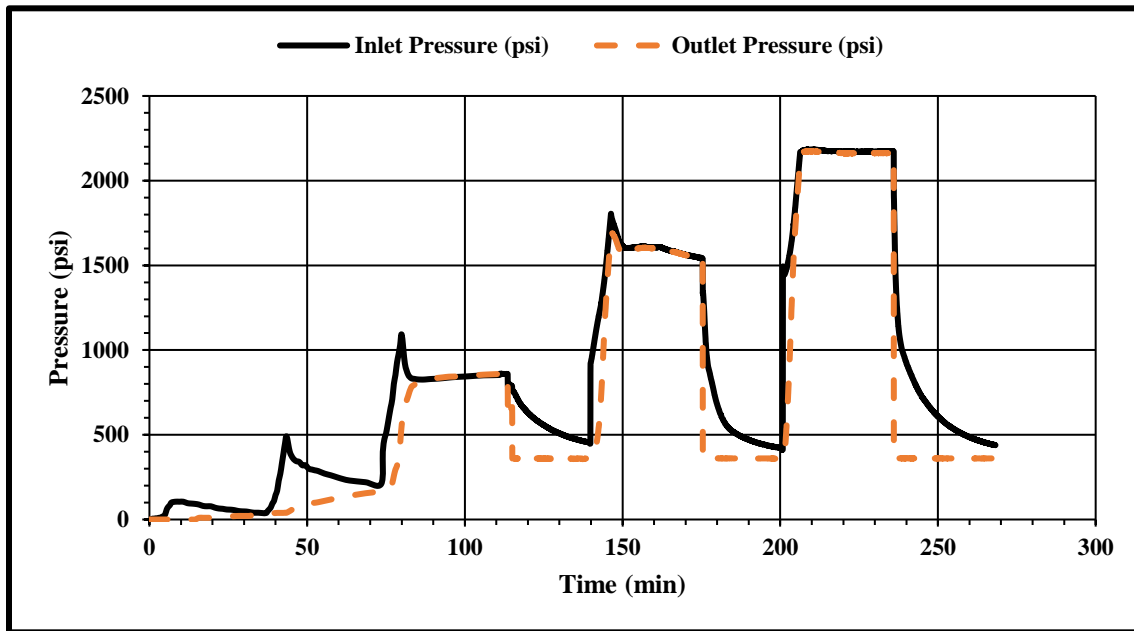


Figure 4.36. The inlet-outlet pressures measured in psi during the 5 successive cycles of stimulating Scioto core using the in-situ HF generating fluids and the thermochemicals.

This behavior of the inlet-outlet pressures across the stimulated core while flowing the brine solution with different injection rates confirms the generation of connected micro fractures inside the core. The generated micro fractures highly enhanced the core permeability leading to decrease the pressure drop across the core. These micro fractures were generated by the action of the pressure pulse generated inside the core from the thermochemicals reaction along with the core mineral dissolution action of the HF generated from the acid generating fluids.

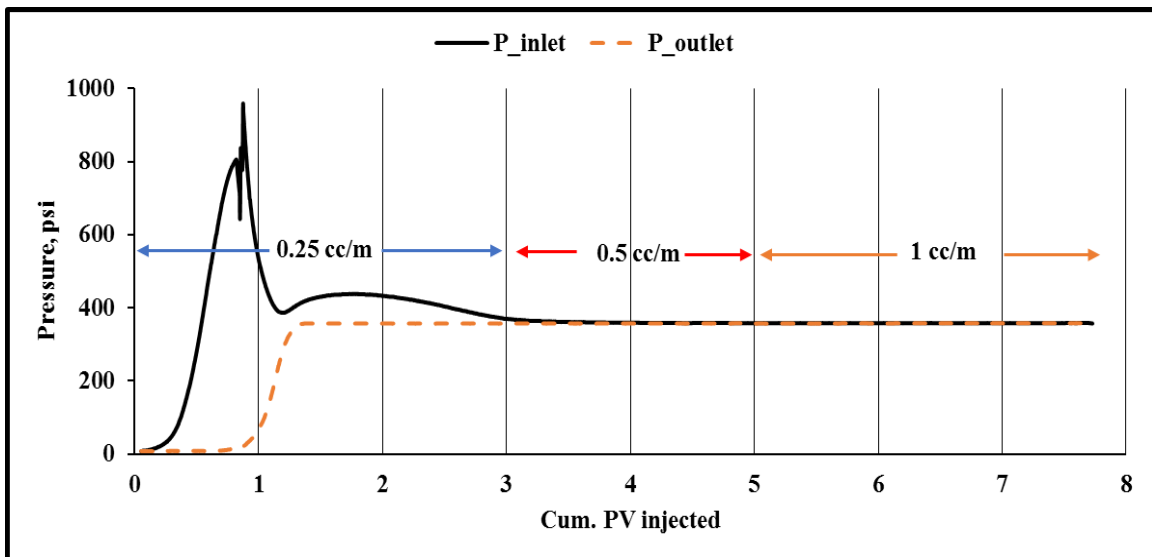


Figure 4.37. The behavior of the inlet-outlet pressures across the stimulated core while flowing the brine solution with different injection rates of 0.25, 0.5 and 1 cm³/min

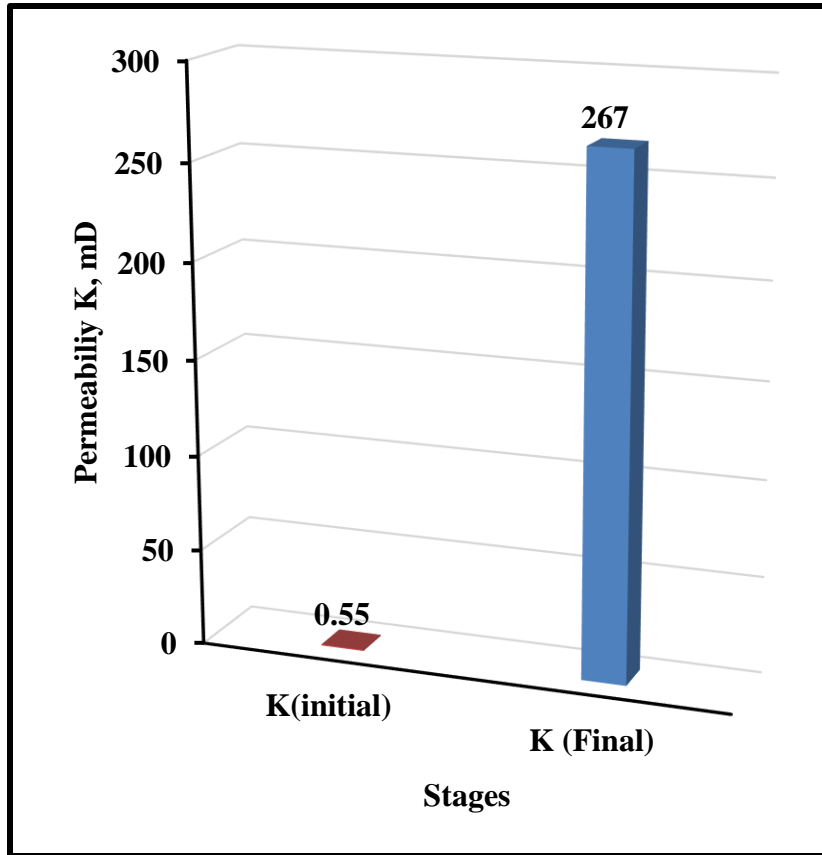


Figure 4.38. A comparison between the core initial permeability and the permeability after acidizing using the in-situ HF generated with the thermochemicals.

The ICP analysis for the effluent from the coreflooding shows the presence of different elements such as Si, Al, Fe, Mg, K and Ca, Figure (4.39). The most abundant element in the effluent is the potassium (K) with a concentration of 6,018 ppm. This is attributed to the presence of illite clay in Scioto sandstone. Illite, which presents up to 18 wt.% of the Scioto cores, is a potassium rich mineral. The injected fluids have a strong capability to dissolve the clay minerals as illustrated before. This leads to the dissolution of the clay mineral from the Scioto core as well as some of the silica particles.

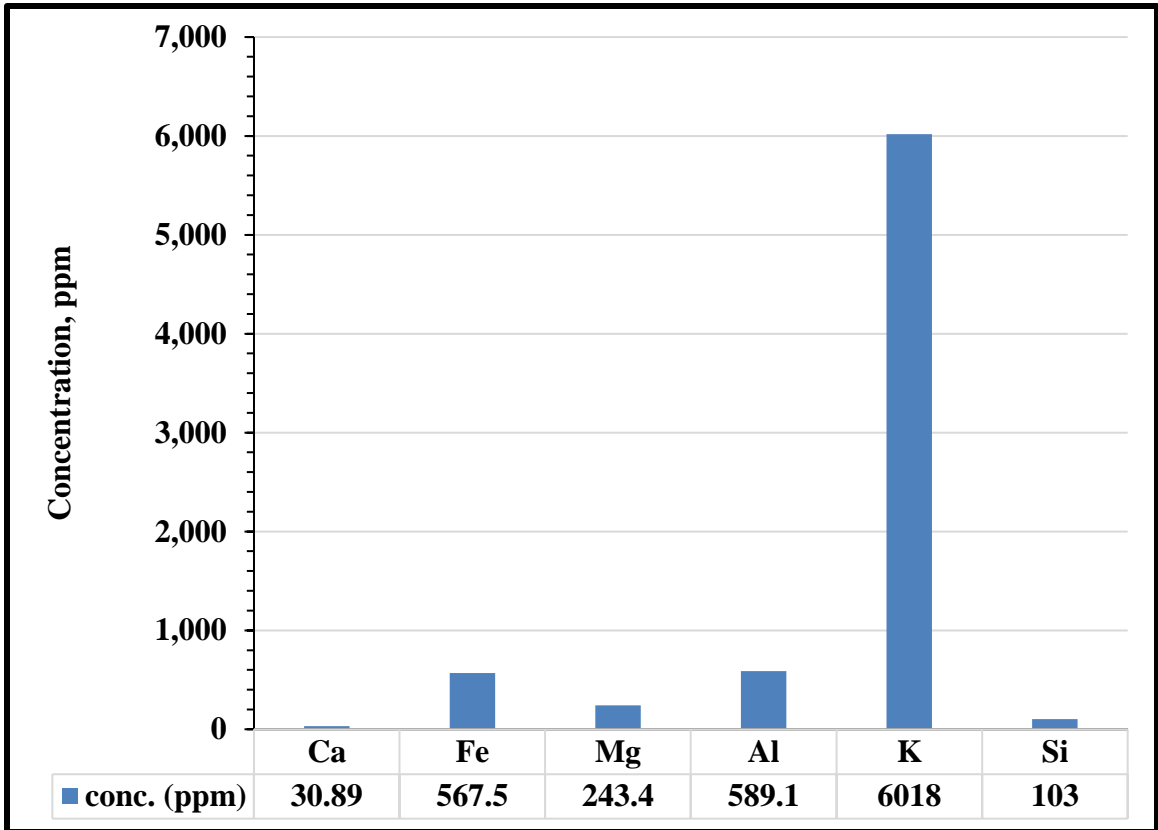


Figure 4.39 The ICP analysis for the elements in the effluent produced after the treatment of the Scioto core with the in-situ generating HF fluids and the thermochemicals.

The NMR scan for the Scioto core before and after the stimulation process is shown in Figure (4.40). The scanning results, again, confirms the generation of the micro fractures generated inside the core. This is represented by the small peak (circled) that appears in the very early relaxation time for the stimulated core scan. In addition, the NMR scan shows a total increase in the core porosity compared to the initial porosity. The increase in core porosity is due to the core mineral dissolution by the action of the generated HF acid. In addition, the micro fractures generated contribute greatly to this increase in core porosity.

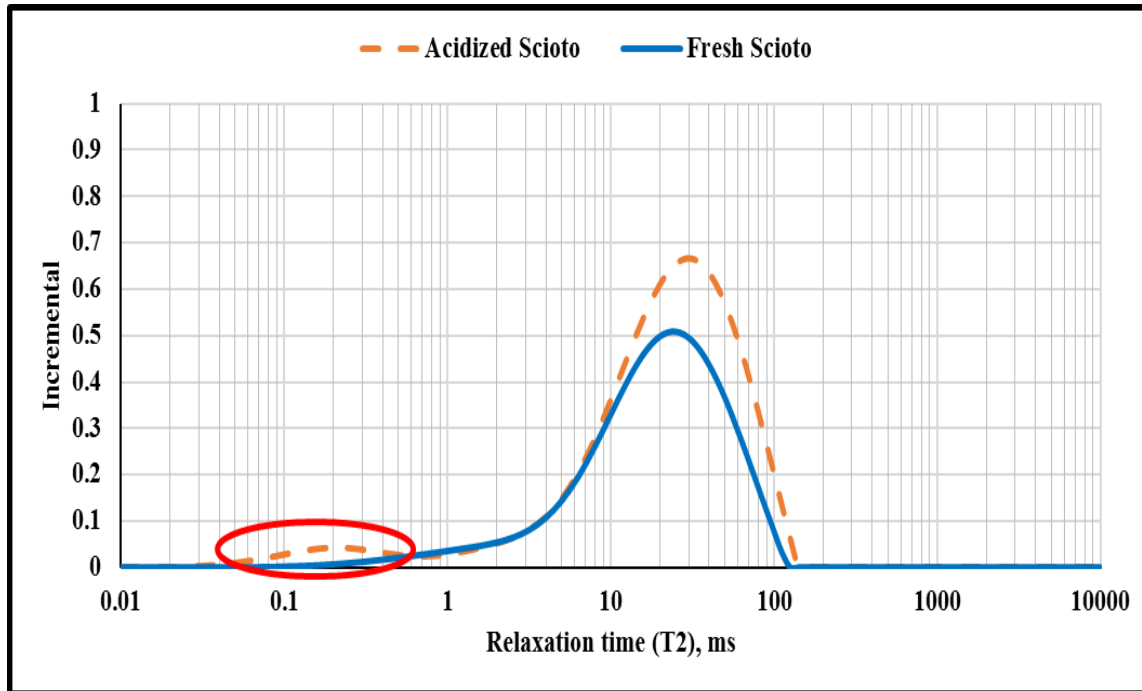


Figure 4.40. The NMR scan for the Scioto core before and after the stimulation process

The Scioto core went through a scratch test before and after the treatment with the in-situ HF generating fluids with the aid of thermochemicals. Figures (4.41 & 4.42) show the groove created along the whole core length by the scratch test cutter along with the recorded UCS value in MPa for the fresh and the acidized cores respectively. The results of the scratch test show a decrease in the core strength (UCS) value from 5,928 psi to 5,172 psi with a difference of 755 psi, Figure (4.43). This is almost the same amount by which the core strength was reduced after being acidized with the HF acid generating fluids only. This means the effect of using the thermochemicals to enhance the acidizing process will not harm the formation integrity that much. However, the use of these chemicals should be carried out under high precautions and after several lab trials.

The acoustic data measured by the scratch test show a decrease in the values of both the compressional and shear waves as shown in Figure (4.44). This is reflected by a decrease in the dynamic Young's modulus value from 2,773 ksi to 2,645 ksi, Figure (4.45). Moreover, the dynamic Poisson's ration was reduced from 0.2 to 0.19, Figure (4.46).

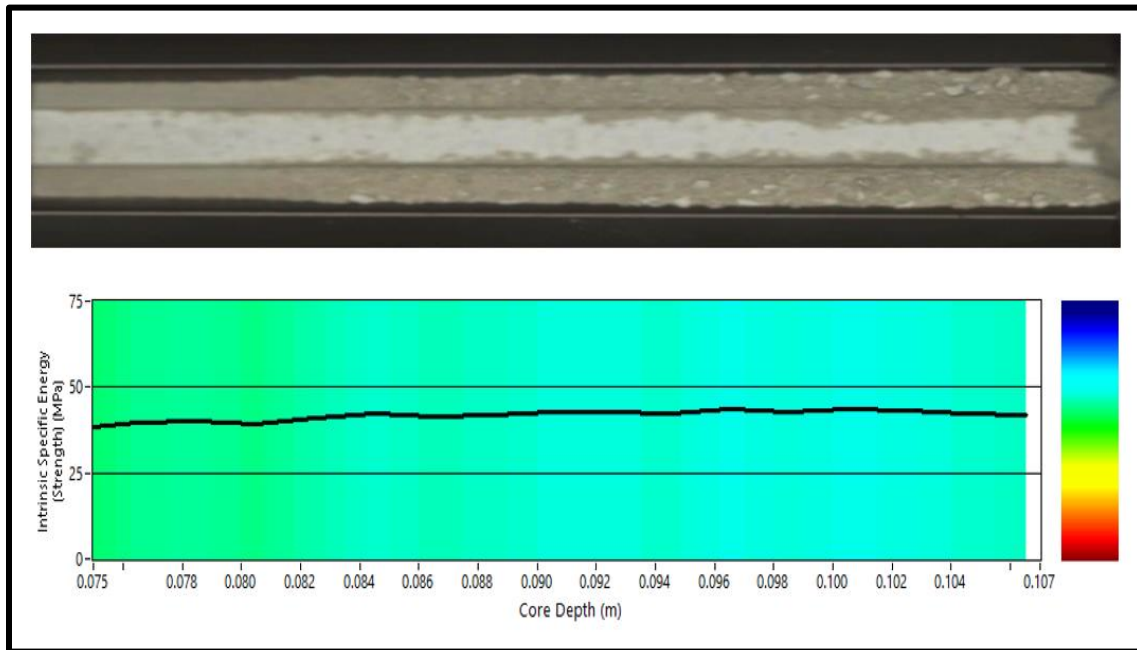


Figure 4.41. The groove created along the whole length of the fresh Scioto core with the recorded rock strength in MPa before being acidized with the in-situ HF generating fluids and the thermochemicals,

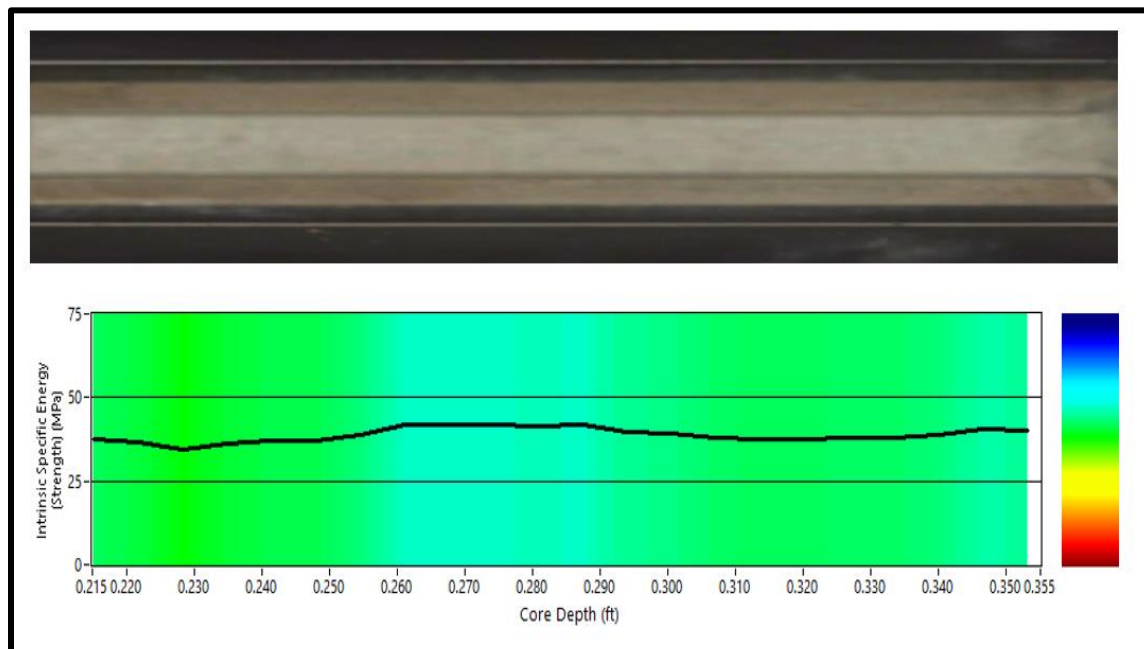


Figure 4.42. The groove created along the whole length of the fresh Scioto core with the recorded rock strength in MPa after being acidized with the in-situ HF generating fluids and the thermochemicals,

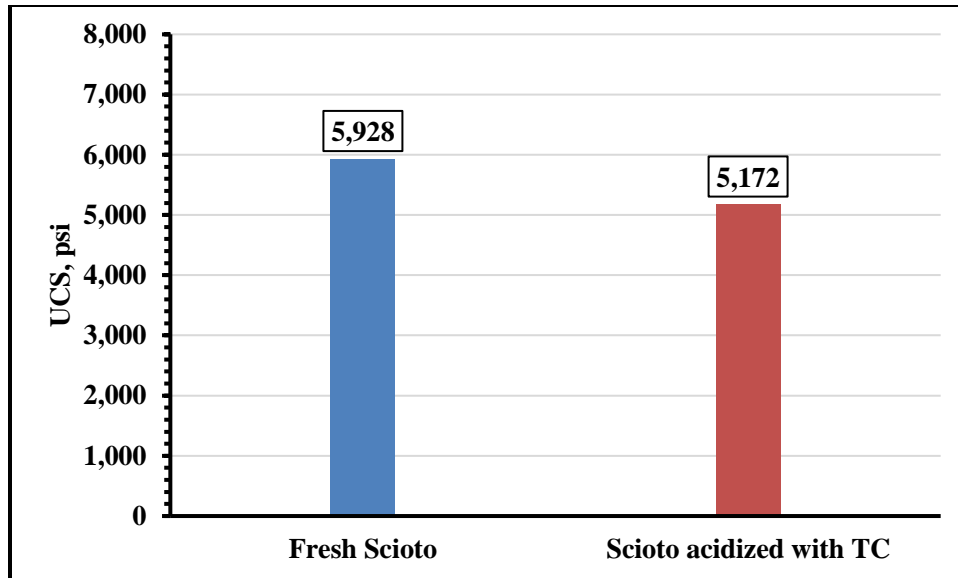


Figure 4.43. The UCS values of the Scioto core measured in psi before and after being stimulated using the acid generating fluids along with the thermochemicals measured by the scratch test.

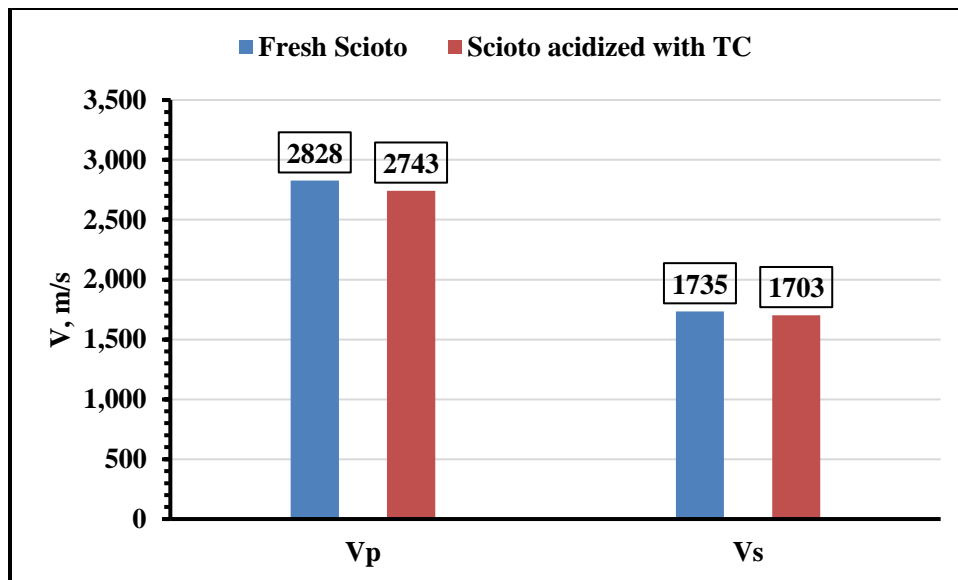


Figure 4.44. The compression and shear waves' velocity of the Scioto core measured in m/s before and after being acidized with the in-situ HF generating fluids and the thermochemicals,

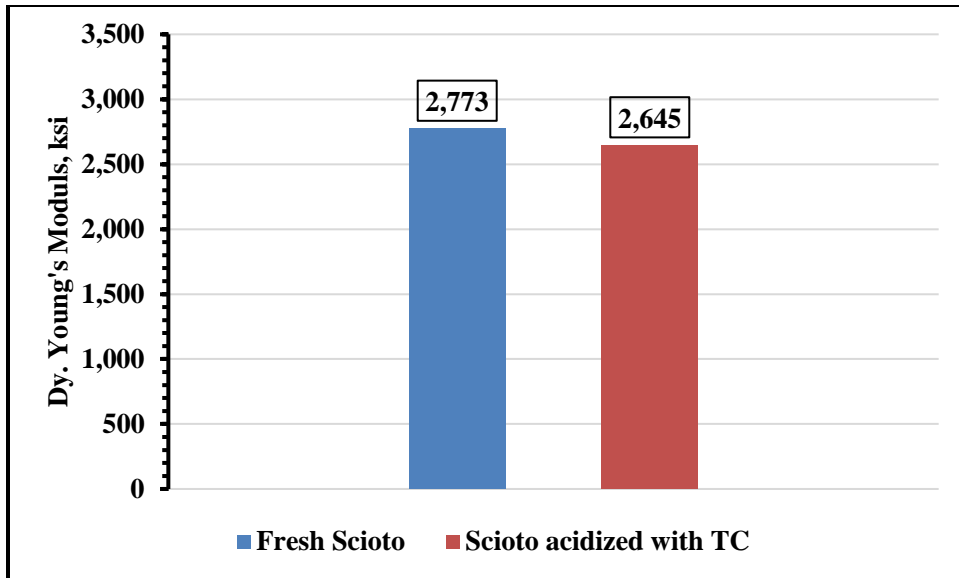


Figure 4.45. The dynamic Young's modulus of the Scioto core measured in ksi before and after being acidized with the in-situ HF generating fluids and the thermochemicals,

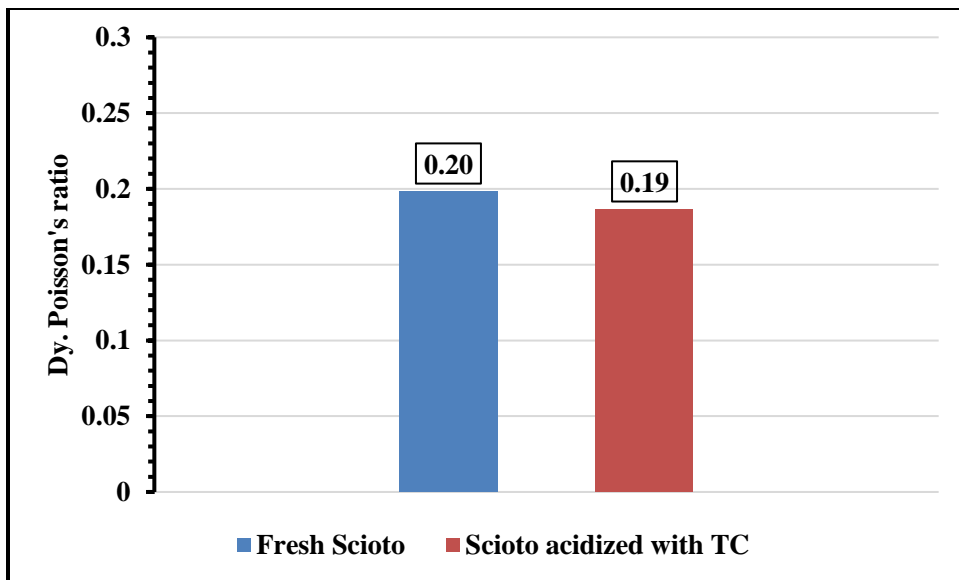


Figure 4.46. The dynamic Poisson's ratio of the Scioto core before and after being acidized with the in-situ HF generating fluids and the thermochemicals,

Chapter 5

Conclusions and Recommendations

5.1 Conclusions

A novel approach for stimulating sandstone formation has been developed and optimized throughout this study. This approach implements the oxidation of ammonium fluoride salt (NH_4F) by a suitable oxidizer in the presence of an exothermic reaction between ammonium chloride (NH_4Cl) and sodium nitrite (NaNO_2). The following conclusions are derived from the results achieved;

- Sodium bromates (NaBrO_3) is a powerful oxidizer that can successfully oxidize ammonium fluoride and produce HF acid. The recommended concentration ratio of NaBrO_3 : NH_4F is 1:2 ratio. Bromine gas may evolve from this reaction. This may arise some safety issues regarding using this oxidizer in the field. However, in the presence of Ca ions, calcium bromide can be formed and dissolved in the solution.
- Ammonium persulfate ($(\text{NH}_4)_2\text{S}_2\text{O}_8$) is another usable oxidizer that reacted with ammonium fluoride and produced HF acid. Tests showed the ability of a mixture of ammonium persulfate and ammonium fluoride to dissolve silica and different clay minerals such as illite, kaolinite and chlorite. The effluents resulted from these showed high stability with no precipitation.
- The generation of the in-situ HF is fully controllable by manipulating the concentration of the used oxidizer used. This will reduce the amount of the hazardous unspent acid as well as reduce the reaction speed and drive the acid deep into the formation.

- The temperature generated from the exothermic reaction between the ammonium chloride (NH_4Cl) and sodium nitrite (NaNO_2) was used to catalyze the ammonium fluoride oxidation reaction and enhance the sandstone stimulation process.
- Gray Berea sandstone core was stimulated using the novel chemical mixture. The stimulation process showed an enhancement in the core permeability by about 40% after three injection cycles of the treating fluids. The ICP analysis for the coreflooding effluent showed that the total chelated amount of Si^+ ions from the core reached 10.5 mg. The scratch test results showed an enhancement in the core strength (UCS) by about 1800 psi while the dynamic Young's modulus and Poisson's ratio increased by 1400 ksi and 0.02 respectively. The NMR scanning for the Berea core before and after the stimulation treatment showed an enhancement in the core total porosity due to the enlargement of the existing pores.
- The optimum number of injection cycles for the acid treatment was found to be only three cycles. After the third cycle, there is no great enhancement in the core permeability and the amount of precipitated silica started to increase. Meanwhile, the soaking time should not be fixed as the core chemicals should be left inside the core until the pressure stabilizes and the reaction finishes.
- Scioto sandstone core was also stimulated using the novel chemical mixture. The core permeability got enhanced by about 37.5% at the end of three successive cycles of the treating fluids. The ICP analysis of the coreflooding effluent showed that the total chelated amount of Si^+ ions from the core reached 49 mg. Unlike Gray Berea core, the scratch test showed a decrease in the Scioto core strength after the acid treatment by

about 770 psi. Moreover, the core dynamic Young's modulus and Poisson's ratio were reduced by 550 ksi and 0.01 respectively. On the other hand, the NMR scanning for Scioto core showed an enhancement in the core total porosity after the acid treatment.

- The generated high-pressure pulse from the thermochemical reaction reached about 2075 psi. This highly increased the efficiency of the Scioto core stimulation process. After applying the proposed injection sequence of the acid generating fluids and the thermochemicals for five successive cycles, the core $K_{\text{fina}}/K_{\text{initial}}$ ratio reached about 485. This came as a result of the tiny micro fractures generated from the thermochemical reaction. NMR scanning for the Scioto core before and after the treatment showed a change in the core pore system due to the micro fractures generated. In addition, the core total porosity increased as indicated by the NMR measurement.
- The generated pressure pulse from the thermochemicals pushes the acid generated deeper into the formation. This overcame the problem of shallower acid penetration when using the conventional treatment methods.
- Since all the chemicals used in this study are safe to handle and are injected separately into the formation, the hazardous effects of HF acid generated are eliminated. Moreover, there will be no special surface equipment required for acid preparation and injection. The in-situ HF generating fluids can be injected using a coiled tubing and spotted directly into the damaged zone. This minimizes the corrosion of the well equipment and reduces the amount of chemicals used.

5.2 Recommendations for Future Work

In order to maximize the output from this research, the following points are highly advised to be taken into consideration;

- Carrying out the coreflooding tests with longer cores (1 ft or more) in order to get a representative response like that of an actual well.
- Examining more types of sandstone formations with different quartz and clay contents to check the effect of the novel fluid mixture on them.
- Carrying out thin-section analysis for the tested sandstone cores in order to characterize the nature of their clay content and know if they will be affected with the acid flow path.
- More fluid analysis is required in order to quantify accurately the amount of acid generated and which types of acids are expected to be produced.
- Using the triaxial compressive strength test to assess the core mechanical properties more comprehensively.

References

- [1] Al Dahlan, M N, Al-Harbi, B G, and Al-Khalidi, M H, (2013). Evaluation of Chelating-Hydrofluoric Systems. Paper IPTC 16969 presented at the International Petroleum Technology Conference, 26-28 March, Beijing, china.
- [2] Al-Anazi, H A, Nasr-El-Din, H A, Hashem, M K, and Hopkins, J K. (2000). Matrix Acidizing of Water Injectors in a Sandstone Field in Saudi Arabia: A Case Study. Paper SPE 62825 presented in the SPE/AAPG Western Regional Meeting, 19-22 June, California, USA.
- [3] Al-Dahlan, M. N., Nasr-El-Din, H. A., & Al-Qahtani, A. A. (2001). Evaluation of Retarded HF Acid Systems. Paper SPE -65032-MS, Presented at *SPE International Symposium on Oilfield Chemistry*, 13-16 Feb., Houston, Texas. <https://doi.org/10.2118/65032-MS>
- [4] Al-Harthy, Salah, Oscar A. Bustos, Mathew Samuel, John Still, Michael Fuller, Nurul Ezalina Hamzah, Mohd Isal Pudim Ismail, and Arthur Parapat. 2009. "Options for High-Temperature Well Stimulation." *Oilfield Rev* 4.20:52–53. <https://goo.gl/1EmCQ>.
- [5] Al-Shaalan, Tareq M., and Hisham A. Nasr-El-Din. 2000. "Mathematical Modeling of Sandstone Stimulation: A Critical Review of Available Models." In *NACE International*. <https://www.onepetro.org/conference-paper/NACE>
- [6] Al-Yaseri AZ, Lebedev M, Vogt SJ, Johns ML, Barifcani A, Iglauer S. (2015). Pore-scale analysis of formation damage in Bentheimer sandstone with in-situ NMR and micro-computed tomography experiments. *J Petrol Sci Eng* 129:48–57
- [7] Amaefule, J. O., Kersey, D. G., Norman, D. L., and Shannon, P. M. 1988. Advances in Formation Damage Assessment and Control Strategies. Paper (PETSOC-88-39-65), presented at Proceedings of the 39th Annual Technical Meeting of Petroleum Society of Canada, June 12–16, Calgary, Alberta.

- [8] Audibert, Annie, Jean-François Argillier, Hemant K. J. Ladva, Paul W. Way, and Arvid O. Hove. 1999. "Role of Polymers on Formation Damage." In Society of Petroleum Engineers. <https://doi.org/10.2118/54767-MS> .
- [9] Bennion, B., "Formation Damage-The Impairment of the Invisible, by the Inevitable and Uncontrollable, Resulting in an Indeterminate Reduction of the Unquantifiable!" *Journal of Canadian Petroleum Technology*, 38(2), February 1999, 11–17.
- [10] Byrn, M. (2009). SPE Distinguished Lecturer Programme. Retrieved from Society of Petroleum Engineers: <https://www.spe.org/dl/slides-graphics.php>
- [11] Chang, Frank, Ronnie L. Thomas, and Walter D. Grant Jr. 2000. Method for acidizing a subterranean formation. World Intellectual Property Organization WO2000070186A1, filed May 10, 2000, and issued November 23, 2000. <https://patents.google.com/patent/WO2000070186A1>.
- [12] Civan, F. (2000). *Reservoir formation damage: fundamentals, modeling, assessment, and mitigation* (1st ed.). Houston, Texas: Gulf Professional Publishing.
- [13] Civan, F. (2005). Advancements in the Evaluation and Mitigation of Formation Damage in Petroleum Reservoirs. *Journal of Energy Resources Technology*, 127(3), 169–170. <https://doi.org/10.1115/1.2000275>.
- [14] Clarke T (2014) Application of a novel clay stabilizer to mitigate formation damage due to clay swelling. MSc Thesis, Texas A&M University
- [15] Coulter, A. W., Hendrickson, A. R., & Martinez, S. J. (1987). *Petroleum Engineering Handbook*, Acidizing chapter 54. Society of Petroleum Engineers.
- [16] Economides, M. J., A. Daniel Hill, Ehlig-Economides, C., & Zhu, D. (2013). *Petroleum production systems* (2. ed). Upper Saddle River, NJ: Prentice Hall.
- [17] El-Aouar, M. (1962). The Effect of Temperature on Clay Minerals In Aqueous Suspension. *Society of Petroleum Engineers Journal*, 2(03), 216–222. <https://doi.org/10.2118/79-pa>.

- [18] Gdanski, R. D. 1985. AlCl₃ Retarded HF Acid for More Effective Stimulation. *Oil & Gas J.* 83 (43): 111–115.
- [19] Haynes, W.M. (ed.) *CRC Handbook of Chemistry and Physics*. 91st ed. Boca Raton, FL: CRC Press Inc., 2010-2011, p. 4-46.
- [20] Hill, A. D., D. M. Lindsay, I. H. Silberberg, and R. S. Schechter. 1981. “Theoretical and Experimental Studies of Sandstone Acidizing.” *Society of Petroleum Engineers Journal* 21 (01): 30–42. <https://doi.org/10.2118/6607-PA>.
- [21] Hull, Katherine L., Amy J. Cairns, and Marium Haq. 2019. “Bromate Oxidation of Ammonium Salts: In Situ Acid Formation for Reservoir Stimulation.” *Inorganic Chemistry* 58 (5): 3007–14. <https://doi.org/10.1021/acs.inorgchem.8b02891>.
- [22] Mahmoud, M. A., Nasr-El-Din, H. A., & De Wolf, C. A. (2015). High-Temperature Laboratory Testing of Illitic Sandstone Outcrop Cores with HCl-Alternative Fluids. *SPE Production & Operations*, 30(01), 43–51. <https://doi.org/10.2118/147395-PA>.
- [23] Kamal, Muhammad Shahzad, Mohamed Mahmoud, Mohammed Hanfi, Salaheldin Elkatatny, and Ibnelwaleed Hussein. 2019. “Clay Minerals Damage Quantification in Sandstone Rocks Using Core Flooding and NMR.” *Journal of Petroleum Exploration and Production Technology* 9 (1): 593–603. <https://doi.org/10.1007/s13202-018-0507-7>.
- [24] Karale, Chaitanya Millikarjun, Rajender Salla, and Ragi Lohidakshan Poyyara. 2016. A Method of Acidizing of Subterranean Formations in Well Operations. WO/2016/126351, issued August 12, 2016. <https://patentscope.wipo.int/search/en/detail.jsf?docId=WO2016126351>.
- [25] Kunze, K.R. and Shaughnessy, C.M.: “Acidizing Sandstone Formations with Fluoboric Acid”, paper SPE 9387 presented at the 1980 SPE Annual Fall Technical Conference and Exhibition, Houston, TX, 21-24 September.
- [26] Li, Gao, Wuqiang Cai, Yingfeng Meng, Liang Wang, Limin Wang, and Xiaobing Zhang. 2017. “Experimental Evaluation on the Damages of Different Drilling Modes

to Tight Sandstone Reservoirs.” *Natural Gas Industry B* 4 (4): 256–63.
<https://doi.org/10.1016/j.ngib.2017.08.008> .

- [27] Li, N, Zhang, Q, Wang, Y, Liu, P, and Zhao, L. A New Multichelating Acid System for High-Temperature Sandstone Reservoirs. *Journal of Chemistry*, vol. 2015, Article ID 594913, 9 pages, 2015.
- [28] Lullo, D.G.: “A New Acid for True Stimulation of Sandstone Reservoirs”, paper SPE 37015 presented at the 1996 SPE Annual Technical Conference and Exhibition held in Denver, CO, 6-9 October.
- [29] Malate, R C M, J C Austria, Z F Sarmiento, G Di Lullo, P A Sookprasong, and E S Francis. 1998. “Matrix Stimulation Treatment of Geothermal Wells Using Sandstone Acid.” *Proceedings. Twenty-Third Workshop on Geothermal Reservoir Engineering Stanford University, Stanford, California*, 4.
- [30] McBride, J.R. Rathbone, M.J. and Thomas, R.L.: “Evaluation of Fluoboric Acid Treatment in Grand Isle Offshore Area Using Multiple Rate Flow Test”. Paper SPE 8399 presented at the 1979 SPE Annual Fall Technical Conference and Exhibition, Las Vegas, Nevada, 23-26 September.
- [31] McCune, C. C., H. S. Fogler, and J. R. Cunningham. 1975. “A New Model of the Physical and Chemical Changes in Sandstone During Acidizing.” *Society of Petroleum Engineers Journal* 15 (05): 361–70. <https://doi.org/10.2118/5157-PA>.
- [32] Portier, S., André, L., Vuataz, F.-D., 2007. “Review on chemical stimulation techniques in oil industry and applications to geothermal systems”. Technical report, Deep Heat Mining Association – DHMA, Switzerland.
- [33] Reyes, E A, Smith, A L, and Beaturbaugh, A. Properties and Applications of an Alternative Aminopolycarboxylic Acid for Acidizing Sandstones and Carbonates, (2013). Paper SPE 165142 presented at SPE European Formation Damage Conference & Exhibition, 5-7 June, Noordwijk, Netherlands.

- [34] Richard, Thomas, Fabrice Dagrain, Edmond Poyol, and Emmanuel Detournay. 2012. "Rock Strength Determination from Scratch Tests." *Engineering Geology* 147–148 (October): 91–100. <https://doi.org/10.1016/j.enggeo.2012.07.011>.
- [35] Rogers, B.A., Burk, M.K., Stonecipher, S.A. (1998). "Designing a Remedial Acid Treatment for Gulf of Mexico Deepwater Turbidite Sands Containing Zeolite Cement". Paper (SPE-39595-MS) presented at the SPE Formation Damage Control Conference, 18-19 February, Lafayette, Louisiana. <https://doi.org/10.2118/39595-MS>.
- [36] Shuchart, C. E., & Gdanski, R. D. (1996). Improved Success in Acid Stimulations with a New Organic-HF System. Paper (SPE-36907-MS) presented at European Petroleum Conference 22-24 October, Milan, Italy. <https://doi.org/10.2118/36907-MS>
- [37] Smith, C. F., and A. R. Hendrickson. 1965. "Hydrofluoric Acid Stimulation of Sandstone Reservoirs." *Journal of Petroleum Technology* 17 (02): 215–22. <https://doi.org/10.2118/980-PA> .
- [38] Sokhanvarian, K, Nasr-El-Din, H A, Wang, G, and De Wolf, C A. Thermal Stability of Various Chelates That Are Used in The Oilfield And Potential Damage Due To Their Decomposition Products. Paper SPE 157426 presented at the SPE international Production and Operations Conference and Exhibition, Doha, Qatar, 14-16 May 2014.
- [39] Templeton, C. C., E. A. Richardson, G. T. Karnes, and J. H. Lybarger. 1975. "Self-Generating Mud Acid." *Journal of Petroleum Technology* 27 (10): 1,199-1,203. <https://doi.org/10.2118/5153-PA> .
- [40] Thomas, R.L. and Crowe, C.W. (1981). "Matrix Treatment Employs New Acid System for Stimulation and Control of Fines Migration in Sandstone Formation". Paper (SPE – 7566) presented at the SPE Annual Fall Meeting of SPE (AIME), 1-3 October, Houston, TX.
- [41] Thomas R.L., Crowe C.W. (1978) Single-stage chemical treatment provides stimulation and clay control sandstone formations. Paper SPE-7124-MS presented at SPE California Regional Meeting, 12-14 April, San Francisco, California.

- [42] Thomas, Ronnie L. 1979. Method for acidizing a subterranean formation. United States US4151879A, filed August 15, 1977, and issued May 1, 1979. <https://patents.google.com/patent/US4151879/en> .
- [43] W.W. Frenier, D. Wilson, D. Crump and L. Jones (2000). "Use of Highly Acid-Soluble Chelating Agents in Well Stimulation Services." In proceeding of the SPE Annual Technical Conference and Exhibition, SPE 63242, Dallas, Texas, USA, October.
- [44] Yang, X. M., and Mukul M. Sharma. 1991. "Formation Damage Caused by Cement Filtrates in Sandstone Cores." SPE Production Engineering 6 (04): 399–405. <https://doi.org/10.2118/19305-PA> .
- [45] Ying-Hsiao, Li, John D. Fambrough, and Carl T. Montgomery. 1998. "Mathematical Modeling of Secondary Precipitation from Sandstone Acidizing." In . Society of Petroleum Engineers. <https://doi.org/10.2118/39420-MS>.
- [46] Yu, Meng, Mohamed A. Mahmoud, and Hisham A. Nasr-El-Din. 2011. "Propagation and Retention of Viscoelastic Surfactants Following Matrix-Acidizing Treatments in Carbonate Cores." SPE Journal 16 (04): 993-1,001. <https://doi.org/10.2118/128047-PA>.
- [47] Bryant, S.L., "An Improved Model of Mud Acid/Sandstone Chemistry," SPE 22855 MS, presented at SPE Annual Technical Conference and Exhibition, 6-9 October, Dallas, Texas, 1991.
- [48] Schechter, R.S., Oil Well Stimulation, Prentice Hall, Englewood Cliffs, NJ, 1992
- [49] Hartman, R.L., Lecerf, B., Frenier, W., Ziauddin, M., and Fogler, H.S., "Acid-Sensitive Aluminosilicates: Dissolution Kinetics and Fluid Selection for Matrix-Stimulation Treatments," SPEPO, 194–204 (May 2006).
- [50] Fogler, H.S., Lund, K., and McCune, C.C., "Predicting the Flow and Reaction of HCl/HF Mixtures in Porous Sandstone Cores," SPEJ, 248–260 (October 1976), Trans. AIME, 234.

- [51] Taylor, K.C., and Nasr-El-Din, H.A., “Measurement of Acid Reaction Rates with the Rotating Disk Apparatus,” *JCPT*, 48(6): 66–70 (June 2009).
- [52] Ayorinde, C. G., & R. L. Thomas. (1992). The Application of Fluoboric Acid in Sandstone Matrix Acidizing: A Case Study. 21st Annual Convention Proceedings (2) 235–261. Retrieved from http://archives.datapages.com/data/ipa/data/021/021002/235_ipa021b0235.htm.
- [53] Hassan, Amjed, Mohamed Mahmoud, Abdulaziz Al-Majed, Olalekan Alade, Ayman Al-Nakhli, Mohammed BaTaweel, and Salaheldin Elktatany. 2019. “Development of A New Chemical Treatment for Removing Water Blockage in Tight Reservoirs.” Paper SPE-194879-MS presented at the SPE Middle East Oil and Gas Show and Conference held in Manama, Bahrain, 18-21 March. <https://doi.org/10.2118/194879-MS>.
- [54] da Motta, E. P., Plavnik, B., Schechter, R. S., & Hill, A. D. (1993). Accounting for silica precipitation in the design of sandstone acidizing. *SPE Production and Facilities*, 8(2), 138–144. <https://doi.org/10.2118/23802-PA>.
- [55] Kalfayan, L. (2008). *Production enhancement with acid stimulation*. 2nd ed. Tulsa, Okla.: PennWell.
- [56] Leong, V. H., & Ben Mahmud, H. (2019). A preliminary screening and characterization of suitable acids for sandstone matrix acidizing technique: a comprehensive review. *Journal of Petroleum Exploration and Production Technology*, 9(1), 753–778. <https://doi.org/10.1007/s13202-018-0496-6>
- [57] McLeod, H. O. (1984). Matrix Acidizing. *Journal of Petroleum Technology*, 36(12), 2055–2069. <https://doi.org/10.2118/13752-PA>
- [58] Economides, M. J., & Nolte, K. G. (1987). *Reservoir stimulation*. (3rd edition), Wiley. http://do.rulitru.ru/docs/4/3081/conv_1/file1.pdf.
- [59] McLeod, H.O., “Significant Factors for Successful Matrix Acidizing,” Paper presented at the SPE Centennial Symposium at New Mexico Tech, Socorro, New Mexico, 1989.

- [60] McLeod, H.O., Jr. and Norman, W.D., "Sandstone Acidizing," Ch. 18 in Reservoir Stimulation, 3rd edition, Economides, M.J., and Nolte, K.G., eds., John Wiley and Sons, Chichester, UK, 2000.
- [61] Hill, A. D., Lindsay, D. M., Silberberg, I. H., & Schechter, R. S. (1981). Theoretical and Experimental Studies of Sandstone Acidizing. Society of Petroleum Engineers Journal, 21(01), 30–42. <https://doi.org/10.2118/6607-PA>.
- [62] Hill, A. D., Sepehrnoori, K., & Wu, P. Y. (1994). Design of the HCl Preflush in Sandstone Acidizing. SPE Production & Facilities, 9(02), 115–120. <https://doi.org/10.2118/21720-PA>.
- [63] Nasr-El-Din, H. A., Al-Nasser, A. H., Al-Habib, N. S., Jemmali, M., Zoraia, G., & Sunbul, A. (2005). New Methodology to Effectively Stimulate Water Disposal Wells Drilled in Acid Sensitive Sandstone formations in Saudi Arabia. Paper SPE-93502-MS, presented in SPE Middle East Oil and Gas Show and Conference 12-15 March, Kingdom of Bahrain. <https://doi.org/10.2118/93502-MS>.
- [64] Gidley, J. L. (1985). Acidizing Sandstone Formations: A Detailed Examination of Recent Experience. Paper (SPE-14164-MS) presented at SPE Annual Technical Conference and Exhibition. <https://doi.org/10.2118/14164-MS>.
- [65] Welton, J. E., "SEM Petrology Atlas," American Association of Petroleum Geologists, Tulsa, Oklahoma, 1984, 237 p.
- [66] Kunze, K. R., & Shaughnessy, C. M. (1983). Acidizing Sandstone Formations with Fluoboric Acid. Society of Petroleum Engineers Journal, 23(01), 65–72. <https://doi.org/10.2118/9387-PA>
- [67] Zhou, L., & Nasr-El-Din, H. A. (2016). Phosphonic-Based Hydrofluoric Acid: Interactions with Clay Minerals and Flow in Sandstone Cores. SPE Journal, 21(01), 264–279. <https://doi.org/10.2118/164472-PA>
- [68] Shafiq, M. U., Shuker, M. T., & Kyaw, A. (2014). Performance Comparison of New Combinations of Acids with Mud Acid in Sandstone Acidizing. Research Journal of

- Applied Sciences, Engineering and Technology, 7(2), 323–328.
<https://doi.org/10.19026/rjaset.7.258>
- [69] Shafiq, M. U., & Mahmud, H. K. Ben. (2016). An Effective Acid Combination for Enhanced Properties and Corrosion Control of Acidizing Sandstone Formation. IOP Conference Series: Materials Science and Engineering, 121(1), 012002.
<https://doi.org/10.1088/1757-899X/121/1/012002>.
- [70] Frenier, W., Brady, M., Al-Harthy, S., Arangath, R., Chan, K. S., Flamant, N., & Samuel, M. (2004). Hot Oil and Gas Wells Can Be Stimulated Without Acids. SPE Production & Facilities, 19(04), 189–199. <https://doi.org/10.2118/86522-PA>.
- [71] Tuedor, F. E., Xiao, Z., Frenier, W. W., Fu, D., Salamat, G., Davies, S. N., & Lecerf, B. (2006). A Breakthrough Fluid Technology in Stimulation of Sandstone Reservoirs. Paper SPE-98314-MS, presented at the SPE International Symposium and Exhibition on Formation Damage Control, 15-17 February, Lafayette, Louisiana, USA.
<https://doi.org/10.2118/98314-MS>.
- [72] Ali, S. A., Ermel, E., Clarke, J., Fuller, M. J., Xiao, Z., & Malone, B. (2005). Stimulation of High-Temperature Sandstone Formations from West Africa with Chelating Agent-Based Fluids. Paper SPE-93805-MS Presented at SPE European Formation Damage Conference, 25-27 May, Sheveningen, The Netherlands.
<https://doi.org/10.2118/93805-MS>.
- [73] Reyes, E. A., Smith, A. L., Beuterbaugh, A., & Calabrese, T. (2015). GLDA/HF Facilitates High Temperature Acidizing and Coiled Tubing Corrosion Inhibition. Paper SPE-174264-MS, presented at SPE European Formation Damage Conference and Exhibition, 3-5 June, Budapest, Hungary. <https://doi.org/10.2118/174264-MS>.
- [74] Rignol, J., Ounsakul, T., Kharrat, W., Fu, D., Teng, L. K., Lomovskaya, I., & Boonjai, P. (2015). Improved Fluid Technology for Stimulation of Ultrahigh-Temperature Sandstone Formation. Paper SPE-173755-MS, presented at SPE International

Symposium on Oilfield Chemistry, 13-15 April, The Woodlands, Texas, USA.
<https://doi.org/10.2118/173755-MS>.

- [75] Al-Harbi, B. G., Al-Khaldi, M. H., & AlDossary, K. A. (2011). Interactions of Organic-HF Systems with Aluminosilicates: Lab Testing and Field Recommendations. Paper SPE-144100-MS presented at SPE European Formation Damage Conference, 7-10 June, Noordwijk, The Netherlands.<https://doi.org/10.2118/144100-MS>
- [76] Andotra G (2014) Investigating the use of chelating agents for clay dissolution and sandstone acidizing purposes. Master's thesis. Texas A&M University, Texas.
- [77] Yang, F., Nasr-El-Din, H. A., & Al-Harbi, B. M. (2012). Acidizing Sandstone Reservoirs Using HF and Formic Acids. Paper SPE-150899-MS, presented at SPE International Symposium and Exhibition on Formation Damage Control, 15-17 February, Lafayette, Louisiana, USA. Society of Petroleum Engineers.
<https://doi.org/10.2118/150899-MS>
- [78] Zhou, L., & Nasr-El-Din, H. A. (2013). Acidizing Sandstone Formations Using a Sandstone Acid System For High Temperatures. Paper SPE-165084-MS, Presented at SPE European Formation Damage Conference & Exhibition 5-7 June, Noordwijk, The Netherlands. <https://doi.org/10.2118/165084-MS>.
- [79] Coffey, J. A., Brewer, K. L., Carroll, R., Bradfield, J., & Meggs, W. J. (2007). Limited efficacy of calcium and magnesium in a porcine model of hydrofluoric acid ingestion. *Journal of Medical Toxicology : Official Journal of the American College of Medical Toxicology*, 3(2), 45–51. <https://doi.org/10.1007/bf03160907>
- [80] Smeđra-Kaźmiraska, A., Kędzierski, M., Barzdo, M., Jurczyk, A., Szram, S., & Berent, J. (2014). Accidental intoxication with hydrochloric acid and hydrofluoric acid mixture. *Archiwum Medycyny Sadowej i Kryminologii*, 64(1), 50–58. Retrieved from <http://www.ncbi.nlm.nih.gov/pubmed/25184427>

- [81] Blodgett, D. W., Suruda, A. J., & Crouch, B. I. (2001). Fatal unintentional occupational poisonings by hydrofluoric acid in the U.S. *American Journal of Industrial Medicine*, 40(2), 215–220. <https://doi.org/10.1002/ajim.1090>
- [82] Ohtani, M., Nishida, N., Chiba, T., Muto, H., & Yoshioka, N. (2007). Pathological demonstration of rapid involvement into the subcutaneous tissue in a case of fatal hydrofluoric acid burns. *Forensic Science International*, 167(1), 49–52. <https://doi.org/10.1016/j.forsciint.2005.12.008>
- [83] Heard, K., & Delgado, J. (2003). Oral decontamination with calcium or magnesium salts does not improve survival following hydrofluoric acid ingestion. *Journal of Toxicology. Clinical Toxicology*, 41(6), 789–792. <https://doi.org/10.1081/CLT-120025343>.
- [84] Burgher, F., Mathieu, L., Lati, E., Gasser, P., Peno-Mazzarino, L., Blomet, J., ... Maibach, H. I. (2011). Experimental 70% hydrofluoric acid burns: histological observations in an established human skin explants ex vivo model. *Cutaneous and Ocular Toxicology*, 30(2), 100–107. <https://doi.org/10.3109/15569527.2010.533316>
- [85] Bajraktarova-Valjakova, E., Korunoska-Stevkovska, V., Georgieva, S., Ivanovski, K., Bajraktarova-Misevska, C., Mijoska, A., & Grozdanov, A. (2018). Hydrofluoric Acid: Burns and Systemic Toxicity, Protective Measures, Immediate and Hospital Medical Treatment. *Open Access Macedonian Journal of Medical Sciences*, 6(11), 2257. <https://doi.org/10.3889/OAMJMS.2018.429>.
- [86] Holman, G. B. (1982). State-of-the-Art Well Stimulation. *Journal of Petroleum Technology*, 34(02), 239–241. <https://doi.org/10.2118/10868-PA>
- [87] Houseworth JE (2014) Advanced well stimulation technologies in California: an independent review of scientific and technical information, executive summary. California Council on Science and Technology. 978-1-930117-94-5\$4
- [88] Davies, S., & Kelkar, S. (2007). Carbonate Stimulation. *Middle East & Asia Reservoir Review*, pp. 51-63.

- [89] Schneider, G. W., "A Geochemical Model of the Solution-Mineral Equilibria Within a Sandstone Reservoir," M.S. Thesis, The University of Oklahoma, 1997, 157 p.
- [90] Schei, G., Fjær, E., Detournay, E., Kenter, C. J., Fuh, G. F., & Zausa, F. (2000). The Scratch Test: An Attractive Technique for Determining Strength and Elastic Properties of Sedimentary Rocks. Paper SPE-63255-MS, Presented at the SPE Annual Technical Conference and Exhibition 1-4 October Dallas, Texas. <https://doi.org/10.2118/63255-MS>.
- [91] Thomas, R. L., Nasr-El-Din, H. A., Lynn, J. D., Mehta, S., & Zaidi, S. R. (2001). Precipitation During the Acidizing of a HT/HP Illitic Sandstone Reservoir in Eastern Saudi Arabia: A Laboratory Study. In SPE Annual Technical Conference and Exhibition. Society of Petroleum Engineers. <https://doi.org/10.2118/71690-MS>.
- [92] Pituckchon, A. Further Investigation of Fluoboric Acid in Sandstone Acidizing Using ¹¹B And ¹⁹F NMR. M. S. Texas A&M University, 2014.
- [93] Sygała, A.; Bukowska, M.; Janoszek, T. High Temperature Versus Geomechanical Parameters of Selected Rocks – The Present State of Research. *J. Sustain. Min.* 2013, 12 (4), 45–51. <https://doi.org/10.7424/JSM130407>.
- [94] Vogt, T. C., & Anderson, M. L. (1974). Optimizing the Profitability of Matrix Acidizing Treatments. *Journal of Petroleum Technology*, 26(09), 1055–1062. <https://doi.org/10.2118/4550-PA>.
- [95] Hongjie, X. (1994). Prediction of Effective Acid Penetration and Acid Volume for Matrix Acidizing Treatments in Naturally Fractured Carbonates. *SPE Production & Facilities*, 9(03), 188–194. <https://doi.org/10.2118/25410-PA>.
- [96] Zou, C., Qin, Y., Yan, X., Zhou, L., & Luo, P. (2014). Study on acidizing effect of cationic β -cyclodextrin inclusion complex with sandstone for enhancing oil recovery. *Industrial and Engineering Chemistry Research*, 53(33), 12901–12910. <https://doi.org/10.1021/ie501569d>.

- [97] Zakaria, A. S., Nasr-El-Din, H. A., & Ziauddin, M. (2015). Flow of Emulsified Acid in Carbonate Rocks. *Industrial & Engineering Chemistry Research*, 54(16), 4190–4202. <https://doi.org/10.1021/ie504167y>.
- [98] Kume, N., Van Melsen, R., Erhahon, L., & Abiodun, A. F. (1999). New HF Acid System Improves Sandstone Matrix Acidizing Success Ratio By 400% Over Conventional Mud Acid System in Niger Delta Basin. Paper (SPE-56527-MS) presented at the SPE Annual Technical Conference and Exhibition, 3-6 October, Houston, Texas. <https://doi.org/10.2118/56527-MS>.
- [99] Zeit, B. (2005). Stimulation of sandstone reservoirs. SPE technology transfer workshop (TTW). A presentation.
- [100] Cheung, S. K., & Van Arsdale, H. (1992). Matrix Acid Stimulation Studies Yield New Results with a Multitap Long-Core Permeameter. *Journal of Petroleum Technology*, 44(01), 98–102. <https://doi.org/10.2118/19737-PA>.
- [101] Crowe C., Masmonteil J., Thomas R. (1992). Trends in matrix acidizing. *Oilfield Rev* 4(4):22–40.
- [102] Priisholm, S., Nielsen, B. L., & Haslund, O. (1987). Fines Migration, Blocking, and Clay Swelling of Potential Geothermal Sandstone Reservoirs, Denmark. *SPE Formation Evaluation*, 2(2), 168–178. <https://doi.org/10.2118/15199-PA>.
- [103] Weaver, C.E., Pollard, L.D. (1973). *The chemistry of clay minerals*. New York, NY, Elsevier Scientific Pub. Co.
- [104] Weaver, C.E. (1989). *Clays, muds, and shales*. 1st ed. Development in Sedimentology, vol. 44. , Amsterdam, Netherlands: Elsevier Pub. Co.
- [105] Grim, R.E. (1942). Modern Concepts of Clay Materials. *J. Geol.* 50, 225-275. <https://doi.org/10.2307/30070578>.

- [106] Hughes, R. V., 1951. The Application of Modern Clay Concepts to Oil Field Development. Paper (API-50-151), presented in Drilling and Production Practice1, New York.
- [107] Ezzat, A. M., 1990. Completion Fluids Design Criteria and Current Technology Weaknesses. Paper (SPE-19434), presented at the SPE Formation Damage Control Symposium, February 22-23, Lafayette, Louisiana.
- [108] Crowe C., Masmonteil J., Thomas R., 1992. Trends in matrix acidizing. Oilfield Rev. 4(4):22–40.
- [109] Thomas, R L, Nasr-El-Din, H A, Lynn, J D, Mehta, S, and Zaidi, S R. (2001). Precipitation During the Acidizing of a HT/HP Illitic Sandstone Reservoir in Eastern Saudi Arabia: A Laboratory Study. Paper (SPE 71690) presented at the Annual Technical Conference and Exhibition, 30 September- 3 October, New Orleans, Louisiana.
- [110] Simon, D. E., & Anderson, M. S. (1990). Stability of Clay Minerals in Acid. In SPE Formation Damage Control Symposium. Society of Petroleum Engineers. <https://doi.org/10.2118/19422-MS>
- [111] Labrid, J. C. (1975). Thermodynamic and Kinetic Aspects of Argillaceous Sandstone Acidizing. Soc Pet Eng AIME J, 15(2), 117–128. <https://doi.org/10.2118/5156-pa>
- [112] Nguyen, D. A., Iwaniw, M. A., & Fogler, H. S. (2003). Kinetics and mechanism of the reaction between ammonium and nitrite ions: Experimental and theoretical studies. Chemical Engineering Science, 58(19), 4351–4362. [https://doi.org/10.1016/S0009-2509\(03\)00317-8](https://doi.org/10.1016/S0009-2509(03)00317-8).
- [113] Singh, P., & Fogler, H. S. (1998). Fused chemical reactions: The use of dispersion to delay reaction time in tubular reactors. Industrial & Engineering Chemistry Research, 37(6), 2203–2207.

Vitae

- Name:** Ibrahim Hassan Ali Gomaa.
- Nationality:** Egyptian.
- Date of Birth:** 20/10/1993
- Email:** ebrahim.hassan5759@gmail.com
- Address:** Benha, Qalubiya, Egypt (13511).
- Education:** B.S of Petroleum Engineering and Gas Technology, The British University in Egypt, Cairo, Egypt, 2016.
- M.S. in Petroleum Engineering, King Fahd University of Petroleum and Minerals, Dhahran, Saudi Arabia, 2019.

Research and Publications

Journal Papers

- **Gomaa, I.**, Mahmoud, M., Kamal, M. S. (2019). "A Novel Approach for Sandstone Acidizing Using In-Situ Generated HF Acid with the Aid of Thermochemicals". ACS Omega, (*under review*).
- Ba Geri, B.S., **Gomaa, I.**, Mahmoud, M., Patil, S. (2019). "Complex Barite Filter Cake Removal Using In-Situ Generated Acids by Thermochemicals". Journal of Petroleum Exploration and Production Technology, (*under review*).
- **Gomaa, I.**, Mahmoud, M. (2019). "A Novel Approach for Stimulating Illitic Sandstone Using In-Situ Generated HF with the Aid of Thermochemicals". J. of Petroleum Science and Engineering (*under review*).
- S. Elkatatny, **I. Gomaa**, T. Moussa, New approach to obtain the rheological properties of drill-in fluid on a real-time using artificial intelligence, Petroleum (2019), doi: <https://doi.org/10.1016/j.petlm.2019.11.004>.
- **Gomaa, I.**, Elkatatny, S., and Abdulaheem, A. (2019). "Real-Time Determination of the Rheological Properties of High

Over-Balanced Drilling Fluid Used for Drilling Ultra-Deep Gas Wells Using Artificial Intelligence”. *Journal of Natural Gas Science & Engineering (under review)*.

Patents

- Ba Geri, B., **Gomaa, I.H.**, Mahmoud, M., and Patil, S. (2019). “In-Situ Barite-Quartz and Calcite-Quartz Filter Cake Removal Method”. Filed, Inv2019-072.
- **Gomaa, I.H.**, Mahmoud, M., Abdelgawad, K.Z., Hasan, A., and Al-Shehri, D. (2019). “Acidizing of Subterranean Formation Using In-Situ Generated HF”. Filed, Inv2019-066-01.

Conference Papers

- **Gomaa, I.**, Elkatatny, S., Abdulraheem, A., and Mahmoud, M. (2019). “Real-Time determination of the rheological properties of High Over-Balanced Drilling Fluid Using Artificial intelligence”. AADE National Technical Conference and Exhibition, April 9-10, Denver, Colorado.
- **Gomaa, I.**, Mahmoud, M., and Hassan, A. (2020). "Novel Approach for Stimulating Sandstone Formations Using In-situ Generated HF Acid with the Aid of Thermochemicals". Paper SPE-200286-MS for presentation as an ePoster at Oman Petroleum & Energy Show (OPES) to be held 9 - 11 March 2020 in Muscat, Oman.

Undergraduate Research

- Designed a **novel viscoelastic surfactant (VES)** to be used for EOR processes under high salinity conditions.
- Created a **Casing Design Computer Application** using MATLAB coding language.
- Created a **Gas Reserve Estimation Application** using MATLAB coding language.